INSTITUTE OF TECHNOLOGY

AIR UNIVERSITY

UNITED STATES AIR FORCE

SCHOOL OF ENGINEERING

THESIS

WRIGHT-PATTERSON AIR FORCE BASE, OHIO

AF-WP-B-SEP 60 5M

AN ANALYSIS
OF A
TRAJECTORY AND VELOCITY MATCH TECHNIQUE
FOR INTERCEPTING
INTERCONTINENTAL BALLISTIC MISSILES

THESIS

Presented to the Faculty of the School of Engineering

of the Institute of Technology

Air University

in Partial Fulfillment of the

Requirements for the Degree of

Master of Science

By

Richard Allen Coffland, B.S. Ch.E.

Capt USAF

and

Charles Allison MacIvor, M.E.

Capt USAF

Graduate Aeronautical Engineering

Air Weapons Option

August 1961

AN ANALYSIS
OF A
TRAJECTORY AND VELOCITY MATCH TECHNIQUE
FOR INTERCEPTING
INTERCONTINENTAL BALLISTIC MISSILES

THESIS

Presented to the Faculty of the School of Engineering

of the Institute of Technology

Air University

in Partial Fulfillment of the

Requirements for the Degree of

Master of Science

By

Richard Allen Coffland, B.S. Ch.E.

Capt USAF

and

Charles Allison MacIvor, M.E.

Capt USAF

Graduate Aeronautical Engineering

Air Weapons Option

August 1961

Preface

In this study, the authors have attempted to lay the groundwork needed to determine the feasibility of a trajectory-match technique for intercepting intercontinental ballistic missiles. In Chapter II, the ballistic trajectory equations and rocket equations of motion are developed in detail, since the authors feel that many readers, who may be interested in ICBM defense, may not be completely familiar with these concepts.

We found the boost-phase analysis in Chapter IV to be the most challenging aspect of the problem. As far as we know, we have developed a new technique for obtaining good approximations to the thrust and weight of boost-rockets required for boosting a given payload onto a specified trajectory.

Figures are used liberally throughout the report so that the reader can more easily follow the geometry involved in some of the more complicated mathematical derivations. There is also a list of definitions included on page vi to explain some terms which are peculiar to this particular study. The computer programs used are included in Appendix A, so that other investigators may reproduce any of the results or expand this study, if they so desire.

We wish to thank Captain H.G. Pringle for suggesting this thesis topic, and for his many helpful ideas throughout the investigation.

The authors are also indebted to their wives and children, for their patience, understanding, and many sacrifices which have greatly contributed to the completion of this work.

R.A.C.

C.A.M.

Table of Contents

		Page
Preface		ii
Definitions		vi
List of Symbols		vii
List of Figures		xi
List of Tables		xiii
Abstract		xiv
I.	Introduction	1
	General Considerations	1
	Statement of the Problem	2
	Analysis of the Problem	3
	Intercept Analysis	3
	Boost Analysis	3
	Effect of Variables	5
II.	Basic Theory	7
	Free-Flight Missile Trajectory	7
	Basic Equations	
	Additional Trajectory Parameters	12
	Time of Flight	1[illegible]
	Minimum Energy Trajectory	1[illegible]
	Energy Ratio Concept	21
	Rocket Equations of Motion	22
	Velocity Equations	22
	Distance Equations	24
	Specific Impulse of Rocket Fuels	25
III.	Determination of Intercept Trajectory	26
	Theoretical Intercept Geometry	26
	Velocity Difference Between Warhead and Interceptor	32
	Correction to Theoretical Intercept Trajectory	33
	Summary	41
IV.	Boost-Phase Analysis	42
	Approximations	43
	The K-Stage Boost Rocket	43
	Optimization	45
	Equations of Motion	47

Table of Contents (cont.)

		Page
	Thrust to Initial Weight Ratio	50
	Technique for Satisfying Burnout Velocity Requirement	52
	Technique for Satisfying Burnout Position Requirement	54
	Determination of Weight and Thrust Requirements	58
	Excess Time	61
	Maximum Acceleration	62
	Summary	64
V.	Procedure for Obtaining Numerical Results	66
	Primary Considerations	66
	Basic Analysis	66
	Warhead Trajectories to be Investigated	67
	Selection of Intercept Points and Launch Sites	70
	Selection of Rocket Parameters	72
	Number of Boost-Phase Stages	73
	Specific Impulse and Structural Factor	73
	Thrust to Initial Weight Ratios	73
	Summary	74
VI.	Results and Conclusions	75
	Results	76
	Effect of β_u on Th_1	76
	Effect of β and β_u on v	78
	Effect of β_u on T_x^*	78
	Effect of β on Th_1	81
	Effect of β on T_x^*	83
	Effect of n on Th_1	83
	Effect of I_s on Th_1	86
	Effect of I_s on T_x^{*1}	86
	Combined Effect of Changes in I_s and n	89
	Effect of ϕ_{LS_m} and ϕ_{wr} on Th_1 and T_x^*	90
	Illustrations of the Use of the Graphs	90
	Summary of Results	100
	Conclusions	107

Table of Contents (cont.)

		Page
List of References		109
Appendix A:	Computer Programs	111
Appendix B:	Check on the Validity of the Boost Approximations	123

Definitions

Interceptor Vehicle — The final payload consisting of the vehicle structure, and equipment necessary for detection and destruction of the enemy warhead.

Velocity-Match Rocket — An assembly consisting of the interceptor vehicle, rocket engine, fuel tanks, etc., needed to accelerate the interceptor vehicle to its final velocity. The velocity match rocket is the payload for the boost-phase rocket.

Interceptor System — The structure consisting of the boost-phase rocket and the velocity-match rocket.

Excess Time — The difference between the flight-times of the enemy warhead and the interceptor vehicle from their launch sites to the intercept point.

Sub-Rocket — An assembly consisting of the payload and the rocket stages not yet jettisoned.

List of Symbols

A	cross sectional area of rocket stage
AP	aiming point
a	speed of sound
b	height above the earth
C_d	coefficient of drag
D	effective mass ratio of boost-phase sub-rocket
D_u	effective mass ratio of velocity-match rocket
D_r	drag force
E	total energy per unit mass
ER	energy ratio
e	eccentricity of elliptical trajectory
f	functional notation
g	acceleration of gravity
g_c	proportionality constant (lb mass per lb force)(ft per sec^2)
h	angular momentum per unit mass
I_s	specific impulse
IP	intercept point
K	kinetic energy per unit mass
k	number of stages
LS	launch site
M	initial sub-rocket mass (lb_m), numerically equal to sea level weight
M	mach number

m	stage mass (lb_m)
m_p	interceptor vehicle mass
m'_p	interceptor rocket mass
n	structural factor
r	length of radius vector from center of the earth
r_I	radius at intercept point
r_{Ia}	radius at aiming point on corrected intercept trajectory
r_m	radius to interceptor trajectory
r_w	radius to enemy warhead trajectory
S	distance
S'	distance travelled by one-stage rocket, starting from rest in field-free, airless space
T_j	thrust force of the jth stage
T^*	flight time from apogee along ballistic trajectory
T_x^*	excess time (See list of definitions)
Th_j	ratio of thrust of jth stage to weight of interceptor vehicle
t	time
u	rocket exhaust velocity
V	potential energy per unit mass
v	velocity
X_e	range over earth's surface
x	horizontal distance
y	vertical distance
α	angle between thrust vector and velocity vector
β	thrust to initial weight ratio of boost-phase sub-rocket
β_u	thrust to initial weight ratio of velocity match rocket

γ	flight path angle (angle between velocity vector and local horizontal)
Γ	flight-path angle at termination of tip-over maneuver
δ	angle between aiming point and intercept point
ϵ	angular difference between launch site and burnout point in rectangular coordinates
μ	gravitational constant of the earth
ν	maximum acceleration in sea-level "g's"
η_b	burnout angle in rectangular coordinates
θ	angle between thrust vector and local horizontal
ϕ	position angle between radius vector and major axis
ϕ_b	burnout range angle of corrected interceptor trajectory
ϕ_{LI}	angle from launch site to intercept point for theoretical intercept trajectory
ϕ_{LIa}	angle from launch site to intercept point for corrected intercept trajectory
ϕ_{LS_m}	interceptor launch site position relative to warhead apogee
ϕ_{mo}	semi-range angle of theoretical intercept trajectory
ϕ_{moa}	semi-range angle of corrected intercept trajectory
ρ	atmospheric density
ψ	stage mass ratio (boost phase)
ψ_o	overall mass ratio (boost phase)
ψ_u	overall mass ratio (velocity match rocket)
λ	thrust angle above horizon in rectangular coordinates

Subscripts

a	corrected values
f	final value
b	burnout conditions.
I	intercept point conditions
m	interceptor
o	initial conditions
w	enemy warhead
x	horizontal component
x	excess
y	vertical component
u	velocity match stage

Other

.	derivative with respect to time
-	vector notation

List of Figures

Figure		Page
2-1	Coordinate System for Trajectory Derivation	7
2-2	Elliptical Ballistic Missile Trajectory	13
2-3	Diagram of Flight Path Angle Relationships	14
2-4	Effects of Total Energy, Angular Momentum and Launch Angle on Ballistic Trajectory	19
2-5	Diagram for Rocket Equation Derivation	22
3-1	"Apogee Intercept" Intercept Point at Apogee of Intercept Trajectory	27
3-2	"Tangent Intercept" Interceptor and Warhead Trajectories Tangent at Intercept Point	28
3-3	Auxiliary Triangle for Solving Equation (3-13) . .	31
3-4	Vector Diagram of Velocities and Displacement for Theoretical Intercept Trajectory	35
3-5	Vector Diagram of Velocities and Displacement for corrected Intercept Trajectory	37
3-6	Geometry for Determining Correction to Theoretical Intercept Trajectory	40
4-1	Coordinate System for Boost-Phase Approximation . .	44
4-2	K-Stage Boost-Phase Rocket	46
4-3a	Trial Number One in Boost-Phase Approximation . . .	55
4-3b	Trial Number Two in Boost-Phase Approximation . . .	57
4-4	Iterative Process for Satisfying Velocity and Position Requirements on the Interceptor Trajectory	59
4-5	Angles for Determining Flight-Times of Warhead and Interceptor	63

Figure		Page
5-1	Position of Launch Site and Intercept Point Relative to Warhead Apogee	71
6-1	Effect of β_u on Th_1	77
6-2	Effect of β_u on ν_u	79
6-3	Effect of β_u on T_x^*	80
6-4	Effect of β on Th_1	82
6-5	Effect of β on T_x^*	84
6-6	Effect of n on Th_1	85
6-7	Effect of I_s on Th_1	87
6-8	Effect of I_s on T_x^*	88
6-9	Plot of Th_1 vs ϕ_{LS_m} for Various ϕ_{WI} - 6000 n.m. Low Angle Warhead Trajectory	91
6-10	Plot of Th_1 vs ϕ_{LS_m} for Various ϕ_{WI} - 6000 n.m. Minimum Energy Warhead Trajectory	92
6-11	Plot of Th_1 vs ϕ_{LS_m} for Various ϕ_{WI} - 6000 n.m. High Angle Warhead Trajectory	93
6-11a	Effect of Time, Thrust, and "g" Limitations on Launch Site and Intercept Point Location	94
6-12	Plot of T_x^* vs ϕ_{LS_m} for Various ϕ_{WI} - 6000 n.m. Low Angle Warhead Trajectory	97
6-13	Plot of T_x^* vs ϕ_{LS_m} for Various ϕ_{WI} - 6000 n.m. Minimum Energy Warhead Trajectory	98
6-14	Plot of T_x^* vs ϕ_{LS_m} for Various ϕ_{WI} - 6000 n.m. High Angle Warhead Trajectory	99
6-15	Plot of Th_1 vs ϕ_{LS_m} for Various ϕ_{WI} - 4000 n.m. Low Angle Warhead Trajectory	101

Figure		Page
6-16	Plot of Th_1 vs ϕ_{LS_m} for Various ϕ_{WI} - 4000 n.m. Minimum Energy Warhead Trajectory	102
6-17	Plot of Th_1 vs ϕ_{LS_m} for Various ϕ_{WI} - 4000 n.m. High Angle Warhead Trajectory	103
6-18	Plot of T_x^* vs ϕ_{LS_m} for Various ϕ_{WI} - 4000 n.m. Low Angle Warhead Trajectory	104
6-19	Plot of T_x^* vs ϕ_{LS_m} for Various ϕ_{WI} - 4000 n.m. Minimum Energy Warhead Trajectory	105
6-20	Plot of T_x^* vs ϕ_{LS_m} for Various ϕ_{WI} - 4000 n.m. High Angle Warhead Trajectory	106

List of Tables

Table		Page
I	Warhead Trajectory Semi-Range and Launch Angles for 6000 and 4000 Nautical Mile Ranges	70
II	Combined Effects of Specific Impulse and Structural Factor on Overall Thrust Requirements	89

Abstract

In this thesis, a mid-course, trajectory-match intercept of intercontinental ballistic missiles is analyzed. The intercept is accomplished by using a multi-stage rocket to boost an interceptor vehicle onto a ballistic trajectory in the same direction of flight as the warhead trajectory, so that the two trajectories are almost tangent at a selected intercept point. Near the intercept point, a final rocket is ignited to accelerate the vehicle and match the warhead's position and velocity.

A simplified analysis is performed for the case of a co-planar intercept over a spherical, non-rotating earth. Intercept trajectories are determined from the trajectory geometry and the rocket equations of motion. An approximate method is derived to estimate the thrusts and rocket weights required to boost an interceptor vehicle onto these trajectories. Equations are programmed for an IBM 1620 digital computer to obtain estimates of thrusts, weights, maximum accelerations, and the difference in the times of flight of the warhead and interceptor. Various combinations of intercept points and interceptor launch sites are used to determine the first stage thrust required per pound of interceptor vehicle for intercept of low angle, minimum energy, and high angle, 6000 and 4000 nautical mile range warhead trajectories. The effects of specific impulse, structural factor, and thrust to initial weight ratio upon overall thrust, time, and acceleration are also determined. It is found that there is an optimum value of thrust to weight ratio which

results in minimum overall thrust requirements.

A numerical solution to the equations of motion is performed on the computer for the boost phase. For the case considered it is found that: the actual burnout velocity is within three percent less than desired and thrust is within eleven percent of that required, thereby proving the validity of the original boost phase approximations.

The computer results are presented graphically, and indicate that this intercept technique is theoretically possible for either a manned or unmanned interceptor system. However, a much broader investigation would be required to definitely determine its usefulness for defense against ICBM's.

AN ANALYSIS
OF A
TRAJECTORY AND VELOCITY MATCH TECHNIQUE
FOR INTERCEPTING
INTERCONTINENTAL BALLISTIC MISSILES

I. Introduction

General Considerations

The high speed and short time of flight of the intercontinental ballistic missile have made the problem of finding an effective ICBM defense system extremely complex. To successfully intercept an ICBM, an interceptor vehicle must be positioned at or near the same point in space as the ICBM, at the same time. The interceptor must also be able to distinguish the warhead from decoys and destroy it.

One system which is presently in the development and test stage is limited to intercepting enemy missiles during the re-entry phase of their trajectories. For this type of intercept, the interceptor vehicle approaches the warhead practically "head on", resulting in extremely high relative velocities. This places very stringent guidance and accuracy requirements upon the system. Furthermore, this system is limited to point-defense of relatively small, strategic target areas. Since this is practically a "last ditch" defense, the question has arisen: Can a successful intercept be made during the boost phase of the warhead trajectory, while the rocket motors are still burning, or during the mid-course, free-flight phase, prior to re-entry?

It would be difficult to intercept a missile during the boost phase because of the very short warning time available, and the usual lack of friendly defense bases in the vicinity of enemy launch sites. Thus, serious disadvantages also exist for this type of intercept.

Now let us consider the possibility of a mid-course intercept, and a method of reducing the relative velocity between the interceptor and the warhead. This can be accomplished by: launching an interceptor vehicle on a ballistic trajectory in the same direction of flight as the warhead; making this intercept trajectory nearly tangent to the warhead trajectory; and accelerating the interceptor vehicle to match the warhead's position and velocity by igniting a final booster rocket near the intercept point. This method offsets the disadvantages inherent in the re-entry and boost phase intercepts. Available warning time would not be as great as for the re-entry intercept, but terminal guidance requirements should not be nearly as critical due to the low relative velocity near the intercept point. Thus, the mid-course, trajectory-match intercept appears to be a promising solution to the problem of ICBM defense.

Statement of the Problem

The purpose of this thesis is to analyze a mid-course, trajectory-match intercept of an ICBM warhead. This analysis consists of determining the interception geometry, the required thrust and weight of the interceptor system, and the difference between the flight times of the ICBM warhead and the interceptor, from launch site to point of intercept.

Since for this type of intercept there is a low relative velocity at the intercept point, there are possible advantages to having a man

in the interceptor vehicle. These include man's ability to make decisio and evaluate data from short range, decoy discrimination equipment. Therefore, the analysis includes a consideration of the maximum acceleration imposed upon this system, and an effort is made to keep acceleration within human tolerances.

Analysis of the Problem

The analysis of an ICBM intercept over the non-spherical, rotating earth, by an interceptor system of unknown performance would be extremely complex. However, this analysis can be greatly simplified by assuming that the earth is spherical and non-rotating, and that the warhead and interceptor trajectories are co-planar. Although these assumptions are unrealistic, the basic concepts and techniques, when established for this special case, could be extended to the general intercept. Should the present investigation show promise.

Intercept Analysis. The first step is the determination of the geometry of the intercept for the tangent trajectory. The equations are developed to allow variable inputs of warhead trajectory, intercept point and interceptor launch site.

Next, the dynamics of the velocity-match phase are considered. It is shown that the equations of motion of a rocket in field free space can be considered to be a perturbation to the theoretical free-flight trajectory, if gravity is assumed constant during the velocity-match phase. The required free-flight trajectory is determined by correcting the theoretical trajectory for the effect of this perturbation.

Boost Analysis. With the required intercept trajectories

established, the next problem is to determine the booster requirements to place the interceptor vehicle on this trajectory. These requirements must be based upon the weight of the velocity-match rocket which in turn depends upon the weight of the interceptor vehicle. Since this is an initial investigation, the weight of the interceptor vehicle is unknown. A vehicle weight could be assumed, but to permit greater flexibility, non-dimensional weight ratios are used to determine rocket weight and thrust requirements per pound of interceptor vehicle. The boost phase analysis is further complicated by the large number of variable rocket parameters. The thrust, weight, specific impulse and structural factor of each stage, as well as the number of stages must be established to continue the analysis. Furthermore, the exact size and shape of the interceptor system and the velocity profile during boost are all unknown. Therefore aerodynamic drag during the boost phase can not be exactly predicted. These complications make a closed-form solution to the boost-phase equations of motion unfeasable.

The following assumptions are made to obtain an approximate solution to these equations:

(1) The structual factor and specific impulse are the same for each stage.

(2) Drag is negligible compared to thrust.

(3) Gravity is constant in magnitude and direction.

(4) Vertical launch and tip-over maneuver can be neglected.

(5) An inertial, rectangular coordinate system can be used.

(6) Thrust for each stage is constant.

(7) The thrust direction is the same (constant direction relative to inertial space) for each stage.

A further simplification is made by making the thrust to initial weight ratio the same for each sub-rocket.

With the use of the above assumptions and simplifications, a set of equations are obtained which give the thrust and weight ratios required to achieve a desired velocity and direction in space. These equations are then combined with the interceptor trajectory equations in a program designed for use on the IBM 1620 digital computer. By means of this program the thrusts and weights of the booster rockets, the flight times from interceptor launch site to intercept point, and maximum accelerations are obtained.

A numerical integration is then performed on the 1620 computer to check the validity of the boost-phase approximations. For the typical intercept situation, it is found that the burnout velocity of the booster rockets differed from that desired by approximately three per cent.

Effect of Variables. The large number of variables require that this investigation be limited to a few of the many possible enemy warhead trajectories.

Two typical ICBM ranges (6000 and 4000 nautical miles) are selected However, this must be further limited since for any particular warhead range there are an infinite number of possible trajectories, characterized by the height of their apogees. In an attempt to adequately consider possible intercept conditions, a high, medium (minimum energy), and low altitude trajectory is considered for each range.

The effect of structual factor, specific impulse, and thrust to weight ratio on thrust requirements, excess time, and maximum acceleration is investigated for a few typical intercepts. Finally, reasonable values of specific impulse and structural factor, and an optimum value of thrust to weight ratio are used to investigate the effect of varying the intercept point and interceptor launch site on thrust and excess time.

II. Basic Theory

The Free-Flight Missile Trajectory

Basic Equations. The motion of a ballistic missile in a vacuum under the influence of a central force field such as the earth's gravitational field, can be analyzed by considering the missile to be a point mass in a polar, inertial coordinate system (Ref 13:2-20).

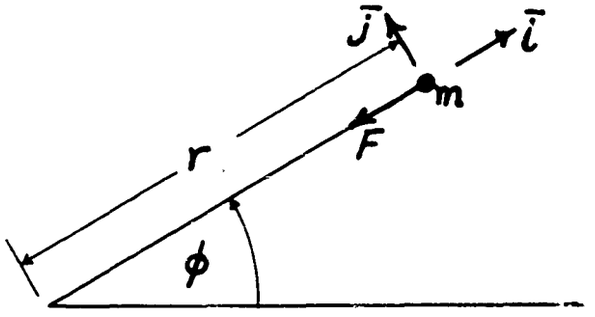

Fig. 2-1
Coordinate System for Trajectory Derivation

Let $\bar{i}$ be a unit vector in the $\bar{r}$ direction and $\bar{j}$ a unit vector perpendicular to $\bar{r}$ as shown in Fig. 2-1. The derivatives of the unit vectors with respect to ϕ are

$$\frac{d\bar{i}}{d\phi} = \bar{j} \qquad \text{and} \qquad \frac{d\bar{j}}{d\phi} = -\bar{i}$$

Then the derivatives with respect to time are

$$\frac{d\bar{i}}{dt} = \frac{d\bar{i}}{d\phi}\frac{d\phi}{dt} = \dot{\phi}\bar{j} \qquad \text{and} \qquad \frac{d\bar{j}}{dt} = \frac{d\bar{j}}{d\phi}\frac{d\phi}{dt} = -\dot{\phi}\bar{i}$$

Now the position vector of the missile is

$$\bar{r} = r\bar{i}$$

Its velocity is

$$\dot{\bar{r}} = \dot{r}\bar{i} + r\frac{d\bar{i}}{dt}$$

or

$$\dot{\bar{r}} = \dot{r}\bar{i} + r\dot{\phi}\bar{j} \tag{2-1}$$

and its acceleration is

$$\ddot{\bar{r}} = \dot{r}\frac{d\bar{i}}{dt} + \ddot{r}\bar{i} + r\dot{\phi}\frac{d\bar{j}}{dt} + (r\ddot{\phi} + \dot{r}\dot{\phi})\bar{j}$$

or

$$\ddot{\bar{r}} = (\ddot{r} - r\dot{\phi}^2)\bar{i} + (2\dot{r}\dot{\phi} + r\ddot{\phi})\bar{j} \tag{2-2}$$

Now

$$\frac{d}{dt}(r^2\dot{\phi}) = 2r\dot{r}\dot{\phi} + r^2\ddot{\phi} = r(2\dot{r}\dot{\phi} + r\ddot{\phi})$$

or

$$\frac{1}{r}\frac{d}{dt}(r^2\dot{\phi}) = 2\dot{r}\dot{\phi} + r\ddot{\phi} \tag{2-3}$$

Substituting Eq (2-3) into Eq (2-2),

$$\ddot{\bar{r}} = (\ddot{r} - r\dot{\phi}^2)\bar{i} + \left[\frac{1}{r}\frac{d}{dt}(r^2\dot{\phi})\right]\bar{j} \tag{2-4}$$

Now, by applying Newton's Second Law of Motion, $\bar{F} = m\bar{a}$

where

$$\bar{F} = -\frac{\mu m}{r^2}\bar{i}$$

m is the mass of the missile

μ is the earth's gravitational constant

we get

$$-\frac{\mu m}{r^2}\bar{i} = m\left[(\ddot{r} - r\dot{\phi}^2)\bar{i} + \left(\frac{1}{r}\frac{d}{dt}[r^2\dot{\phi}]\right)\bar{j}\right] \tag{2-5}$$

Then by equating the $\bar{j}$ components of Eq (2-5)

$$\frac{1}{r}\frac{d}{dt}(r^2\dot{\phi}) = 0$$

Now, since r is not infinite,

$$\frac{d}{dt}\left(r^2\dot{\phi}\right)=0$$

or $$r^2\dot{\phi} = \text{"a constant"}$$

But $r^2\dot{\phi}$ is the polar coordinate expression for the angular momentum per unit mass. Therefore, the angular momentum of the missile is a constant during the free-flight phase. Let us call the angular momentum per unit mass, h. Then

$$h = r^2\dot{\phi} \tag{2-6}$$

Now, equating the $\bar{I}$ components of Eq (2-5),

$$-\frac{\mu}{r^2} = \ddot{r} - r\dot{\phi}^2 \tag{2-7}$$

In order to solve Eq (2-7), let us define a dummy variable,

$$p = \frac{1}{r}$$

Then, in terms of p, Eq (2-6) becomes

$$h = r^2\dot{\phi} = \frac{\dot{\phi}}{p^2} \qquad \text{or} \qquad \dot{\phi} = p^2h \tag{2-8}$$

Also

$$\dot{r} = \frac{dr}{d\phi}\frac{d\phi}{dt} = p^2h\left[\frac{d}{d\phi}\left(\frac{1}{p}\right)\right] \tag{2-9}$$

But

$$\frac{d}{d\phi}\left(\frac{1}{p}\right) = -\frac{1}{p^2}\frac{dp}{d\phi} \tag{2-10}$$

Combining Eqs (2-9) and (2-10),

$$\dot{r} = \left(p^2h\right)\left(-\frac{1}{p^2}\right)\frac{dp}{d\phi} = -h\frac{dp}{d\phi} \tag{2-11}$$

Then

$$\ddot{r} = \frac{d}{dt}\left(-h\frac{dp}{d\phi}\right)$$

$$= -h\left[\frac{d}{d\phi}\left(\frac{dp}{d\phi}\right)\frac{d\phi}{dt}\right]$$

$$= -\dot{\phi}h\frac{d^2p}{d\phi^2}$$

or
$$\ddot{r} = -p^2 h^2 \frac{d^2 p}{d\phi^2} \tag{2-12}$$

Substituting Eqs (2-8 and (2-12) into Eq (2-7), with $r = \frac{1}{p}$, we get

$$-\mu p^2 = -p^2 h^2 \frac{d^2 p}{d\phi^2} - \frac{1}{p}(p^2 h)^2 \tag{2-13}$$

Dividing Eq (2-13) by $-p^2h^2$ gives

$$(-\mu/h^2) = \frac{d^2 p}{d\phi^2} + p \tag{2-14}$$

Equation (2-14) is a non-homogeneous, second order, linear differential equation which can be solved by the method of undetermined coefficients (Ref. 14:36-41).

The solution of this equation is

$$p = \frac{\mu}{h^2} + A\cos(\phi - \phi') \tag{2-15}$$

where A and ϕ' are constants which must be determined from the bounda conditions.

The evaluation of these constants depends upon the fact that th· .otal energy of the missile must be a constant for free-flight in a central force field. Thus,

$$E = K + V = \text{"a constant"}$$

where: E = total energy of the missile per unit mass

K = kinetic energy of the missile per unit mass

V = potential energy of the missile per unit mass

By defining potential energy, V, as zero when r is infinite we can say that
$$V = -\frac{\mu}{r} \tag{2-16}$$

Also, kinetic energy is defined as $K = \frac{1}{2}v^2$

or
$$K = \frac{1}{2}(\dot{r}^2 + r^2\dot{\phi}^2) \tag{2-17}$$

Thus

$$E = \frac{1}{2}(\dot{r}^2 + r^2\dot{\phi}^2) - \frac{\mu}{r} \tag{2-}$$

Equation (2-18) can be rewritten in terms of p by the use of Eqs (2-1) and (2-8).

$$E = \frac{1}{2}\left[h^2\left(\frac{dp}{d\phi}\right)^2 + \left(\frac{1}{p^2}\right)(p^2h)^2\right] - \mu p$$

$$E = \frac{h^2}{2}\left[\left(\frac{dp}{d\phi}\right)^2 + p^2\right] - \mu p \tag{2-}$$

Differentiating Eq (2-15) gives

$$\frac{dp}{d\phi} = -A\sin(\phi - \phi') \tag{2-20}$$

By using Eqs (2-15) and (2-20), p is eliminated from Eq (2-19, giving an expression for E in terms of A and h.

$$E = \frac{h^2A^2}{2} - \frac{\mu^2}{2h^2} \tag{2-19a}$$

Rearranging Eq (2-19a) and solving for A,

$$A = \pm\sqrt{\frac{2E}{h^2} + \frac{\mu^2}{h^4}} = \pm\frac{\mu}{h^2}\sqrt{1 + \frac{2Eh^2}{\mu^2}} \tag{2-}$$

Substituting Eq (2-21) into Eq (2-15),

$$p = \frac{\mu}{h^2} \pm \frac{\mu}{h^2}\sqrt{1 + \frac{2Eh^2}{\mu^2}}\cos(\phi - \phi')$$

$$p = \frac{\mu}{h^2}\left[1 \pm \sqrt{1 + \frac{2Eh^2}{\mu^2}}\cos(\phi - \phi')\right] \tag{2-22}$$

But

$$r = \frac{1}{p} = \frac{h^2/\mu}{1 \pm \sqrt{1 + \frac{2Eh^2}{\mu^2}}\cos(\phi - \phi')} \tag{2-}$$

Now if we choose our coordinate system so that r is a maximum when $\phi = 0$, then $\phi' = 0$ and Eq (2-23) becomes

$$r = \frac{h^2/\mu}{1 - \sqrt{1 + \frac{2Eh^2}{\mu^2}} \cos \phi} \tag{2-24}$$

This equation is similar to the equation of an ellipse in polar coordinates, which is

$$r = \frac{l}{1 - e \cos \phi} \tag{2-25}$$

where l = the semi-lattice rectum of the ellipse

e = the eccentricity of the ellipse

Therefore we can state that the equation of the trajectory of a ballistic missile in free-flight over a spherical non-rotating earth is an ellipse with the center of the earth at one focus. The eccentricity of the ellipse is defined by the equation

$$e = \sqrt{1 + \frac{2Eh^2}{\mu^2}} \tag{2-26}$$

and the semi-lattice rectum by

$$l = \frac{h^2}{\mu} \tag{2-27}$$

Thus the trajectory of a ballistic missile is completely defined if the total energy and angular momentum of the missile are known, and is given by the equation

$$r = \frac{h^2/\mu}{1 - e \cos \phi} \tag{2-28}$$

<u>Additional Trajectory Parameters.</u> Figure 2-2 shows the elliptical trajectory plus several other parameters which are useful for analyzing ballistic trajectories. These parameters are defined as follows:

γ - the angle between the flight path and the local horizontal

γ_o - theoretical launch angle at the earth's surface

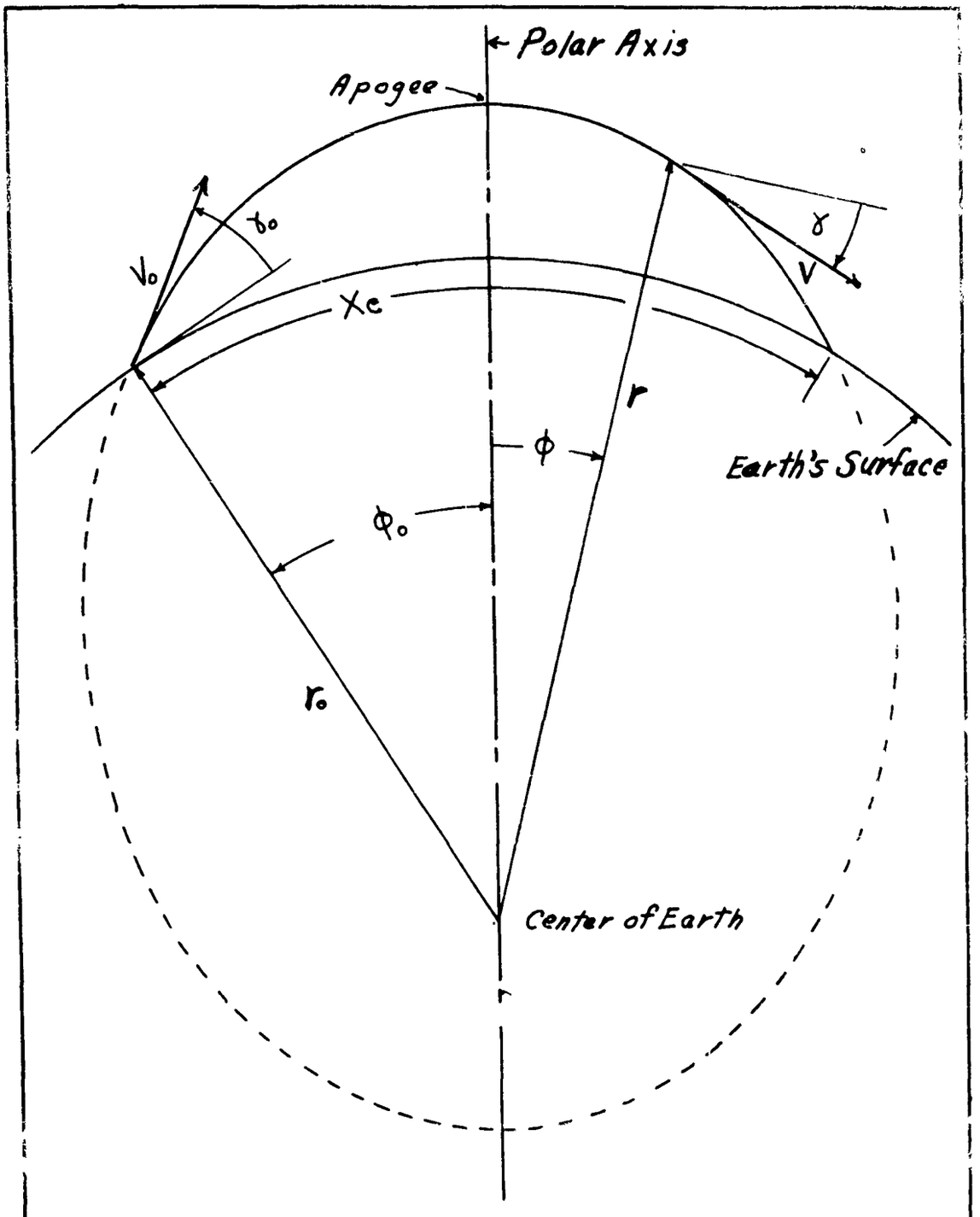

Fig. 2-2

Elliptical Ballistic Missile Trajectory

v_o - theoretical launch velocity at the earth's surface

X_e - range over the earth's surface from theoretical launch site to theoretical impact point

r_o - radius of the earth

ϕ_o - semi-range angle of the trajectory

ϕ - angle from major axis of the ellipse to the radius vector (measured positive clockwise)

The angle of the tangent to the trajectory, γ, can be determined from the ellipse equation and Fig. 2-3.

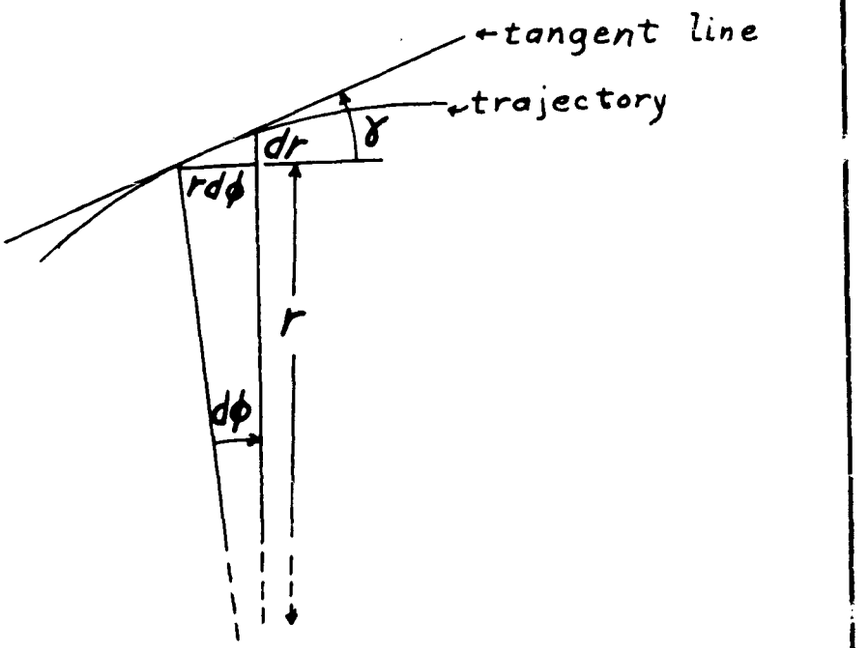

Fig. 2-3
Diagram of Flight Path Angle Relationships

$$\tan \gamma = \frac{dr}{r d\phi} = \frac{1}{r} \frac{dr}{d\phi} \tag{2-29}$$

Differentiating Eq (2-25),

$$\frac{dr}{d\phi} = \frac{-l e \sin \phi}{(1 - e \cos \phi)^2} \tag{2-30}$$

Then

$$\tan \gamma = \frac{-e \sin \phi}{1 - e \cos \phi} \tag{2-31}$$

From Eq (2-31), the theoretical launch angle is defined by the equation

$$\tan \gamma_o = \frac{e \sin \phi_o}{1 - e \cos \phi_o} \tag{2-32}$$

Notice that the negative sign is dropped because the launch angle must always be positive. The sense of the angle is lost when the semi-range angle, an absolute quantity, is substituted into the equation.

The relationship between h, γ_o, and v_o is given by the equation

$$h = r_o v_o \cos \gamma_o \tag{2-33}$$

An alternate equation for eccentricity, knowing ϕ_o and γ_o, can be derived from Eq (2-31). The result is

$$e = \frac{1}{\cos \phi_o + \sin \phi_o \cot \gamma_o} \tag{2-34}$$

If the desired range of the trajectory over the earth's surface is known, the semi-range angle is determined by the equation

$$\phi_o = \frac{X_e}{2 r_o} \tag{2-35}$$

Time of Flight. One very important parameter of the trajectory remains to be determined. This is the time of flight during the free-flight trajectory (Ref. 13:17-19). An inspection of Fig. 2-3 shows that

the incremental area between two radial lines, $d\phi$ apart, is

$$dA = \frac{1}{2}(r\,d\phi)(r) = \frac{1}{2}r^2 d\phi \tag{2-36}$$

Equation (2-36) can be written as

$$\frac{dA}{dt} = \frac{1}{2}r^2\frac{d\phi}{dt} = \frac{1}{2}r^2\dot{\phi}$$

but
$$r^2\dot{\phi} = h \tag{2-6}$$

and so
$$\frac{dA}{dt} = \frac{1}{2}h \qquad \text{(constant)} \tag{2-37}$$

For one complete orbit or revolution,

$$A = \frac{1}{2}hT \tag{2-38}$$

where A = the total area of the ellipse

T = the period of revolution

Since the time rate of change of the area of a sector of the ellipse is a constant,

$$\frac{T^*}{T} = \frac{A^*}{A} \tag{2-39}$$

where T* is the time required to travel along the arc of a sector of area A*.

Then
$$T^* = \frac{T}{A}A^* \tag{2-40}$$

But, by rearranging Eq (2-38), $\frac{T}{A} = \frac{2}{h}$

Thus
$$T^* = \frac{2}{h}A^* \tag{2-41}$$

Now, since A* is the area of any sector of the trajectory, let us

evaluate A* for a sector from the apogee radial line (where $\phi = 0$) to the general angle, ϕ, downrange from apogee.

From Eq (2-36)

$$dA = \frac{1}{2} r^2 d\phi$$

Squaring Eq (2-25) gives

$$r^2 = \frac{l^2}{(1 - e\cos\phi)^2} = \frac{h^4}{\mu^2(1 - e\cos\phi)^2} \tag{2-42}$$

Combining Eqs (2-36) and (2-42)

$$dA = \frac{h^4 d\phi}{2\mu^2(1 - e\cos\phi)^2} \tag{2-43}$$

Then

$$A^* = \frac{h^4}{2\mu^2}\int_0^{\phi} \frac{d\phi}{(1 - e\cos\phi)^2} \tag{2-44}$$

This integral may be evaluated by the use of a table of integrals (Ref. 8:41,42). The result is

$$A^* = \left(\frac{h^4}{2\mu^2}\right)\left(\frac{1}{1-e^2}\right)\left[\frac{e\sin\phi}{1 - e\cos\phi} + \frac{2}{\sqrt{1-e^2}}\tan^{-1}\left(\frac{\sqrt{1-e^2}\tan\frac{\phi}{2}}{1-e}\right)\right] \tag{2-45}$$

Substituting Eq (2-45) into Eq (2-41) we obtain the equation for the time of flight from apogee to any angle, ϕ, downrange from apogee.

$$T^* = \left(\frac{h^3}{\mu^2}\right)\left(\frac{1}{1-e^2}\right)\left[\frac{e\sin\phi}{1 - e\cos\phi} + \frac{2}{\sqrt{1-e^2}}\tan^{-1}\left(\frac{\sqrt{1-e^2}\tan\frac{\phi}{2}}{1-e}\right)\right] \tag{2-46}$$

Since the trajectory is symmetric about the apogee radius (or polar axis), Eq (2-46) can also be used to determine the time to apogee from any angle up-range by substituting the absolute value of the position angle in the formula.

The time of flight between any two points on the trajectory is

$$T_t^* = T^*(\phi_1) - T^*(\phi_2) \tag{2-47}$$

where $\phi_1 > \phi_2$ and the correct signs are used for the position angles.

Minimum Energy Trajectory. (Ref. 13:1924) Previously, we have shown that the trajectory of a ballistic missile is completely defined by the total energy, E, and the angular momentum, h. Now we will investigate the effect of each of these parameters on the trajectory.

First, let us note from Eq (2-48) that as the total energy increases, the theoretical launch velocity, v, increases.

$$E = \frac{1}{2} V_o^2 - \frac{\mu}{r_o} \tag{2-48}$$

But

$$h = r_o V_o \cos \gamma_o \tag{2-33}$$

Thus for a constant launch angle, the angular momentum also increases with an increase in total energy.

Rearranging Eq (2-28) gives an equation which relates the angular momentum and eccentricity to the semi-range angle

$$\cos \phi_o = \frac{1}{e}\left(1 - \frac{h^2}{\mu r_o}\right) \tag{2-49}$$

Substituting Eq (2-26) into Eq (2-49) gives

$$\cos \phi_o = \frac{1 - \frac{h^2}{\mu r_o}}{\sqrt{1 + \frac{2Eh^2}{\mu^2}}} \tag{2-50}$$

Inspection of Eq (2-50) shows that as E increases with h held constant, cos ϕ_o decreases or ϕ_o, and therefore range, increases (See Fig. 2-4a).

Examination of Eqs (2-33, 48, and 50) shows that for a constant launch angle, an increase in the total energy increases both the range

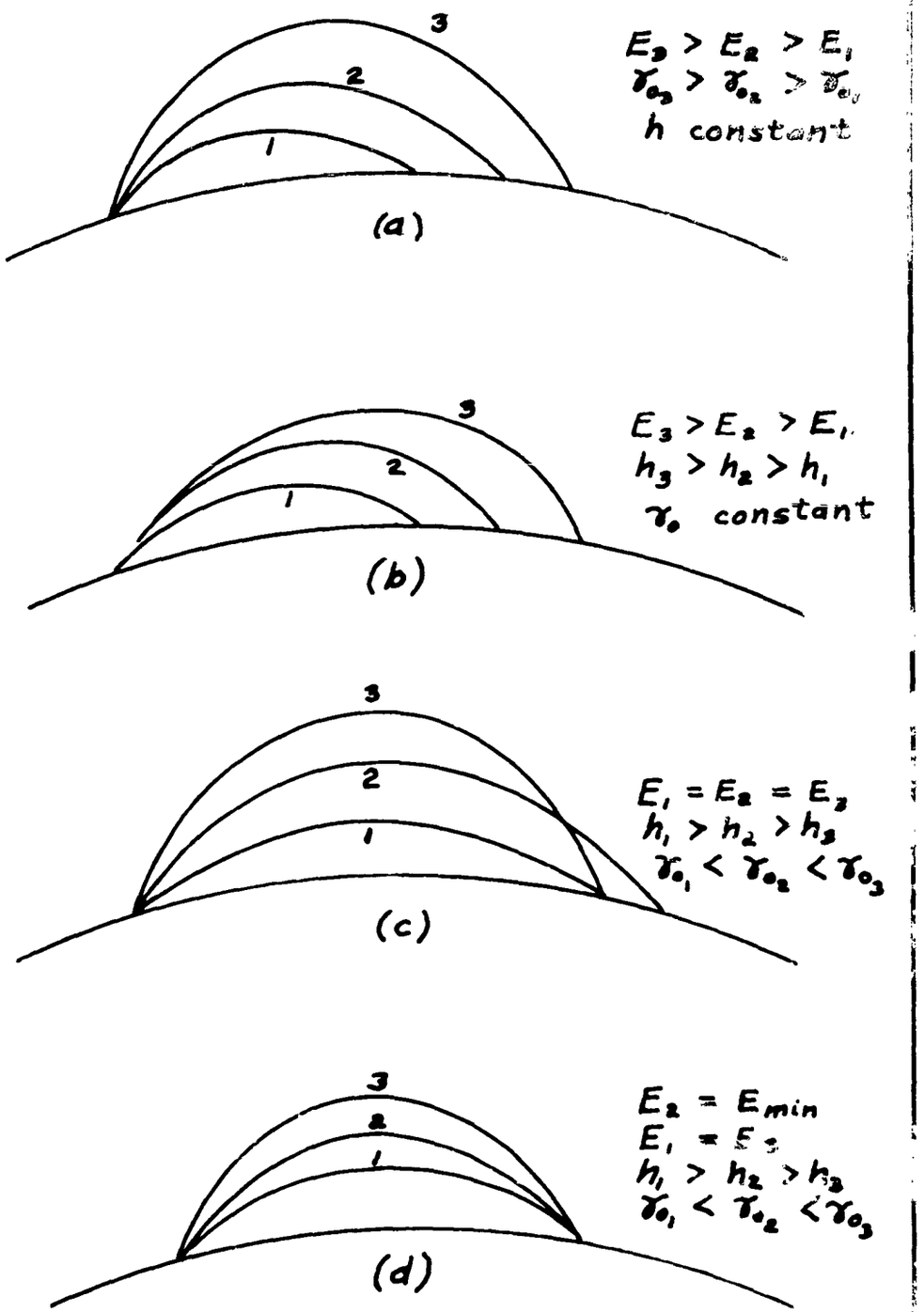

Fig. 2-4
Effects of Total Energy, Angular Momentum and Launch Angle on the Ballistic Trajectory

and the angular momentum (Fig. 2-4b).

Now let us determine the effect of angular momentum on the total energy required for a fixed range. Equation (2-50) can be written as

$$E = \frac{1}{2}\left[\left(\frac{\frac{\mu}{h} - \frac{h}{r_o}}{\cos \phi_o}\right)^2 - \left(\frac{\mu}{h}\right)^2\right] \tag{2-51}$$

If there is a minimum energy for a given range, we can determine the value that h must have for minimum energy by differentiating Eq (2-51) with respect to h, equating the result to zero, and solving for h.

$$\left(\frac{\partial E}{\partial h}\right)_{\phi_o} = \frac{h^4 - \mu^2 r_o^2}{h^3 r_o^2 \cos^2 \phi_o} + \frac{\mu^2}{h^3} = 0 \tag{2-52}$$

Then

$$h^2 = \mu r_o \sin \phi_o \tag{2-53}$$

and

$$h_{ME} = \sqrt{\mu r_o \sin \phi_o} \tag{2-54}$$

Substituting the value of h_{ME} into Eq (2-51)

$$E_{min} = -\frac{\mu}{r_o}\left(\frac{1}{1 + \sin \phi_o}\right) \tag{2-55}$$

Note that E is negative. This must be true for any ballistic trajectory since positive E would be sufficient energy to escape from the earth's gravitational field.

Now, since there is a minimum energy requirement for a given range, there must also be a maximum range for a given amount of total energy. This maximum range is attained with the optimum value of angular momentum and launch angle. If the launch angle is either greater or less than the optimum value, the range will be less than maximum (See Fig. 2-4c).

Finally, for a given range there is an almost unlimited number of trajectories possible depending on the values of E and h. For any particular value of E which is greater than E_{min}, there are two possible trajectories for the same range. These two trajectories converge to the minimum energy trajectory as the total energy approaches E_{min} (See Fig. 2-4d).

Now that we have established the existence of a minimum energy trajectory, let us derive a few minimum energy relationships. Substitution of Eqs (2-54) and (2-55) into Eq (2-26) gives the eccentricity of the minimum energy trajectory as

$$e_{M.E.} = \frac{\cos \phi_o}{1 + \sin \phi_o} \tag{2-56}$$

The optimum launch angle is determined by substitution of Eq (2-56) into Eq (2-32).

$$\tan \gamma_{o_{M.E.}} = \frac{\cos \phi_o}{1 + \sin \phi_o} \tag{2-57}$$

Notice for the minimum energy case,

$$e_{M.E.} = \tan \gamma_{o_{M.E.}}$$

Energy Ratio Concept. The energy ratio (Ref. 6: 134) is a measure of the energy available for the trajectory, and is defined as,

$$ER = \frac{r_o V_o}{\mu}$$

If the range, or ϕ_o, and the energy ratio are specified, the launch angle needed to achieve this range is determined. The equation is

$$\tan \gamma_o = \frac{1}{2}\left[\frac{ER}{\tan \phi_o} \pm \sqrt{\left(\frac{ER}{\tan \phi_o}\right)^2 - 4(1 - ER)}\right] \tag{2-58}$$

This equation is used to specify the high and low angle trajectories which are investigated in the latter portion of this report.

Rocket Equations of Motion

Velocity Equations. The motion of a rocket can best be described by considering the case of a rocket in field-free space (no external forces). Let us assume that we have a rocket in this environment, traveling horizontally with velocity, v, and mass, M, at time, t. (Fig. 2-5).

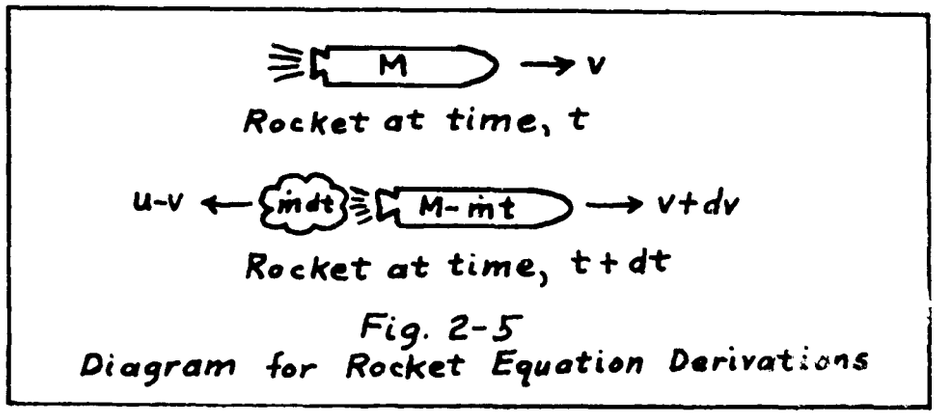

Fig. 2-5
Diagram for Rocket Equation Derivations

Let t_b = the total burning time of the rocket

M_o = the mass of the rocket before ignition

M_f = the mass of the rocket at burnout

v_o = the velocity of the rocket when $t = 0$

v_b = the velocity of the rocket when $t = t_b$

s_o = the displacement (position) of the rocket at $t = 0$

s_b = the displacement of the rocket at $t = t_b$

$\dot{m}$ = mass rate of flow (burning rate) of fuel, a constant

u = the exhaust gas velocity relative to the rocket

Since no external forces are acting on the rocket of Fig. 2-5, the momentum must be a constant for the rocket system (including exhaust

gases). Then the momentum at time, t, and at time, t + dt, must be equal.

$$Mv = (M - \dot{m}\,dt)(v + dv) - (u - v)(\dot{m}\,dt) \tag{2-59}$$

$$Mv = Mv - \dot{m}v\,dt + M\,dv - \dot{m}\,dv\,dt - \dot{m}u\,dt + \dot{m}v\,dt \tag{2-60}$$

Neglecting the products of infinitesimals, Eq (2-60) can be written as

$$M\,dv = \dot{m}u\,dt \tag{2-61}$$

but

$$\dot{m} = -\frac{dM}{dt} \tag{2-62}$$

Then

$$M\,dv = -u\frac{dM}{dt}\,dt \tag{2-63}$$

or

$$dv = -u\frac{dM}{M} \tag{2-64}$$

Equation (2-64) can be integrated for the general situation from t = 0 to t = t.

$$\int_{v_o}^{v} dv = \int_{M_o}^{M} -u\frac{dM}{M} \tag{2-65}$$

$$v - v_o = -u \ln \frac{M}{M_o} \tag{2-66}$$

or

$$v = v_o + u \ln \frac{M_o}{M} \tag{2-67}$$

For the case where the burning of the fuel is complete,

$$v_b = v_o + u \ln \frac{M_o}{M_f} \tag{2-68}$$

Now let us define the ratio of the initial to final mass as the effective mass ratio of the rocket, D.

$$D = \frac{M_o}{M_f} \tag{2-69}$$

Then Eq (2-68) can be written as

$$V_b = V_o + u \ln D \tag{2-70}$$

Distance Equations. To determine the distance traveled during the burning of a rocket, Eq (2-67) can be integrated from t = 0 to t = t_b where v = ds/dt.

$$\int_{s_o}^{s} ds = \int_{o}^{t} \left[V_o + u \ln \frac{M_o}{M} \right] dt \tag{2-71}$$

$$s - s_o = V_o t + \int_{o}^{t} u \ln \frac{M_o}{M} \, dt \tag{2-72}$$

But
$$M = M_o - \dot{m} t \tag{2-73}$$

Then combining Eqs (2-72) and (2-73),

$$s = s_o + V_o t + u \int_{o}^{t} \ln \frac{M_o}{M_o - \dot{m} t} \, dt \tag{2-74}$$

Hence
$$s = s_o + V_o t + ut - \frac{uM}{\dot{m}} \ln \frac{M_o}{M} \tag{2-75}$$

For the burnout conditions, Eq (2-75) becomes

$$s_b = s_o + V_o t_b + s' \tag{2-76}$$

where
$$s' = u t_b - \frac{u M_f}{\dot{m}} \ln \frac{M_o}{M_f} \tag{2-77}$$

or
$$s' = u \left[t_b - \frac{M_f}{\dot{m}} \ln D \right] \tag{2-78}$$

Equations (2-70, 76, and 78) are the basic rocket equations which are used in the analysis of the problem. They can be modified as necessary to account for the effects of gravity and atmospheric drag.

Specific Impulse of Rocket Fuels. The velocity and distance equations of rocket motion are both functions of the velocity of the rocket exhaust gases. Usually, the exhaust velocity, which is a characteristic of a given fuel, is not stated explicitly. Instead, the specific impulse of the fuel is used to define the exhaust velocity by the equation (Ref. 10 : 20)

$$u = I_s g_c \tag{2-79}$$

where I_s, the specific impulse, is the pounds of thrust per pound of mass flow per second, and g_c is a proportionality constant numerically equal to the sea-level acceleration of gravity.

The derivations which follow in Chapters III and IV have the exhaust velocity, u, as a variable. However, the computer programs used to solve the equations have I_s, rather than u, as an input variable.

III. Determination of Intercept Trajectory

Theoretical Intercept Geometry

As a first step in determining the interceptor trajectory let us compare two possible cases as shown in Figs. 3-1 and 3-2. In the "apogee" intercept, the point of intersection between the warhead and intercept trajectories occurs when the interceptor is at the apogee of its trajectory. On the other hand, for the "tangent" intercept, the intersection is at the common tangent to both the warhead and intercept trajectories, and this point is "down range" from the interceptor's apogee. By comparing Figs. 3-1 and 3-2 it is seen that for the same intercept point and interceptor launch site, the tangent intercept will result in a smaller vector velocity difference between the warhead and the interceptor. This is an important fact, since the weight of the velocity-match rocket increases exponentially with the magnitude of this velocity difference. Therefore this investigation is limited to the tangent intercept technique.

The most direct approach would be to fix the desired intercept point and interceptor launch site, and then determine the intercept trajectory parameters. However, this leads to several transcendental equations which can not be solved explicitly for the desired quantities. As an alternative, the following indirect approach is considered. From Chapter II, the equation of the warhead trajectory, over a spherical, non-rotating earth is

$$r_w = \frac{h_w^2}{\mu(1 - e_w \cos \phi_w)} \tag{3-1}$$

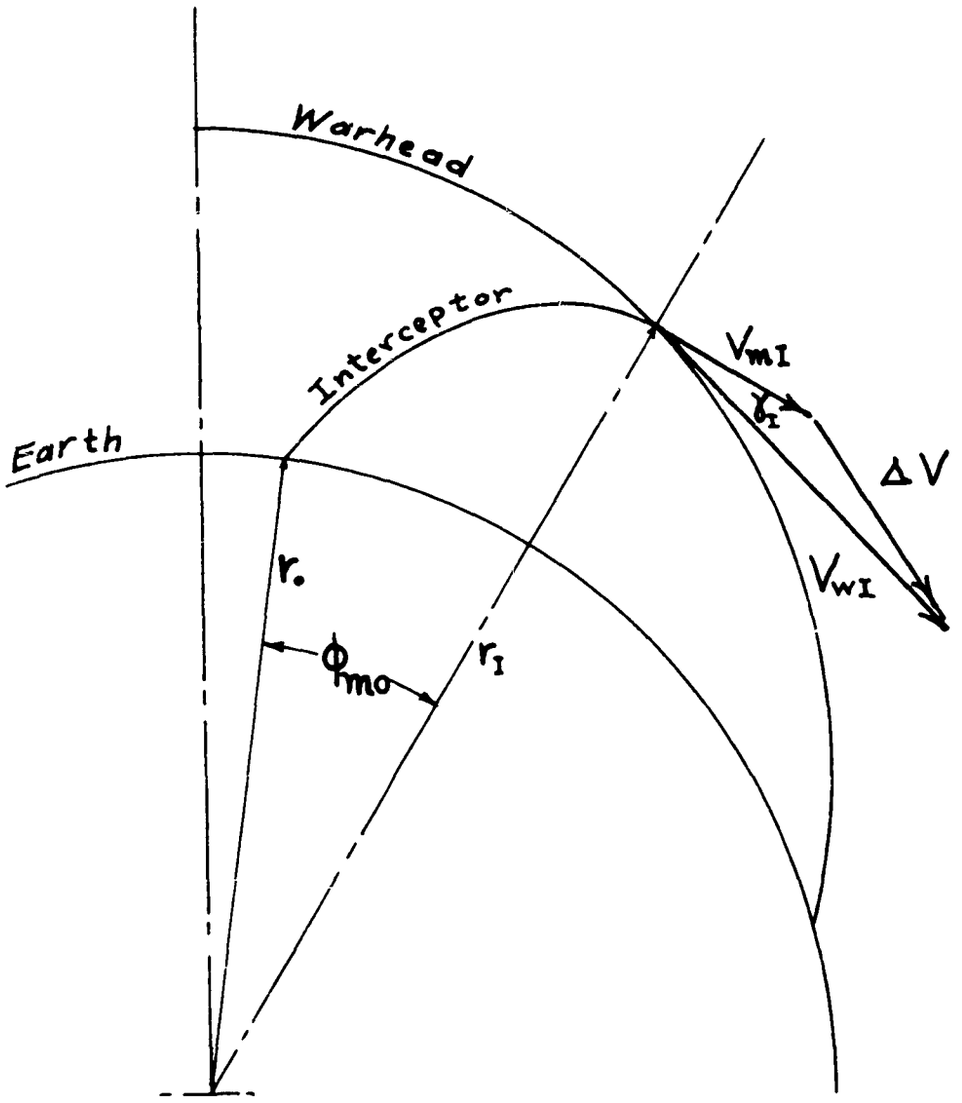

Fig. 3-1
"Apogee Intercept" Intercept Point at Apogee of Interceptor Trajectory

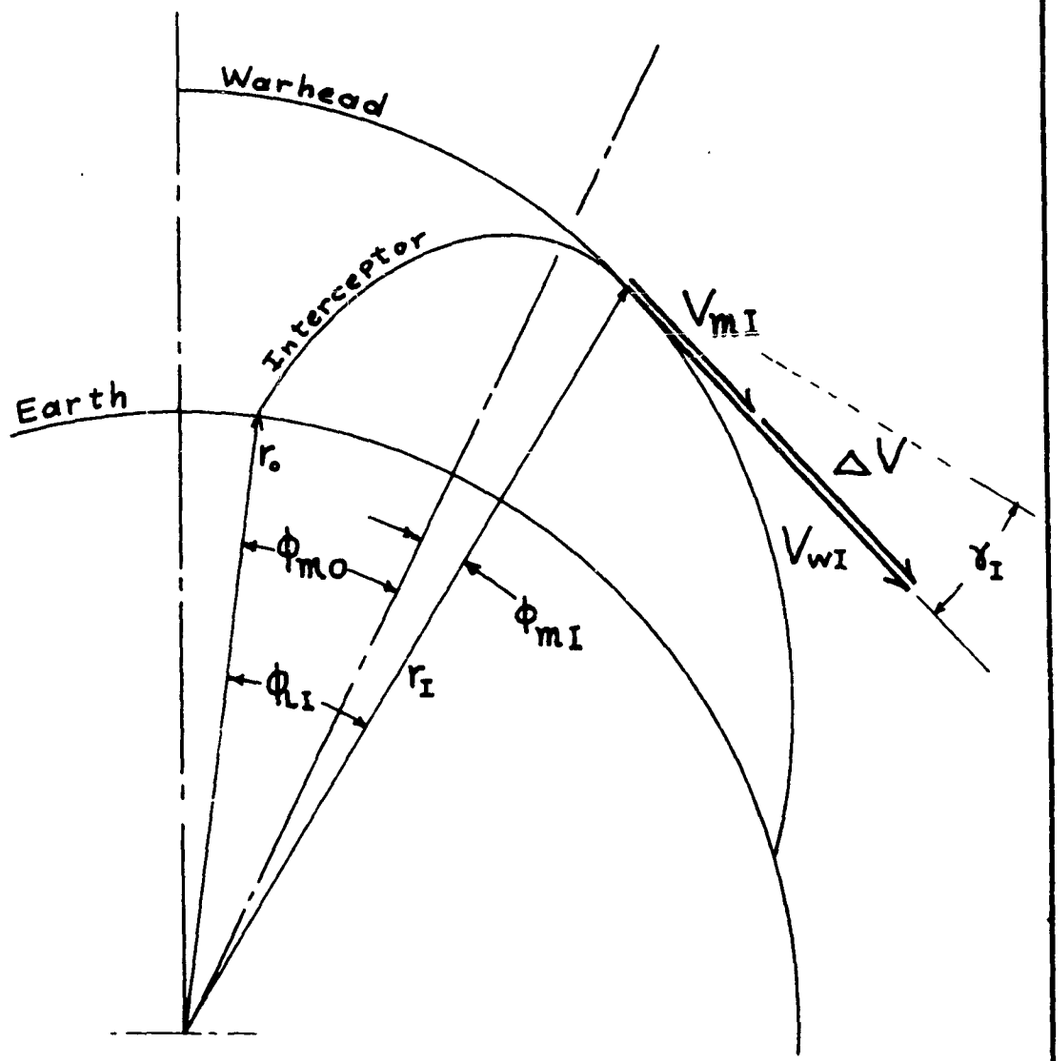

Fig. 3-2
"Tangent Intercept" Interceptor and Warhead Trajectories Tangent at Intercept Point

where r_w is the distance from the center of the earth

h_w is the angular momentum per unit mass

e_w is the eccentricity of the ellipse

ϕ_w is the angle measured from the warhead polar axis

Similarly, the equation of the interceptor trajectory, coplanar with the warhead trajectory, is

$$r_m = \frac{h_m^2}{\mu(1 - e_m \cos \phi_m)} \tag{3-2}$$

Now at the point of intercept, the radii of both the intercept and warhead trajectories must be equal, or

$$r_{mI} = r_{wI} = r_I \tag{3-3}$$

where r_I is defined as the distance from the center of the earth to the intercept point. Furthermore, if we specify that the two trajectories are tangent at the intercept point, the path angles must be the same for both, or

$$\gamma_{mI} = \gamma_{wI} = \gamma_I \tag{3-4}$$

where γ_I is the angle measured from the local horizontal to the tangent to the trajectories (positive counterclockwise). This angle, γ_I, can be found by using Eq (2-31). Therefore

$$\tan \gamma_I = \frac{-e_w \sin \phi_{wI}}{1 - e_w \cos \phi_{wI}} \tag{3-5}$$

or

$$\tan \gamma_I = \frac{-e_m \sin \phi_{mI}}{1 - e_m \cos \phi_{mI}} \tag{3-5a}$$

Rewriting Eq (3-2) for the intercept point, and by using Eq (3-3) we get

$$r_I = \frac{h_m^2}{\mu(1 - e_m \cos \phi_{mI})} \tag{3-6}$$

We can also write Eq (3-2) for the initial conditions, or launch site on the earth's surface, for which case

$$r_o = \frac{h_m^2}{\mu(1 - e_m \cos \phi_{mo})} \tag{3-7}$$

where ϕ_{mo} is the semi-range angle of the intercept trajectory.

For a fixed warhead trajectory and intercept point we know e_w, h_w ϕ_{wI}, r_I and γ_I. Equations (3-5a, 6 and 7) contain four variables, e_m h_m, ϕ_{mI} and ϕ_{mo}. Therefore, if we fix ϕ_{mo}, we have three equations and three unknowns and the theoretical intercept trajectory parameters are completely determined. To find these parameters, we first divide Eq (3-6) by Eq (3-7) to give

$$\frac{r_I}{r_o} = \frac{1 - e_m \cos \phi_{mo}}{1 - e_m \cos \phi_{mI}} \tag{3-8}$$

Now solving Eq (3-5a) for e_m, we get

$$e_m = \frac{-\tan \gamma_I}{\sin \phi_{mI} - \tan \gamma_I \cos \phi_{mI}} \tag{3-9}$$

Substituting Eq (3-9) into Eq (3-8) and simplifying,

$$\frac{r_I}{r_o} = \frac{\sin \phi_{mI} - \tan \gamma_I \cos \phi_{mI} + \tan \phi_{mI} \cos \phi_{mo}}{\sin \phi_{mI}} \tag{3-10}$$

By rearranging Eq (3-10) we can get

$$\frac{\sin \phi_{mI}}{\tan \gamma_I}\left(\frac{r_I}{r_o} - 1\right) + \cos \phi_{mI} = \cos \phi_{mo} \tag{3-11}$$

Next, let us define a new quantity which is a constant for the intercept point. Let

$$\frac{1}{\tan \gamma_I}\left(\frac{r_I}{r_o} - 1\right) \equiv S \tag{3-12}$$

Substitute Eq (3-12) into Eq (3-11) and rearrange.

$$\cos \phi_{mI} + \zeta \sin \phi_{mI} = \cos \phi_{mo} \tag{3-13}$$

Equation (3-13) contains only one unknown, ϕ_{mI}, and this can be solved as follows: Construct a right triangle as shown in Fig. 3-3. By referring to Fig. 3-3 it can be seen that

$$1 = \sqrt{1+\zeta^2} \sin A \tag{3-14}$$

$$\zeta = \sqrt{1+\zeta^2} \cos A \tag{3-15}$$

$$A = \tan^{-1}\left(\frac{1}{\zeta}\right) \tag{3-16}$$

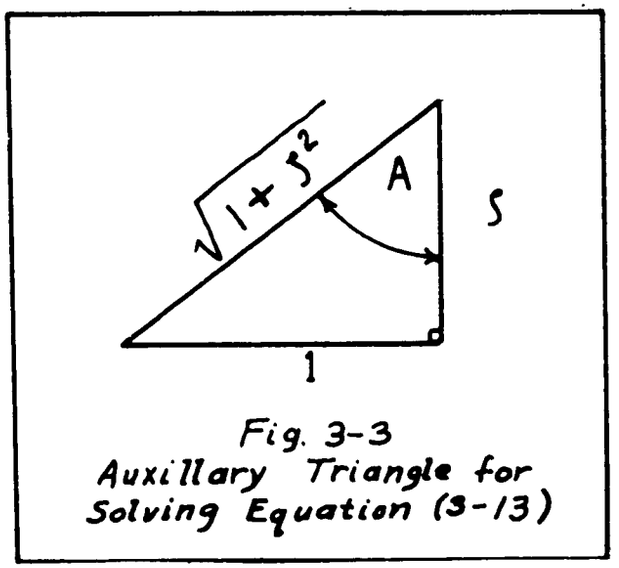

Fig. 3-3
Auxillary Triangle for
Solving Equation (3-13)

If we substitute Eqs (3-14) and (3-15) into Eq (3-13) the result is

$$\sqrt{1+\zeta^2} \sin A \cos \phi_{mI} + \sqrt{1+\zeta^2} \cos A \sin \phi_{mI} = \cos \phi_{mo} \tag{3-17}$$

which can be rewritten as

$$\sin(A + \phi_{mI}) = \frac{\cos \phi_{mo}}{\sqrt{1+\zeta^2}} \tag{3-18}$$

By solving Eq (3-18) for ϕ_{mI}, and using Eq (3-16), the final result is

$$\phi_{mI} = \sin^{-1}\left(\frac{\cos\phi_{mo}}{\sqrt{1+s^2}}\right) - \tan^{-1}\left(\frac{1}{s}\right) \tag{3-19}$$

With ϕ_{mI} now determined, we can solve for the intercept trajectory parameters e_m, and h_m, by using Eqs (3-9) and (3-7). We have also indirectly determined the theoretical launch site of the interceptor system since the angle from launch site to intercept point, ϕ_{LI}, is just (See Fig. 3-2)

$$\phi_{LI} = \phi_{mo} + \phi_{mI} \tag{3-20}$$

Velocity Difference Between Warhead and Interceptor

With the theoretical intercept trajectory now completely defined, we wish to find the difference in velocities between the warhead and interceptor, so that we may determine how large a rocket is required to perform the velocity-match, i.e. reduce the velocity difference to zero. Ignition of the velocity-match rocket causes the actual trajectory to depart from the theoretical trajectory, and an approximate method of correcting for this departure is discussed later. By referring to Eq (2-33) it is seen that the angular momentum per unit mass of the warhead or the interceptor can be written as

$$h_w = r_I V_{wI} \cos\gamma_I \tag{3-21}$$

and

$$h_m = r_I V_{mI} \cos\gamma_I \tag{3-22}$$

If we now divide Eq (3-21) by Eq (3-22) we get

$$\frac{h_m}{h_w} = \frac{V_{mI}}{V_{wI}} \tag{3-23}$$

which can be solved for v_{mI} to give

$$V_{mI} = V_{wI} \frac{h_m}{h_w} \tag{3-24}$$

The velocity difference, Δ v is given by

$$\Delta \bar{V} = \bar{V}_{wI} - V_{mI} \tag{3-25}$$

By making use of the fact that v_{mI} and v_{wI} are co-linear, and substituting Eq (3-24) into Eq (3-25) we find the magnitude of the velocity difference to be

$$\Delta V = V_{wI} \left(1 - \frac{h_m}{h_w}\right) \tag{3-26}$$

It is interesting to note that if the angular momentum of the interceptor approaches that of the warhead, Δ v approaches zero, but with the intercept conditions we have imposed, this occurs only when the two trajectories are identical ... a highly impractical case.

Correction to Theoretical Intercept Trajectory.

In order to correct the theoretical intercept trajectory for the effect of the velocity-match rocket, we must make use of the rocket equations of motion which were developed in Chapter II. Equation (2-70) can be written in vector notation as

$$\bar{V}_b = \bar{V}_o + \bar{u} \ln D \tag{3-27}$$

Equation (2-76) can also be written in vector notation as

$$\bar{s}_b = \bar{s}_o + \bar{V}_o t_b + \bar{s}' \tag{3-28}$$

where $\bar{s}'$ is now defined by

$$\bar{s}' = \bar{u}\left(t_b - \frac{M_f}{\dot{m}} \ln D\right) \tag{3-29}$$

If we let our coordinate system coincide with the point where the velocity-match rocket is ignited, then $\bar{s}_o = 0$ and Eq (3-28) becomes

$$\bar{s}_b = \bar{v}_o t_b + \bar{s}' \tag{3-30}$$

Now if we re-write Eqs (3-27) and (3-30) and assume that the motion takes place in a gravitational field, where $\bar{g}$ is constant in magnitude and direction, these equations are modified to

$$\bar{v}_b = \bar{v}_o + \bar{u} \ln D \tag{3-31}$$

and

$$\bar{s}_b = \bar{v}_o t_b + \bar{s}' + \tfrac{1}{2} \bar{g} t_b^2 \tag{3-32}$$

Let us now refer to Fig. 3-4 and assume that our interceptor rocket is in free-flight on the theoretical interceptor trajectory. If we did not fire the velocity-match rocket, we would coast to the intercept point, IP, and arrive there with velocity equal to $\bar{v}_{mI}$. But we want to match the warhead's velocity, $\bar{v}_{wI}$, at the intercept point. Therefore the velocity-match rocket must be ignited some time before we get to point IP. Let us assume that the velocity-match rocket has a burning time equal to the free-flight time from point A to IP. Then, when the rocket arrives at point A with velocity $\bar{v}_o$, the velocity-match rocket is fired so that the exhaust velocity vector, $\bar{u}$, is parallel to the trajectory-tangent at point IP. If the effective mass ratio, D, of the velocity-match rocket is of the right magnitude, then the burnout velocity, $\bar{v}_b$, will be approximately equal to $\bar{v}_{wI}$, as seen in Fig. 3-4. However, Fig. 3-4 also shows that the position at burnout is point B rather than that desired (IP).

Suppose we correct this discrepancy by the method shown in

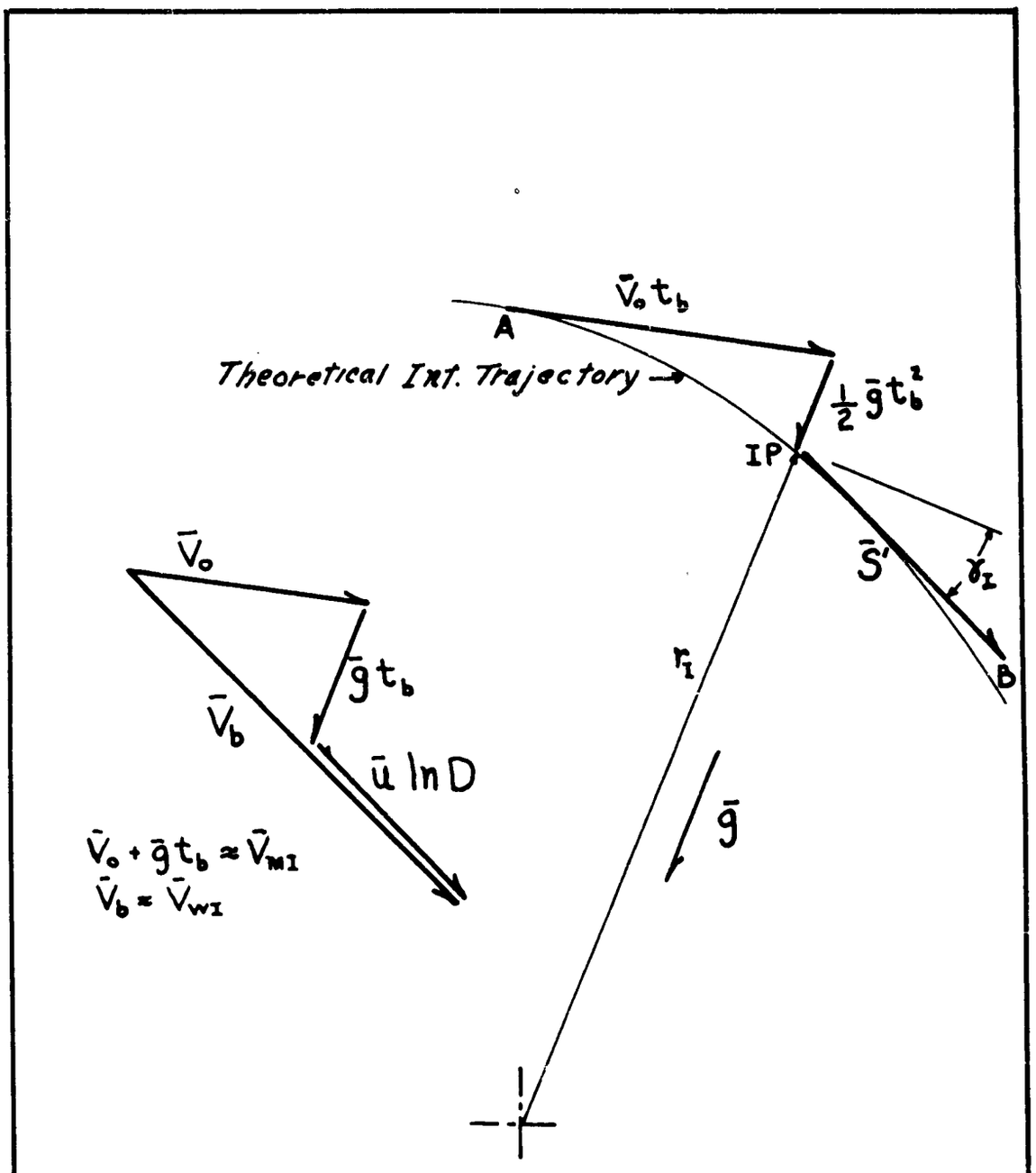

Fig. 3-4

Vector Diagram of Velocities and Displacement for Theoretical Intercept Trajectory

Fig. 3-5. First we extend the tangent line "up-range" to an aiming point, AP, so that AP-IP is equal to IP-B. Next we adjust the trajectory, so that a free-flight interceptor will arrive tangent to point AP with the same velocity, $\bar{v}_{mI}$, that existed at point IP of the theoretical trajectory. Now, if the velocity-match rocket is fired at some point A', where A' is chosen so that the free-flight time from A' to AP is equal to t_b, the burnout position will be at IP. The actual boosted trajectory will be along the dotted line in Fig. 3-5.

If we assume that the burning time is short, we can say that

$$|\bar{s}'| << |\bar{r}_I| \tag{3-33}$$

Then the change in direction and magnitude of gravity between points A' and IP will be extremely small, and by referring to the velocity vector diagram in Fig. 3-5 we can say that

$$\bar{v}_o + \bar{g} t_b \approx \bar{v}_{mI} \tag{3-34}$$

$$\bar{u} \ln D = \bar{v}_b - \bar{g} t_b - \bar{v}_o \tag{3-35}$$

or

$$\bar{u} \ln D = \bar{v}_b - \bar{v}_{mI} \tag{3-36}$$

However, we want $\bar{v}_b$ to be equal to $\bar{v}_{wI}$, and since $\bar{u}$, $\bar{v}_{wI}$ and $\bar{v}_{mI}$ are all parallel we can write Eq (3-36) as

$$u \ln D = v_{wI} - v_{mI} = \Delta v \tag{3-37}$$

where Δv is given by Eq (3-26). By solving Eq (3-37) for D we find that

$$D = \epsilon^{\Delta v/u} \tag{3-38}$$

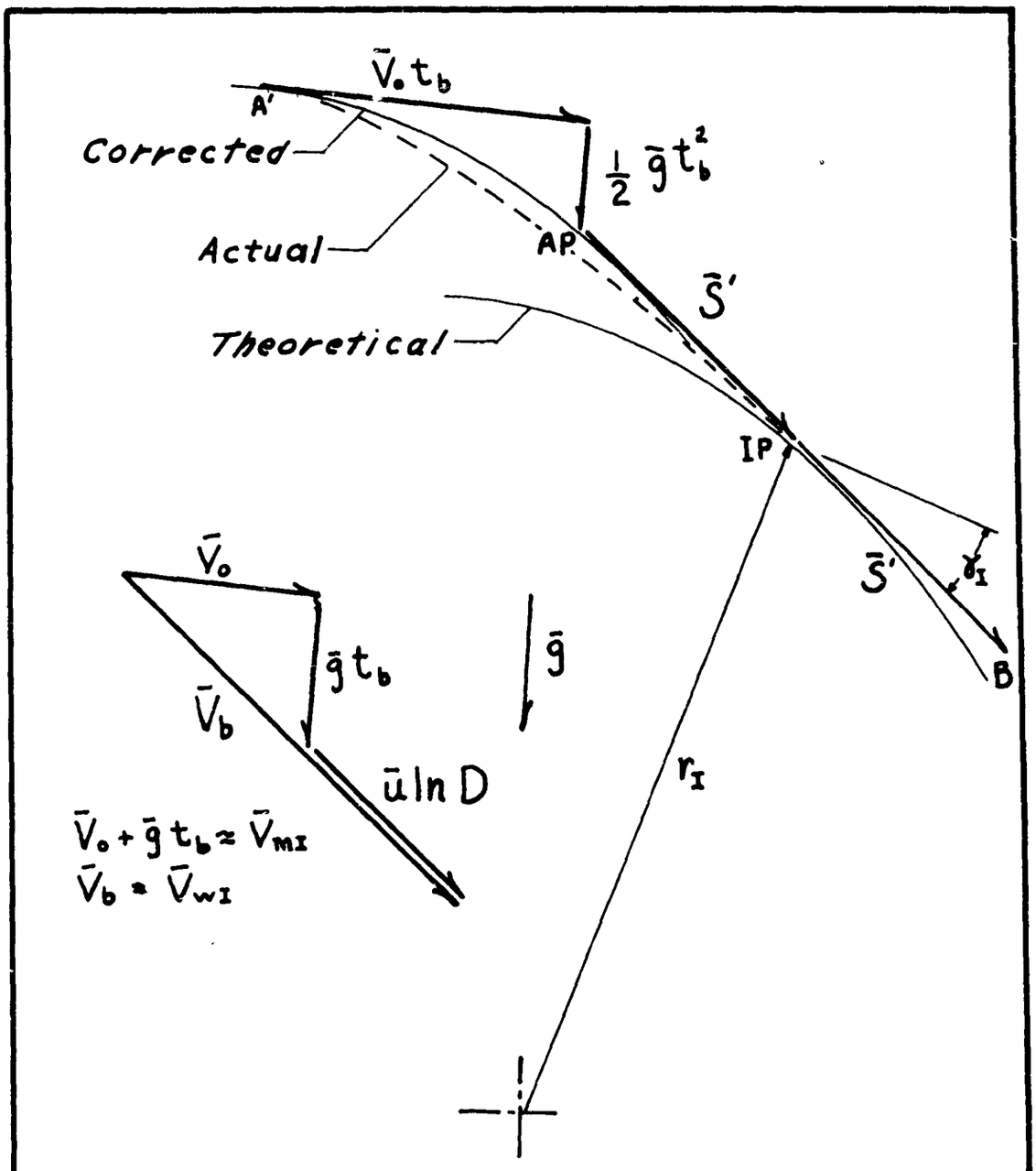

Fig. 3-5

Vector Diagram of Velocities and Displacement for Corrected Intercept Trajectory

In Chapter IV it will be shown that if we specify the thrust to initial weight ratio, β, of a rocket, we can find s' such that

$$s' = f(u, \beta, D)$$

With D and s' known we can calculate the corrected intercept trajectory parameters.

By referring to Fig. 3-6 it is seen that

$$\measuredangle F = 90° - \gamma_I \tag{3-39}$$

Note that γ_I is <u>negative</u> for intercept points down-range from the warhead apogee. We can also show that

$$\tan \delta = \frac{s' \sin F}{r_I - s' \cos F} \tag{3-40}$$

or using Eq (3-39)

$$\tan \delta = \frac{s' \cos \gamma_I}{r_I - s' \sin \gamma_I} \tag{3-41}$$

Then with δ known we can show that the flight-path angle at point AP is

$$\gamma_{Ia} = \gamma_I - \delta \tag{3-42}$$

where δ is always a positive angle and the correct signs must be used for γ_{Ia} and γ_I. By using the law of sines we find that

$$r_{Ia} = \frac{s' \sin F}{\sin \delta} \tag{3-43}$$

or

$$r_{Ia} = \frac{s' \cos \gamma_I}{\sin \delta} \tag{3-44}$$

With γ_{Ia}, r_{Ia}, and v_{mI} known at the point AP we can procede to find the trajectory parameters.

Re-writing Eq (3-22) for the corrected trajectory at the point

AP, we get

$$h_{ma} = r_{Ia}\, V_{mI} \cos \gamma_{Ia} \tag{3-45}$$

where h_{ma} is the corrected angular momentum per unit mass. The total energy per unit mass of the trajectory can be found from Eq (2-48) applied to the aiming point, in which case

$$E_{ma} = \frac{1}{2} V_{mI}^2 - \frac{\mu}{r_{Ia}} \tag{3-46}$$

With the energy known we can find the eccentricity by using Eq (2-26).

$$e_{ma} = \sqrt{1 + \frac{2 E_{ma} h_{ma}^2}{\mu^2}} \tag{3-47}$$

The equation of the corrected intercept trajectory is therefore

$$r_{ma} = \frac{h_{ma}^2}{\mu(1 - e_{ma} \cos \phi_{ma})} \tag{3-48}$$

By applying Eq (3-48) at the earth's surface and at the aiming point, we can find the corrected semi-range angle, ϕ_{moa}, and the angle from the polar axis to the aiming point, ϕ_{mIa} (See Fig. 3-6). These equations are

$$\cos \phi_{moa} = \frac{1}{e_{ma}} \left(1 - \frac{h_{ma}^2}{\mu r_a}\right) \tag{3-49}$$

and

$$\cos \phi_{mIa} = \frac{1}{e_{ma}} \left(1 - \frac{h_{ma}^2}{\mu r_{Ia}}\right) \tag{3-50}$$

The angle from the corrected interceptor launch site to the actual intercept point is

$$\phi_{LIA} = \phi_{moa} + \phi_{mIa} + \delta \tag{3-51}$$

where δ is given by Eq (3-41).

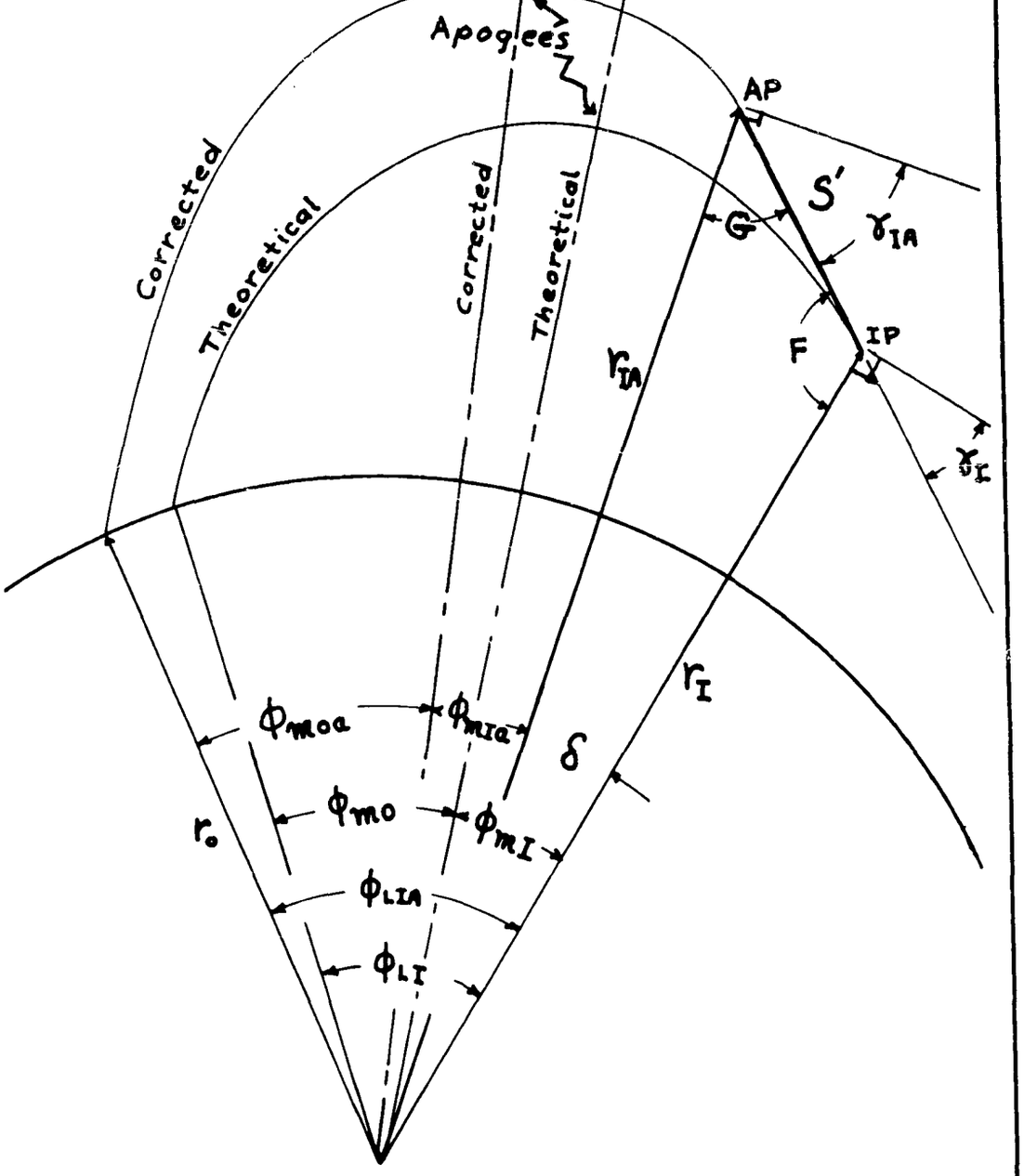

Fig. 3-6

Geometry for Determining Correction to Theoretical Intercept Trajectory

Summary

In this chapter, first we derived the theoretical intercept trajectory equations by fixing the warhead trajectory and the intercept point, and imposing the condition that at the intercept point the warhead and intercept trajectories had the same radius, r_I, and the same path-angle, γ_I. By assuming a short burning time for the velocity-match rocket, and that $\bar{g}$ was constant in the vicinity of the intercept point, we then corrected the theoretical intercept trajectory for the effect of the rocket dynamics, and obtained the parameters for the corrected intercept trajectory. We also determined the effective mass ratio required for the velocity-match rocket. With this trajectory completely determined, and the effective mass ratio of the velocity-match rocket known, we can now consider the boost-phase of the intercept.

IV. Boost-Phase Analysis

In Chapter III it was shown that if the warhead trajectory, intercept point, and semi-range angle for the interceptor were fixed, a unique, free-flight trajectory is determined. We also found the required mass ratio for the velocity-match rocket. In effect, we are now at the point where we have a "payload", and a desired trajectory, and must find the booster rocket requirements needed to get this payload onto this trajectory.

There are an infinite number of points where we can enter this intercept trajectory, and for each point the required burnout velocity and direction is different. This point must also be at some altitude above the earth because of the time required to accelerate to the final desired boost-phase burnout velocity. If we also consider the fact that most rocket launchings consist of a vertical flight segment, a segment at constant angle of attack, a segment at zero lift, and a constant attitude segment, it can be seen that there are many possible flight paths from the launch site to the burnout point. The problem is further complicated by atmospheric drag, variable gravity, and the variation of rocket thrust with altitude. Thus there does not appear to be a neat, closed-form solution to the problem, although many approximate methods have been devised (Ref 12).

In WADC TR 57-724 (Ref 2) a method for the preliminary design and optimization of a long-range, ballistic missile is outlined. Basically, it is a trial and error method, and while it

is well suited to the design of one particular missile, it does not lend itself to this investigation, where we have many trajectories to consider.

Approximations

To proceed with the problem, let us make some assumptions which enable us to develop a method for approximating the required thrusts and weights, and the available warning time for the interceptor system. First we assume that the boost-phase is a small portion of the intercept trajectory, allowing us to consider gravity as a constant vector. This enables us to choose an inertial, rectangular coordinate system on the earth's surface near the launch site, as in Fig. 4-1. Next we neglect the vertical, tip-over, and constant angle of attack segments of the boost-phase, and assume that the thrust vectors of each stage are applied at a constant direction relative to the inertial coordinate system. Although this is not practical for an actual launching, this is a reasonable approximation since the vertical and tip-over segments are usually a small portion of the boost-phase. Then we assume that the aerodynamic drag is small compared to the booster rocket thrust, and can be neglected. Finally, we neglect the variation of thrusts due to altitude, and assume that the specific impulse and structural factor are the same for each stage.

The K-Stage Boost Rocket

With these assumptions in mind, let us develop some equations for the k-stage rocket as shown in Fig. 4-2. Some useful relation-

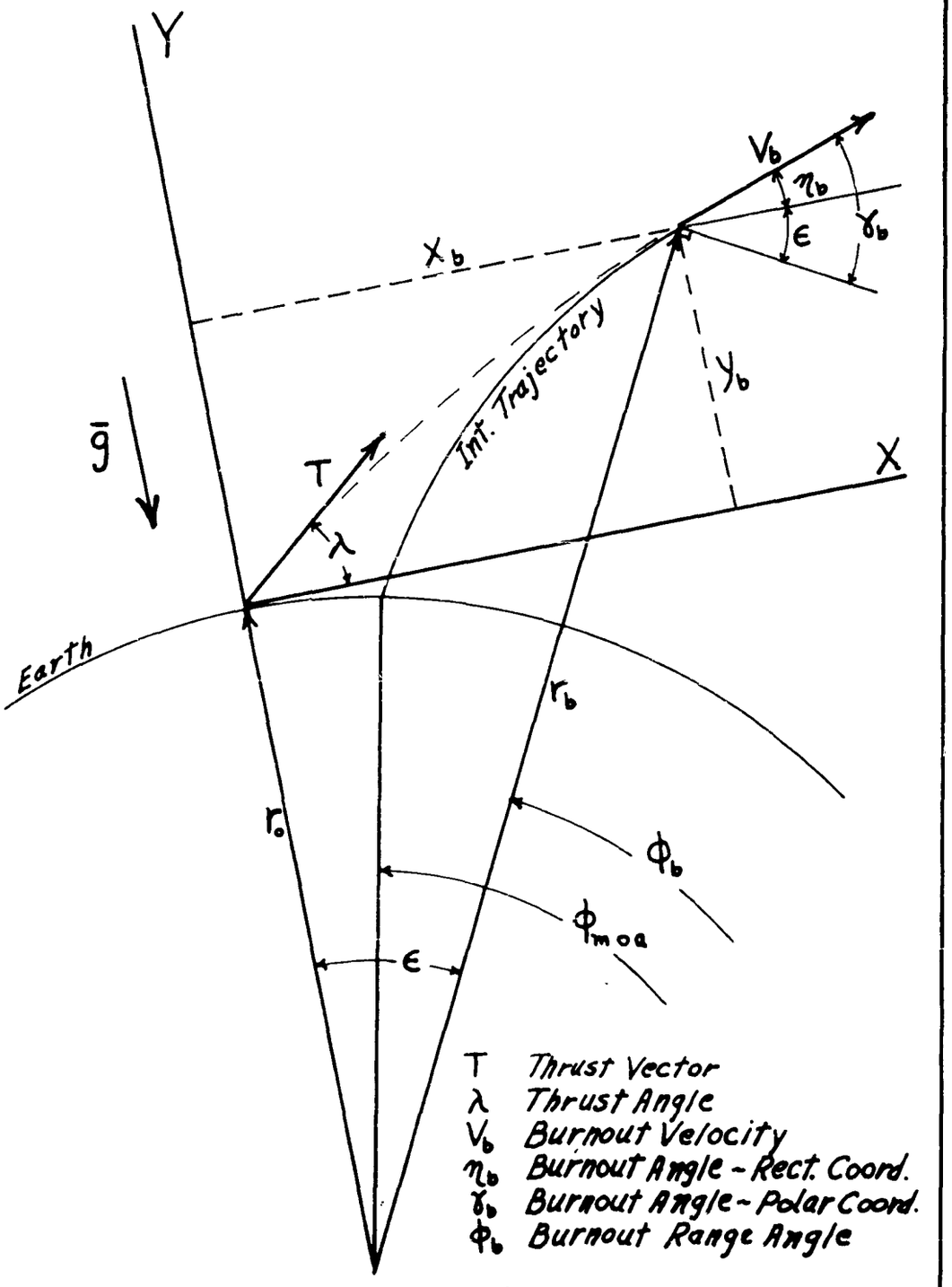

Fig. 4-1
Coordinate System For Boost-Phase Approximation

ships for this rocket are listed as follows (Ref 3). The symbols used are shown in Fig. 4-2.

Structural factor:

$$n_j = \frac{\text{initial mass of the } j^{th} \text{ stage}}{\text{burnout mass of the } j^{th} \text{ stage}}$$

or

$$n_j = \frac{m_j}{m_{j_f}} \tag{4-1}$$

effective mass ratio of the j^{th} sub-rocket:

$$D_j = \frac{M_j}{M_{j_f}} = \frac{m_j + m_{j+1} + \cdots + m_K + m_p'}{\frac{m_j}{n_j} + m_{j+1} + m_{j+2} + \cdots + m_K + m_p'} = \frac{M_j}{M_j - \left(\frac{n_j - 1}{n_j}\right) m_j} \tag{4-2}$$

where M_{j_f} is the burnout mass of the j^{th} sub-rocket.

stage mass ratio:

$$\psi_j = \frac{m_j}{m_p'} \tag{4-3}$$

overall mass ratio:

$$\psi_o = \frac{M_o}{m_p'} \tag{4-4a}$$

or

$$\psi_o = 1 + \psi_1 + \psi_2 + \cdots + \psi_K \tag{4-4b}$$

Optimization. It can be shown that the optimum arrangement of sub-rocket masses, which results in a maximum final burnout velocity (vacuum conditions, constant $\bar{g}$), for a rocket of constant overall mass, with the same exhaust velocity of each stage, is given by the equation (Ref 3)

$$\frac{D_1}{n_1} = \frac{D_2}{n_2} = \cdots = \frac{D_K}{n_K} \tag{4-5}$$

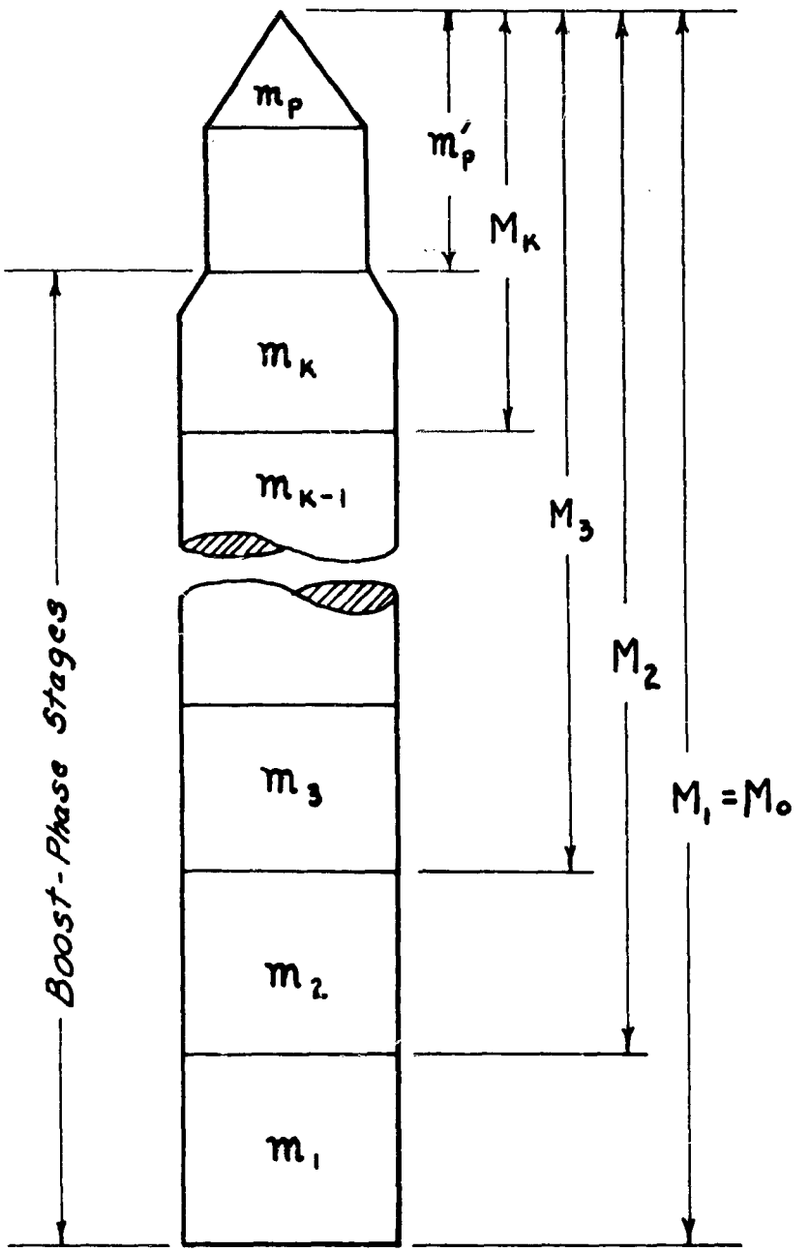

m_p *Interceptor Vehicle*
m'_p *Velocity-Match Rocket*
m_j j^{th} *Stage*
M_j j^{th} *Sub-Rocket*

Fig. 4-2
K-Stage Boost-Phase Rocket

If the structural factors of each stage are the same then the equation for optimization becomes

$$D_1 = D_2 = \cdots = D_K \tag{4-6}$$

The overall mass ratio for optimum staging, with the stage structural factors and exhaust velocities equal, is

$$\Psi_o = \left[\frac{(n-1)D}{n-D}\right]^K \tag{4-7}$$

The sub-rocket mass ratios are then

$$\Psi_j = (\Psi_o - \Psi_1 - \Psi_2 - \cdots - \Psi_{j-1})\left(1 - \frac{1}{\sqrt[K]{\Psi_o}}\right) \tag{4-8}$$

Equations of Motion. In Chapter II it was shown that the equations of motion of a one stage rocket in field-free space are

$$\bar{V}_b = \bar{V}_o + \bar{u} \ln D \tag{2-70}$$

$$\bar{S}_b = \bar{S}_o + \bar{V}_o t_b + \bar{S}' \tag{2-76}$$

If we re-write these equations in scalar form for our rectangular coordinate system and consider the effect of gravity they become

$$\dot{x}_b = \dot{x}_o + u \cos\lambda \ln D \tag{4-9}$$

$$\dot{y}_b = \dot{y}_o + u \sin\lambda \ln D - g t_b \tag{4-10}$$

$$x_b = \dot{x}_o t_b + s' \cos\lambda \tag{4-11}$$

$$y_b = \dot{y}_o t_b + s' \sin\lambda - \frac{g t_b^2}{2} \tag{4-12}$$

where $s_o = 0$

$\dot{x}_b$ = the horizontal component of burnout velocity

$\dot{y}_b$ = the vertical component of burnout velocity

$\dot{x}_o$ = the horizontal component of initial velocity

$\dot{y}_o$ = the vertical component of initial velocity

λ = the angle between the thrust vector and the horizon

and
$$s' = u\left[t_b - \frac{M_f}{\dot{m}} \ln D\right] \tag{2-78}$$

Let us now find the components of burnout velocity and displacement for a k-stage rocket, starting from rest.

Velocity:

Stage 1.
$$\dot{x}_{b_1} = u \cos\lambda \ln D_1 \tag{4-13}$$

$$\dot{y}_{b_1} = u \sin\lambda \ln D_1 - g t_{b_1} \tag{4-14}$$

Stage 2
$$\dot{x}_{b_2} = \dot{x}_{b_1} + u \cos\lambda \ln D_2 \tag{4-15}$$

$$\dot{y}_{b_2} = \dot{y}_{b_1} + u \sin\lambda \ln D_2 - g t_{b_2} \tag{4-16}$$

Stage k.
$$\dot{x}_{b_K} = \dot{x}_{b_{K-1}} + u \cos\lambda \ln D_K \tag{4-17}$$

$$\dot{y}_{b_K} = \dot{y}_{b_{K-1}} + u \sin\lambda \ln D_K - g t_{b_K} \tag{4-18}$$

Displacement:

Stage 1.
$$x_{b_1} = s_1' \cos\lambda \tag{4-19}$$

$$y_{b_1} = s_1' \sin\lambda - \frac{g t_{b_1}^2}{2} \tag{4-20}$$

Stage 2.
$$x_{b_2} = x_{b_1} + \dot{x}_{b_1} t_{b_2} + s_2' \cos\lambda \tag{4-21}$$

$$y_{b_2} = y_{b_1} + \dot{y}_{b_1} t_{b_2} + s_2' \sin\lambda - \frac{g t_{b_2}^2}{2} \tag{4-22}$$

Stage k. $$x_{b_K} = x_{b_{K-1}} + \dot{x}_{b_{K-1}} t_{b_K} + s'_K \cos\lambda \tag{4-23}$$

$$y_{b_K} = y_{b_{K-1}} + \dot{y}_{b_{K-1}} t_{b_K} + s'_K \sin\lambda - \frac{g t_{b_K}^2}{2} \tag{4-24}$$

If we now assume that we have a rocket with optimum staging (D's all equal), and further assume that the burning times, t_b, for all stages are equal, we can say that

$$\dot{x}_{b_2} = 2u \cos\lambda \ln D \tag{4-25}$$

$$\dot{y}_{b_2} = 2u \sin\lambda \ln D - 2g t_b \tag{4-26}$$

$$\dot{x}_{b_K} = ku \cos\lambda \ln D \tag{4-27}$$

$$\dot{y}_{b_K} = ku \sin\lambda \ln D - kg t_b \tag{4-28}$$

$$x_{b_2} = 2s' \cos\lambda + \dot{x}_{b_1} t_b \tag{4-29}$$

$$y_{b_2} = 2s' \sin\lambda + \dot{y}_{b_1} t_b - 2\left(\frac{g t_b^2}{2}\right) \tag{4-30}$$

$$x_{b_K} = ks' \cos\lambda + \left(\dot{x}_{b_1} + \dot{x}_{b_2} + \cdots + \dot{x}_{b_{K-1}}\right) t_b \tag{4-31}$$

$$y_{b_K} = ks' \sin\lambda + \left(\dot{y}_{b_1} + \dot{y}_{b_2} + \cdots + \dot{y}_{b_{K-1}}\right) t_b - k\left(\frac{g t_b^2}{2}\right) \tag{4-32}$$

Now from Eqs (4-27) and (4-28)

$$\dot{x}_{b_1} + \dot{x}_{b_2} + \cdots + \dot{x}_{b_{K-1}} = \dot{x}_{b_1}\left[1 + 2 + \cdots + (k-1)\right] \tag{4-33}$$

$$\dot{y}_{b_1} + \dot{y}_{b_2} + \cdots + \dot{y}_{b_{K-1}} = \dot{y}_{b_1}\left[1 + 2 + \cdots + (k-1)\right] \tag{4-34}$$

But

$$\left[1 + 2 + \cdots + (k-1)\right] = \frac{k(k-1)}{2} \tag{4-35}$$

By combining Eqs (4-27, 28, 31, 32, 33, 34 and 35) we get

$$x_{b_K} = k s' \cos\lambda + t_b u \cos\lambda \ln D\left[\frac{k(k-1)}{2}\right] \tag{4-36}$$

$$y_{b_K} = k s' \sin\lambda + t_b\left(u \sin\lambda \ln D - g t_b\right)\left[\frac{k(k-1)}{2}\right] - k\left(\frac{g t_b^2}{2}\right) \tag{4-37}$$

Thrust to Initial Weight Ratio. Equations (4-27, 28, 36 and 37) are put in a more useful form by defining a new quantity, the thrust to initial mass ratio of a sub-rocket (Ref 11). Let

$$\beta_j = \frac{T_j}{M_j} \tag{4-38}$$

where β_j = the thrust to initial mass ratio of the j^{th} sub-rocket

T_j = the thrust of the j^{th} sub-rocket motor.

Note that at sea level, pounds-mass and pounds force are numerically equal, and therefore β can also be used to express the thrust to sea level weight ratio. The thrust of a rocket engine is given by (Ref. 10:17)

$$T_j = \frac{\dot{m}_j u_j}{g_c} \tag{4-39}$$

where $\dot{m}$ is expressed in pounds-mass per second.

By combining Eqs (4-38) and (4-39) we find that

$$\dot{m}_j = \frac{g_c \beta_j M_j}{u_j} \tag{4-40}$$

Now the burning time of the j^{th} stage rocket is

$$t_{b_j} = \frac{\text{mass of fuel in the } j^{th} \text{ stage}}{\text{burning rate of the } j^{th} \text{ stage}}$$

or $$t_{b_j} = \frac{\left(\frac{n_j - 1}{n_j}\right) m_j}{\dot{m}_j} \tag{4-41}$$

By combining Eqs (4-40) and (4-41) we find that

$$t_{b_j} = \frac{u_j}{g_c \beta_j} \frac{\left(\frac{n_j - 1}{n_j}\right) m_j}{M_j} \tag{4-42}$$

But from Eq (4-2) we can show that

$$\frac{\left(\frac{n_j - 1}{n_j}\right) m_j}{M_j} = \frac{D_j - 1}{D_j} \tag{4-43}$$

Therefore, by combining Eqs (4-43) and (4-42), we find that

$$t_{b_j} = \frac{u_j}{g_c \beta_j} \left(\frac{D_j - 1}{D_j}\right) \tag{4-44}$$

We can also show that

$$S_j' = \frac{u_j^2}{g_c \beta_j} \left(\frac{D_j - 1 - \ln D_j}{D_j}\right) \tag{4-45}$$

From Eq (4-44) it is seen that if the exhaust velocities, sub-rocket effective mass ratios, and thrust to initial weight ratios are all the same, then the burning times are also all the same. This is exactly the assumption we made to get Eqs (4-27, 28, 36 and 37). By using Eqs (4-44) and (4-45) it can be shown that the final velocity and displacements at burnout of the k^{th} stage are

$$\dot{x}_{b_k} = k u \ln D \cos \lambda \tag{4-46}$$

$$\dot{y}_{b_k} = k u \ln D \sin \lambda - \frac{k u}{\beta} \left(\frac{D - 1}{D}\right) \tag{4-47}$$

$$x_{b_k} = \frac{k u^2 \cos \lambda}{2 g_c \beta} \left[\frac{2(D - 1 - \ln D) + (k-1)(D-1) \ln D}{D}\right] \tag{4-48}$$

$$y_{b_K} = \frac{ku^2 \sin\lambda}{2g_c\beta}\left[\frac{2(D-1-\ln D)+(k-1)(D-1)\ln D}{D}\right] - \frac{1}{2g_c}\left[\frac{ku(D-1)}{\beta D}\right]^2 \qquad (4\text{-}49)$$

Thus, with the burning time eliminated from the equations by use of the thrust to weight ratio, we can say that

$$\text{Burnout Conditions} = f(k, u, \lambda, \beta, D) \qquad (4\text{-}50)$$

We must now combine these equations with the corrected trajectory equations of Chapter III, so that we may find a method for evaluating a function of the form

$$D = f(k, u, \lambda, \beta, \text{Burnout Conditions}) \qquad (4\text{-}51)$$

Technique for Satisfying Burnout Velocity Requirement

First let us solve the problem by satisfying only the conditions of burnout velocity and direction, and later consider what must be done to also satisfy the condition of burnout position. Assume that we are given a required burnout velocity, v_b, and burnout angle, η_b, as shown in Fig. 4-1, and that we want to find the required sub-rocket mass ratios, D. We assume also that k, and β are given. We can say that

$$\tan\eta_b = \frac{\dot{y}_b}{\dot{x}_b} \qquad (4\text{-}52)$$

where $\dot{x}_b$ and $\dot{y}_b$ are given by Eqns (4-46) and (4-47) with the

k subscripts omitted for simplicity. Then

$$\tan \eta_b = \tan \lambda - \frac{D-1}{\beta D \ln D \cos \lambda} \tag{4-53}$$

If we multiply both sides of Eq (4-53) by the quantity, cos λ cos η_b and rearrange, the resulting equation is

$$\sin \lambda \cos \eta_b - \cos \lambda \sin \eta_b = \frac{(D-1)\cos \eta_b}{\beta D \ln D} \tag{4-54}$$

Then

$$\sin (\lambda - \eta_b) = \frac{(D-1)\cos \eta_b}{\beta D \ln D} \tag{4-54a}$$

Solving Eq (4-54a) for λ,

$$\lambda = \sin^{-1}\left[\frac{(D-1)\cos \eta_b}{\beta D \ln D}\right] + \eta_b \tag{4-55}$$

or

$$\lambda = \eta_b + \sin^{-1} \xi \tag{4-56}$$

where

$$\xi = \frac{(D-1)\cos \eta_b}{\beta D \ln D} \tag{4-57}$$

From Fig. 4-1 the horizontal component of burnout velocity is

$$\dot{x}_b = V_b \cos \eta_b \tag{4-58}$$

By combining Eqs (4-46, 55, 57, and 58) we can show that

$$ku \ln D \cos(\eta_b + \sin^{-1} \xi) - V_b \cos \eta_b = 0 \tag{4-59}$$

or

$$f(D) = 0 \tag{4-60}$$

Now we have an equation with one unknown, D, which would be

difficult, if not impossible, to solve explicitly for D. A numerical solution is found by using Newton's iteration method (Ref 14:495). With this method, we choose a trial value for D, say D_i. For this value we evaluate $f(D_i)$ and $f'(D_i)$ where

$$f'(D) = \frac{d[f(D)]}{dD} \tag{4-61}$$

The equation for f'(D) can be shown to be

$$f'(D) = ku\left[\frac{(D-1)\cos\lambda + \left(\frac{\xi}{\sqrt{1-\xi^2}}\right)(D-1-\ln D)\sin\lambda}{D(D-1)}\right] \tag{4-61a}$$

Then our new trial value for D is given by the formula

$$D_{i+1} = D_i - \frac{f(D_i)}{f'(D_i)} \tag{4-62}$$

This process converges quite rapidly in this particular case, and is repeated until the required degree of accuracy is attained. Thus we can find D, the sub-rocket effective mass ratio required to achieve a given burnout velocity and direction.

Technique for Satisfying Burnout Position Requirement

In order to simultaneously satisfy the condition of burnout altitude, y_b, or radius, r_b, we must resort to a second trial and error process. To do this, first choose a trial value for burnout range angle, ϕ_b, (See Fig. 4-3a). With the chosen ϕ_b and the corrected interceptor trajectory parameters, we use the general trajectory equations of Chapter II to determine r_{b_1}, v_{b_1}, and γ_{b_1}. As a first approximation let us assume that the launch site in the rectangular coordinate system coincides with the theoretical launch site in the polar coordinate system. Then we can say that

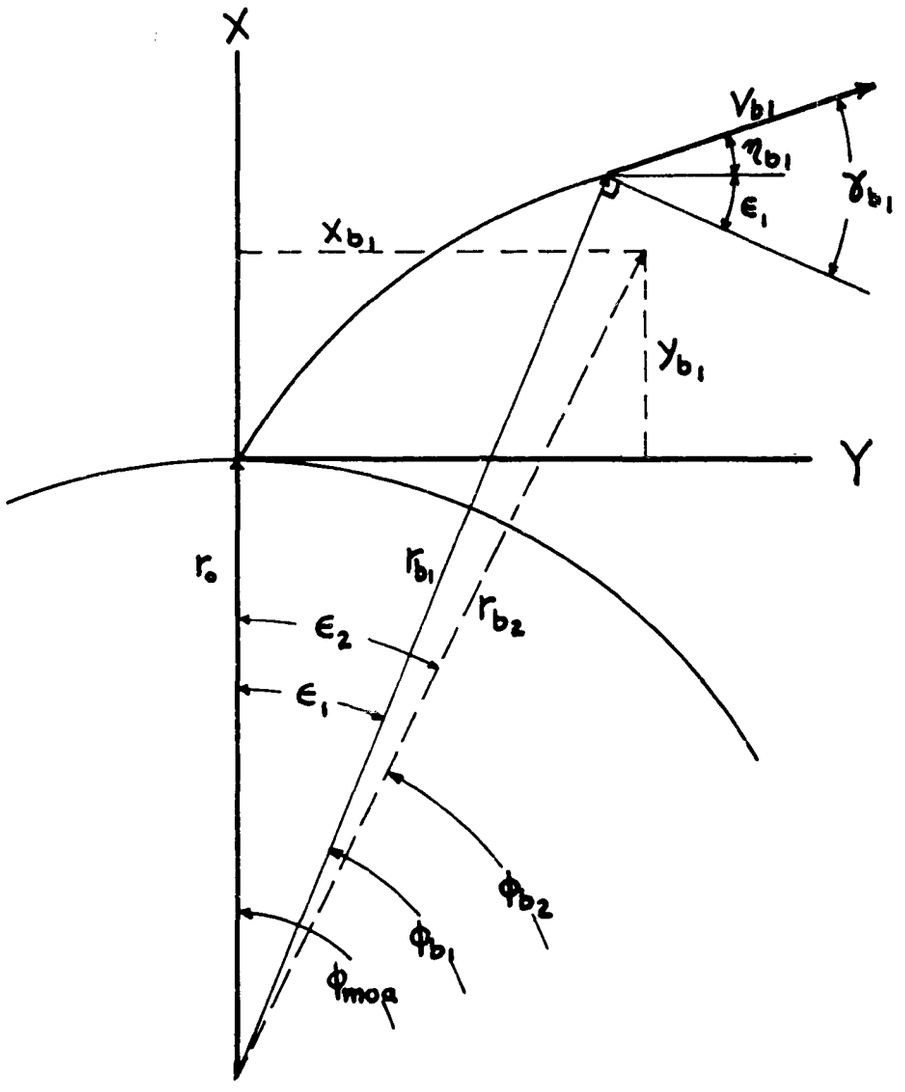

Fig. 4-3a

Boost Phase Approximation

Trial One

$$\epsilon_1 = \phi_{moa} - \phi_{b_1} \tag{4-63}$$

where these angles are shown in Fig. 4-3a. Therefore the first trial burnout angle in rectangular coordinates is

$$\eta_{b_1} = \gamma_{b_1} - \epsilon_1 \tag{4-64}$$

Then by using Eq (4-59) we can find a value for D_1. With D_1 known, Eqs (4-48) and (4-49) are used to find x_{b_1} and y_{b_1}.

We can now compute the actual value of r_b, which is designated r_{b_2}. using the relationship (See Fig. 4-3a)

$$r_{b_2} = \sqrt{(r_o + y_{b_1})^2 + x_{b_1}^2} \tag{4-65}$$

Now we can remove the restriction that the rectangular and polar launch sites are coincident by finding that

$$\epsilon_2 = \tan^{-1}\left(\frac{x_{b_1}}{r_o + y_{b_1}}\right) \tag{4-66}$$

and change from the coordinate system of Fig. 4-3a to the adjusted coordinate system of Fig. 4-3b. With the value of r_{b_2} from Eq (4-65) and the interceptor trajectory equations we can find new values of ϕ_{b_2}, v_{b_2}, and γ_{b_2}. Now substituting ϵ_2 and γ_{b_2} into Eq (4-64) we find η_{b_2}. Then again using Eqs (4-59, 48, and 49) we find values for D_2, x_{b_2} and y_{b_2}. The iteration process is continued until

$$r_{b_{i+1}} \approx r_{b_i} \tag{4-67}$$

Note that we use the previous value of ϵ to compute a new value

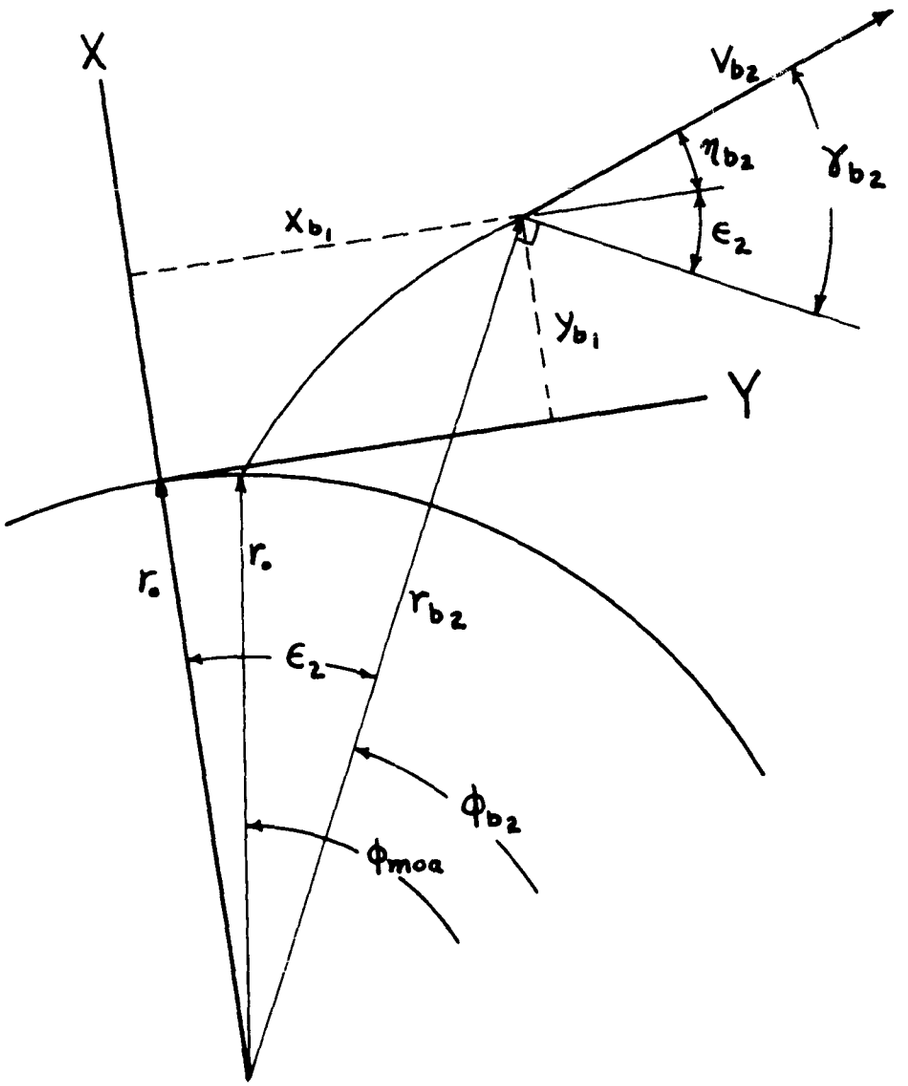

Fig. 4-3b
Boost Phase Approximation
Trial Two

for η_b. This introduces a small error for the first few trials since in all likelihood the relative positions of the rectangular and polar launch sites will be different from one trial to the next. However, since this process is convergent, as the number of trials increases, ϵ will approach a constant value and the error will approach zero. An exaggerated illustration of how this iteration process might converge is shown in Fig. 4-4. Thus, by using this double iteration process, we find the effective sub-rocket mass ratio, D, for the boost-phase rockets, and values for ϕ_b and r_b.

We are now prepared to achieve our objective, and determine the weights and thrusts required, and calculate the excess time. First let us find the weights and thrusts.

Determination of Weight and Thrust Requirements

The effective sub-rocket mass ratio for the velocity-match rocket is found by using Eq (3-38). Let us also specify a thrust to initial weight ratio for this rocket, and call this quantity β_u, where the u subscript is used to avoid confusion with the boost-rocket parameters. Assuming a one-stage velocity-match rocket, the overall mass ratio of this rocket is found from Eq (4-7) and Fig. 4-2 to be

$$\psi_u = \frac{m'_p}{m_p} = \frac{(n-1)\,D_u}{(n-D_u)} \tag{4-68}$$

where ψ_u is the non-dimensional mass (or weight) ratio of the velocity-match rocket (lb of int. rocket per lb of int. vehicle). The thrust required for the velocity-match rocket is found from Eq (4-38) to be

$$T_u = \beta_u M_u \tag{4-69}$$

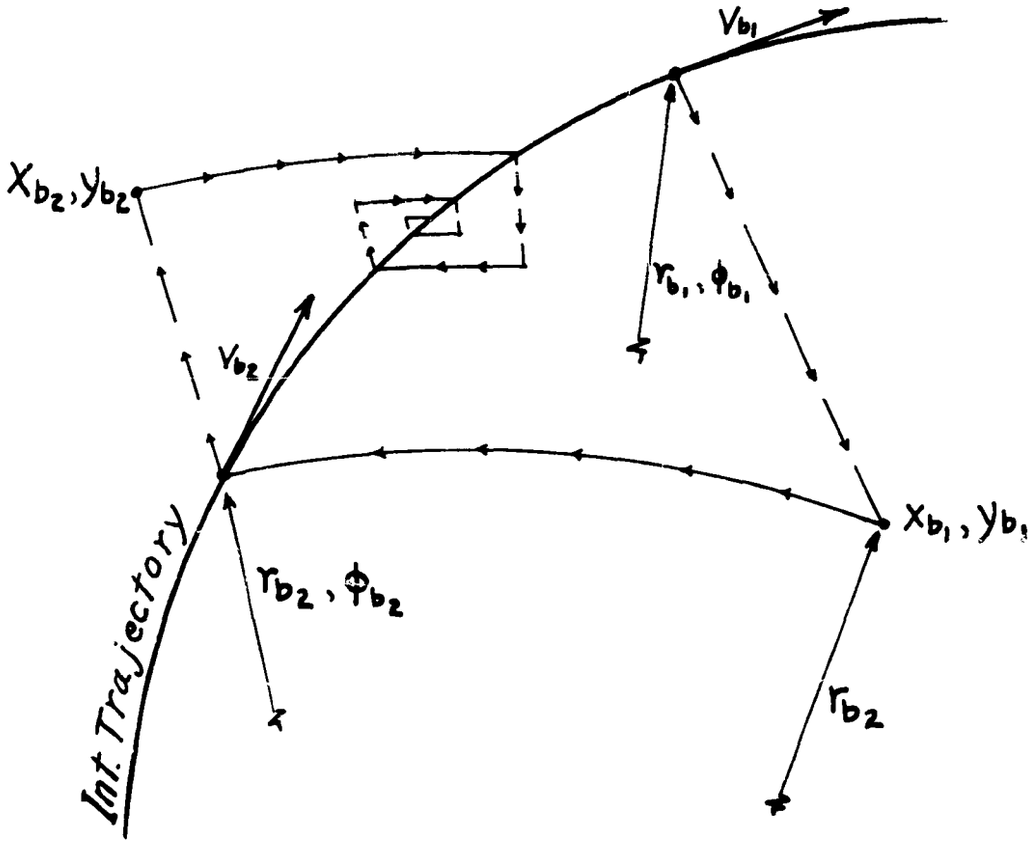

Fig. 4-4

Iterative Process for Satisfying Velocity and Position Requirements of the Intercept Trajectory

or in non-dimensional form

$$Th_u = \beta_u \Psi_u \tag{4-70}$$

where T_u = the thrust of the velocity-match rocket

M_u = the weight (or lb mass) of the velocity-match rocket

Th_u = the lb of thrust required per lb of interceptor vehicle.

The mass ratios of the boost-stages are found by using Eqs (4-7) and (4-8). These mass ratios are

$$\Psi_0 = \left[\frac{(n-1)\,D}{n-D}\right]^K \tag{4-7}$$

$$\Psi_1 = \Psi_0\left[1 - \frac{1}{\sqrt[K]{\Psi_0}}\right] \tag{4-71}$$

$$\Psi_2 = (\Psi_0 - \Psi_1)\left[1 - \frac{1}{\sqrt[K]{\Psi_0}}\right] \tag{4-72}$$

$$\Psi_K = (\Psi_0 - \Psi_1 - \Psi_2 - \cdots - \Psi_{K-1})\left[1 - \frac{1}{\sqrt[K]{\Psi_0}}\right] \tag{4-73}$$

The thrusts required for each stage are, from Eq (4-38) and Fig. 4-2

$$T_1 = \beta M_1 = \beta\left(m_1 + m_2 + \cdots + m_K + m_p'\right) \tag{4-74}$$

$$T_2 = \beta M_2 = \beta\left(m_2 + m_3 + \cdots + m_K + m_p'\right) \tag{4-75}$$

$$T_K = \beta M_K = \beta\left(m_K + m_p'\right) \tag{4-76}$$

By dividing through by m_p'. and using Eq (4-68) we can write these equations in non-dimensional form.

$$Th_1 = \beta \Psi_u \left(\Psi_1 + \Psi_2 + \cdots + \Psi_K + 1 \right) \tag{4-77}$$

$$Th_2 = \beta \Psi_u \left(\Psi_2 + \Psi_3 + \cdots + \Psi_K + 1 \right) \tag{4-78}$$

$$Th_K = \beta \Psi_u \left(\Psi_K + 1 \right) \tag{4-79}$$

By using Eqs (4-4b) and (4-8) we can further reduce these equations and show that

$$Th_1 = \beta \Psi_o \Psi_u \tag{4-80}$$

$$Th_2 = \frac{\beta \Psi_2 \Psi_u}{\left[1 - \frac{1}{\sqrt[K]{\Psi_o}} \right]} \tag{4-81}$$

$$Th_K = \frac{\beta \Psi_K \Psi_u}{\left[1 - \frac{1}{\sqrt[K]{\Psi_o}} \right]} \tag{4-82}$$

Therefore, the mass (or weight) and thrust ratios are determined, and numerical values of weights and thrusts can be found if m_p, the weight of the interceptor vehicle, and k, the number of boost-phase stages are known.

Excess Time

To find the excess time it is necessary to determine the flight times to the intercept point for both the warhead and the interceptor. The difference between these times is defined as the excess time.

Let us assume that the burning time of the enemy booster rockets can be neglected and that the total flight time of the warhead from its launch site to the intercept point is the same as its free-flight time. This time can be found by using the warhead

trajectory parameters and evaluating Eqs (2-46) and (2-47) at the angles ϕ_{wo}, and ϕ_{wI} as shown in Fig. 4-5. Let this time be T_w^*. The time of the interceptor from its launch site, LS_m, to the boost-phase burnout point, BO, can be found by multiplying Eq (4-44) by K, the number of booster stages. Let this time be T_b^*. From Fig. 3-5 it can be seen that the flight-time of the interceptor from point A' to the intercept point, IP, is the same as the free-flight time (without velocity-match rocket ignited) from point A' to the aiming point, AP. Thus the free-flight time from point BO to IP (Fig. 4-5) can be found by using the intercept trajectory parameters and evaluating Eqs (2-46) and (2-47) at the angles ϕ_b, and ϕ_{mIa}. Let this time be T_c^*. Then the excess time, T_x^*, is given by the equation

$$T_x^* = T_w^* - (T_b^* + T_c^*) \tag{4-83}$$

Therefore, by assuming that the enemy missile is detected at the instant it is launched, the interceptor must be launched T_x^* seconds later, if the warhead and interceptor vehicle are to arrive at the intercept point simultaneously.

Maximum Acceleration

An important consideration, especially if a manned vehicle is used in the interceptor system, is the maximum acceleration imposed upon the system. There is a peak acceleration at the instant of burnout of each sub-rocket, and this is found by using Newton's second law to be

$$\nu_j = \frac{T_j}{M_{j_f}} \tag{4-84}$$

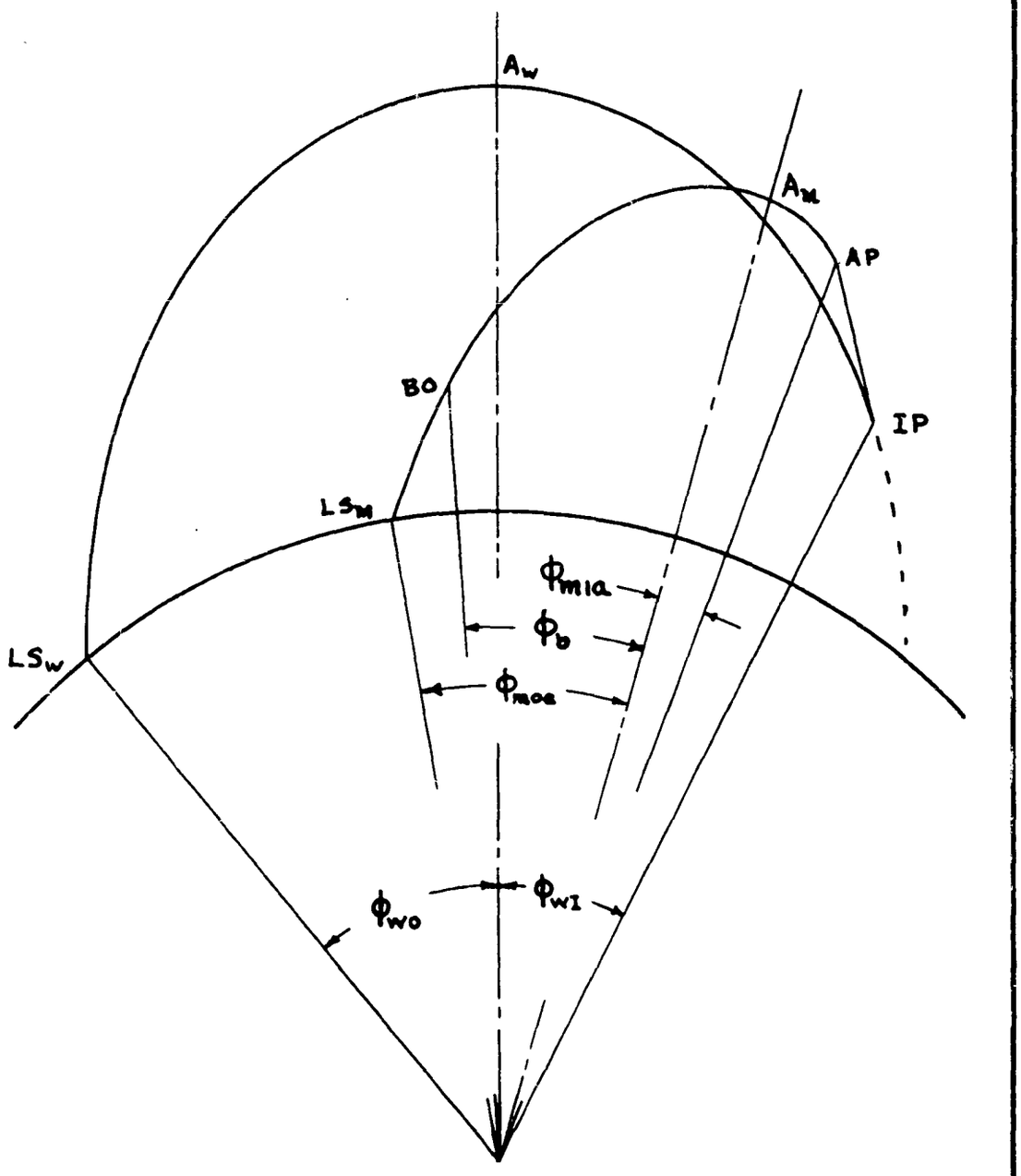

Fig. 4-5

Angles for Determining Flight-Times of Warhead and Interceptor

where ν_j = the maximum acceleration in sea level "g's"

T_j = the thrust of the j^{th} stage

M_{j_f} = the burnout weight of the j^{th} stage.

But from Eq (4-38)

$$T_j = \beta_j M_j \tag{4-85}$$

By combining Eqs (4-84) and (4-85) it is found that

$$\nu_j = \frac{\beta_j M_j}{M_{j_f}} \tag{4-86}$$

But

$$\frac{M_j}{M_{j_f}} = D_j \tag{4-2}$$

By combining Eq (4-2) and (4-86) we get

$$\nu_j = \beta_j D_j \tag{4-87}$$

Since we have specified that the β's and D's of each sub-rocket are equal, Eq (4-87) shows us that the peak accelerations during the boost-phase are the same. Similarly, the maximum acceleration during the velocity-match phase would then be

$$\nu_u = \beta_u D_u \tag{4-88}$$

During an actual launching there would be other components of acceleration (eg. angular and centripetal accelerations during the tip-over maneuver) but these are considered to be of secondary importance for this investigation.

Summary

In this chapter a method for determining the booster-rocket requirements was developed. This was accomplished by making several

simplifying assumptions, developing the equations of motion of a k-stage rocket and introducing the concept of thrust to weight ratio. The equations derived in this manner were then combined with the interceptor trajectory equations of Chapter III to determine thrust and weight ratios, available warning time, and maximum accelerations of the boost-phase and velocity-match rockets.

Because of the many equations, and two iteration processes involved, numerical results are very difficult to obtain without the aid of an electronic computer. For this reason, the equations are programmed on the IBM 1620 digital computer to permit the investigation of many different intercept conditions. The computer programs used in the analysis are described in Appendix A.

V. Procedure for Obtaining Numerical Results

Primary Considerations

The overall vehicle weight, the thrust of the first boost stage, the excess time, and the maximum "g" forces on the interceptor vehicle are the principal factors to be determined.

The excess time is certainly the most important factor in the analysis, for without adequate excess time, the intercept technique is impractical or even impossible. Therefore we wish to determine what intercept conditions allow the most excess time, and the effects of the boost parameters on excess time.

The overall vehicle weight is also quite important, since as weight increases, the thrust required to launch the vehicle increases. Since there are limits on the amount of thrust available to perform the intercept, thrust rather than weight is the factor which we attempt to minimize in the analysis.

Finally, the accelerations which exist during the boost phases are also an important factor if the system is manned. Man is capable of withstanding approximately ten transverse "g's" or 322 feet per second per second applied with the pilot perpendicular to the acceleration vector (Ref. 4:14). Therefore we shall indicate the intercept conditions which result in accelerations in excess of ten "g's".

Basic Analysis

The basic analysis consists of fixing the warhead trajectory,

intercept point, and the boost parameters and then varying the position of the interceptor launch site. This procedure is repeated for different intercept points on the warhead trajectory. Finally the complete procedure is repeated for other warhead trajectories. Once the basic analysis is complete, the effects of varying I_s with n fixed, varying n with I_s fixed, and varying I_s and n in combination are determined.

Warhead Trajectories to be Investigated

In Chapters III and IV we have laid the mathematical groundwork for evaluating the trajectory-match intercept. Now a decision must be made as to what missile trajectories should be used in the analysis.

A 6000 nautical mile trajectory is selected because it is a typical range for ICBM trajectories. A 4000 nautical mile trajectory is also selected because less time is available to complete the interception of a shorter range ICBM trajectory. Now Eq (2-35) can be used to determine the semi-range angles for these two trajectories. For the 6000 nautical mile trajectory,

$$\phi_o = \frac{X_e}{2r_o} = \frac{6000}{2(3437.747)} = 0.87266456 \text{ radian}$$

and for the 4000 mile trajectory,

$$\phi_o = \frac{4000}{2(3437.747)} = 0.58177638 \text{ radian}$$

It was shown in Chapter II, that for any given range there is an almost unlimited number of trajectories, depending upon the amount of total energy available. Thus we must stipulate more than just the range to define the exact trajectory. In order to more completely consider the possible intercept situations, three different trajectories are chosen for each range. One is the minimum-energy trajectory, and the others are a high angle (high altitude) and a low angle (low altitude) trajectory. These trajectories can be completely defined if we now specify the theoretical launch angle, γ_o, of the warhead. For the minimum energy trajectories, we can use Eq (2-57) to determine γ_o. For the 6000 mile trajectory

$$\tan \gamma_{o_{ME}} = \frac{\cos \phi_o}{1 + \sin \phi_o} = \frac{0.64278759}{1.76604431} = 0.36192092$$

and $$\gamma_{o_{ME}} = 0.34906588 \text{ radian.}$$

For the 4000 mile trajectory,

$$\tan \gamma_{o_{ME}} = \frac{0.83548776}{1.54950890} = 0.53919520$$

and $$\gamma_{o_{ME}} = 0.49450997 \text{ radian.}$$

To establish the high and low angle warhead trajectories for each range, we can fix the total energy available for the trajectory.

This then determines the energy ratio of the trajectory, which in turn determines the theoretical launch angle. Since the choice of total energy is an arbitrary one as long as reasonable values are used, it is more convenient to specify the energy ratio. An energy ratio of 0.9 is chosen for the 6000 mile trajectory, and 0.8 for the 4000 mile trajectory. Then for the 6000 mile trajectory

$$\tan \gamma_o = \frac{1}{2}\left[\frac{ER}{\tan \phi_o} \pm \sqrt{\left(\frac{ER}{\tan \phi_o}\right)^2 - 4(1 - ER)}\right] \qquad (2\text{-}58)$$

$$= \frac{1}{2}\left[\frac{0.9}{1.1917534} \pm \sqrt{\left(\frac{0.9}{1.1917534}\right)^2 - 4(1 - 0.9)}\right]$$

$$= 0.58389717 \quad \text{and} \quad 0.17126302$$

or γ_o = 0.52849701 radian (high angle)

and γ_o = 0.16961984 radian (low angle)

For the 4000 mile trajectory

$$= \frac{1}{2}\left[\frac{0.8}{0.65771029} \pm \sqrt{\left(\frac{0.8}{0.65771029}\right)^2 - 4(1 - 0.8)}\right]$$

$$= 1.02032565 \quad \text{and} \quad 0.19601585$$

or γ_o = 0.79544624 radian (high angle)

and γ_o = 0.19356362 radian (low angle)

These values of ϕ_o and γ_o which are listed in Table I, are necessary inputs to the computer solution of the boost-phase approximations (Appendix A), since the computer is programmed to determine all other parameters of the warhead trajectory from these values.

Table I

Warhead Trajectory Semi-Range and Launch Angles for 6000 and 4000 Nautical Mile Ranges

Warhead Range (n.m.)	Trajectory Angle	Semi-Range Angle (radians)	Launch Angle (radians)
4000	Low	0.58177638	0.19356362
	Minimum Energy	"	0.49450997
	High	"	0.79544624
6000	Low	0.87266456	0.16961984
	Minimum Energy	"	0.34906588
	High	"	0.52849701

Selection of Intercept Points and Launch Sites

To facilitate the discussion of the position of intercept points and launch sites, we will use the angular position of the

points relative to the warhead apogee in an earth-centered, polar coordinate system. This is illustrated in Fig. 5-1.

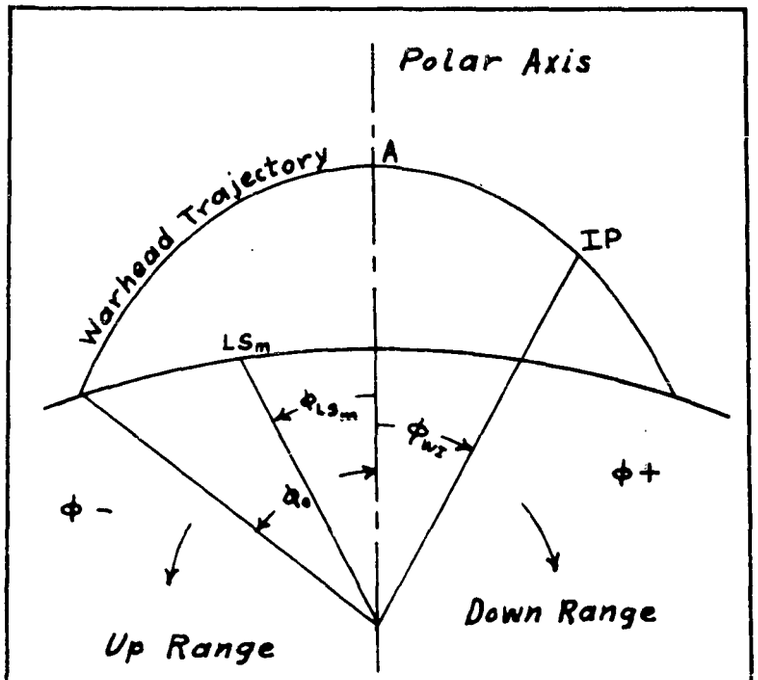

Fig. 5-1
Position of Launch Site and Intercept Point Relative to Warhead Apogee

An intercept point is defined by ϕ_{wI} and is understood to be on the warhead trajectory. The position of the interceptor launch site, ϕ_{LS_m}, is determined in the same manner, but its position is on the earth's surface. Note that ϕ is positive clockwise and the warhead apogee is at $\phi = 0$. With these definitions established we can proceed with the selection of intercept points and launch sites.

The intercept points to be investigated are arbitrarily chosen

so that a representative sample of points on the warhead trajectory is checked. These points are approximately equally spaced along each trajectory between warhead apogee and atmospheric re-entry point.

The interceptor launch sites are determined indirectly by using the theoretical intercept trajectory semi-range angles as inputs to the computer program. Then the approximate position of the interceptor launch site relative to the warhead apogee is $\phi_{WI} - \phi_{mo}$. The exact position, which is $\phi_{WI} - \phi_{LIA}$ is slightly further up-range than the approximate position (Fig. 3-6), but this is not critical since we are merely trying to select a representative group of launch site positions. The up-range positions of interceptor launch sites are limited by practical considerations; e.g. no launch sites in enemy territory. The down-range position of the interceptor launch site is also limited. As the angular position of the launch site approaches the intercept point, the interceptor trajectory becomes almost vertical and the trajectory-match technique is not practical.

With these limitations in mind, the interceptor launch sites are arbitrarily chosen to determine enough points to plot curves which show the effect of launch site position on the boost requirements.

Selection of Rocket Parameters

The five remaining variables to be investigated are:

(1) k, the number of stages for the boost rocket

(2) I_s, the specific impulse of the fuel

(3) n, the structural factor

(4) β, the thrust to weight ratio for the boost-phase

(5) β_u, the thrust to weight ratio for the velocity-match rocket.

In order to continue the investigation some particular values of these variables must be selected.

Number of Boost-Phase Stages. For this investigation three boost stages were selected as a compromise between the decreased reliability of a large number of stages and the large thrust and weight requirements for a small number of stages. This reduces the number of variable boost parameters to four.

Specific Impulse and Structural Factor. Specific impulse is determined by the choice of propellant. Values of I_s vary from 160 seconds for some old-type solid propellants, to 364 seconds for liquid hydrogen-liquid oxygen (Ref 10: 112, 113, 312, 313). Instead of selecting a particular fuel, a reasonable value of I_s, 250 seconds, is selected for the basic analysis. Later in the investigation the effect of different values of I_s for a few typical intercept situations is determined.

A similar approach is used to determine the value of the structural factor since it depends upon the density of the fuel and the detailed structural design of a rocket. A value of n equal to ten is selected for the basic analysis.

Thrust to Initial Weight Ratios. The choice of numerical values for β and β_u appears to be completely arbitrary. Then to determine the values to be used in the analysis, it is necessary to fix the value for one at an arbitrary value, and determine the effect

of the other on overall weight and thrust requirements. Once these effects are known, the most promising values are used in the basic analysis.

Summary

This chapter outlines the general approach used to obtain the desired data from the digital computer solution of the intercept analysis. These results are presented in Chapter VI.

VI. Results and Conclusions

A numerical integration was performed using computer program CM-12 (Appendix A), for one particular intercept trajectory. In this integration, the effects of drag and the vertical, constant angle of attack, zero lift, and constant attitude flight segments of a rocket launching are considered. This was accomplished to verify the validity of the assumptions made in the boost-phase analysis. For the case considered, the actual burnout velocity came within three percent of that required. The results of this integration are summarized in Appendix B.

Since the results are only good approximations to the actual values because of the many simplifying assumptions made, the computed data is presented in graphical rather than tabular form. This also gives a better overall picture of this intercept technique, and allows important trends to be interpreted more easily. Angular inputs and print-outs of the computer are in radians and therefore all angles are plotted on the graphs in radians.

In order to avoid complicating some of the graphs, a code is used to identify the intercept conditions. For example, 6H:45:30 is interpreted as follows:

6H	6000 nautical mile, high angle warhead trajectory
45	intercept point on warhead trajectory is 0.45 radians down range from the apogee
30	semi-range angle of the theoretical intercept trajectory

is 0.30 radians

The theoretical semi-range angle is selected for this code rather than the corrected value, because this is the angle used as the computer input to obtain the numerical results which are plotted.

Results

Effect of β_u on Th_1. Figures 6-1, 2, 3 were obtained for two intercept conditions: 6H:45:30 and 6H:45:60. Thrust to interceptor vehicle weight ratio, β_u, was varied while the other rocket parameters were held constant. These values are

I_s = 250 seconds

n = 10

β = 1.5

k = 3

For the case, 6H:45:60, β_u has a negligible effect on Th_1 (Fig. 6-1). thus little advantage is gained by using a more powerful engine for the velocity-match rocket. The top curve shows that a reduction in thrust, Th_1, of approximately 3.5% can be obtained by increasing β_u from one to three; however, since the curve appears to be leveling off, little will be gained by using a more powerful engine. A comparison of the curves in Fig. 6-1 shows that β_u has more effect for the intercept trajectory with the smaller theoretical semi-range angle (.3 vs .6). This is due to the larger difference, Δv, between warhead and interceptor velocities. A larger β_u decreases the distance s' (See Eq 4-45 and Fig. 3-6). This also decreases r_{Ia} and therefore we can say that

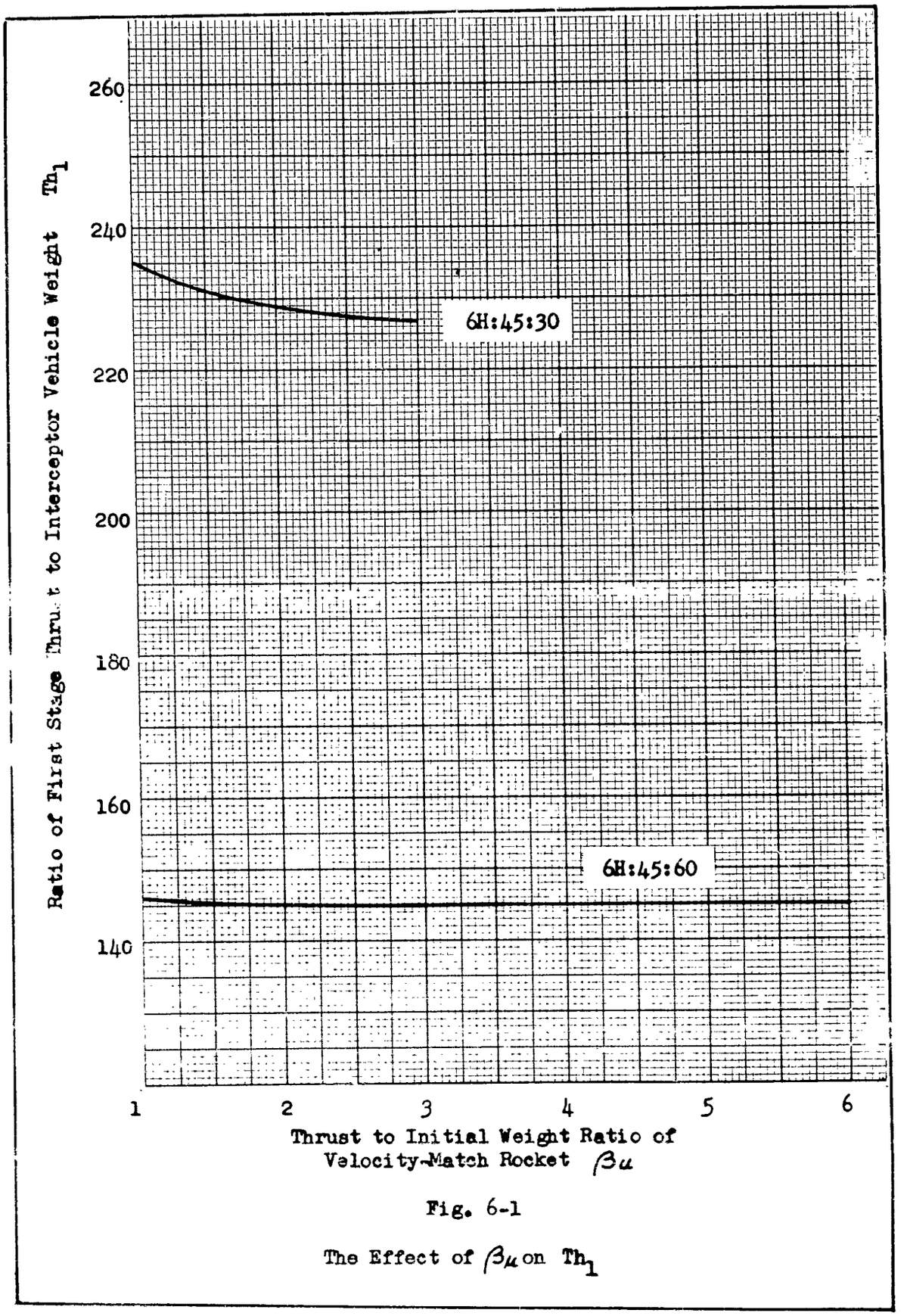

Fig. 6-1

The Effect of β_u on Th_1

$$\lim_{\beta_u \to \infty} (\text{corrected int. trajectory}) = (\text{theoretical int. trajectory})$$

In other words we can say that as r_{Ia} approaches r_I, the total energy, E, of the intercept trajectory approaches a constant value (E of the theoretical intercept trajectory), thus explaining why the curves in Fig. 6-1 level off.

Effect of β and β_u on v. The computer data indicated that for the values of β used, the maximum acceleration during the boost-phase ranged from approximately 3.0 to 4.5 "g's", and thus this acceleration is not considered to be a problem. Therefore no graphs are plotted for this data.

Figure 6-2 shows that the maximum acceleration of the velocity-match rocket is a linear function of β_u. This is also apparent from Eq (4-88),

$$v_u = \beta_u D_u$$

where D_u is a constant for a particular intercept point. Since D_u is a function of Δv, and Δv increases with decreasing semi-range angles, the maximum acceleration can be a limiting factor on a choice of β_u for intercept trajectories with small semi-range angles, especially for a manned interceptor vehicle. For the two cases shown in Fig. 6-2, it can be seen that for a given β_u, the acceleration is more than doubled, when the semi-range angle is halved.

Effect of β_u on T_x^*. The same reasoning that was used to analyze the effect of β_u on Th_1 is used for the effect of β_u on T_x^* (Fig. 6-3). Here again, the effect of β_u is more pronounced for

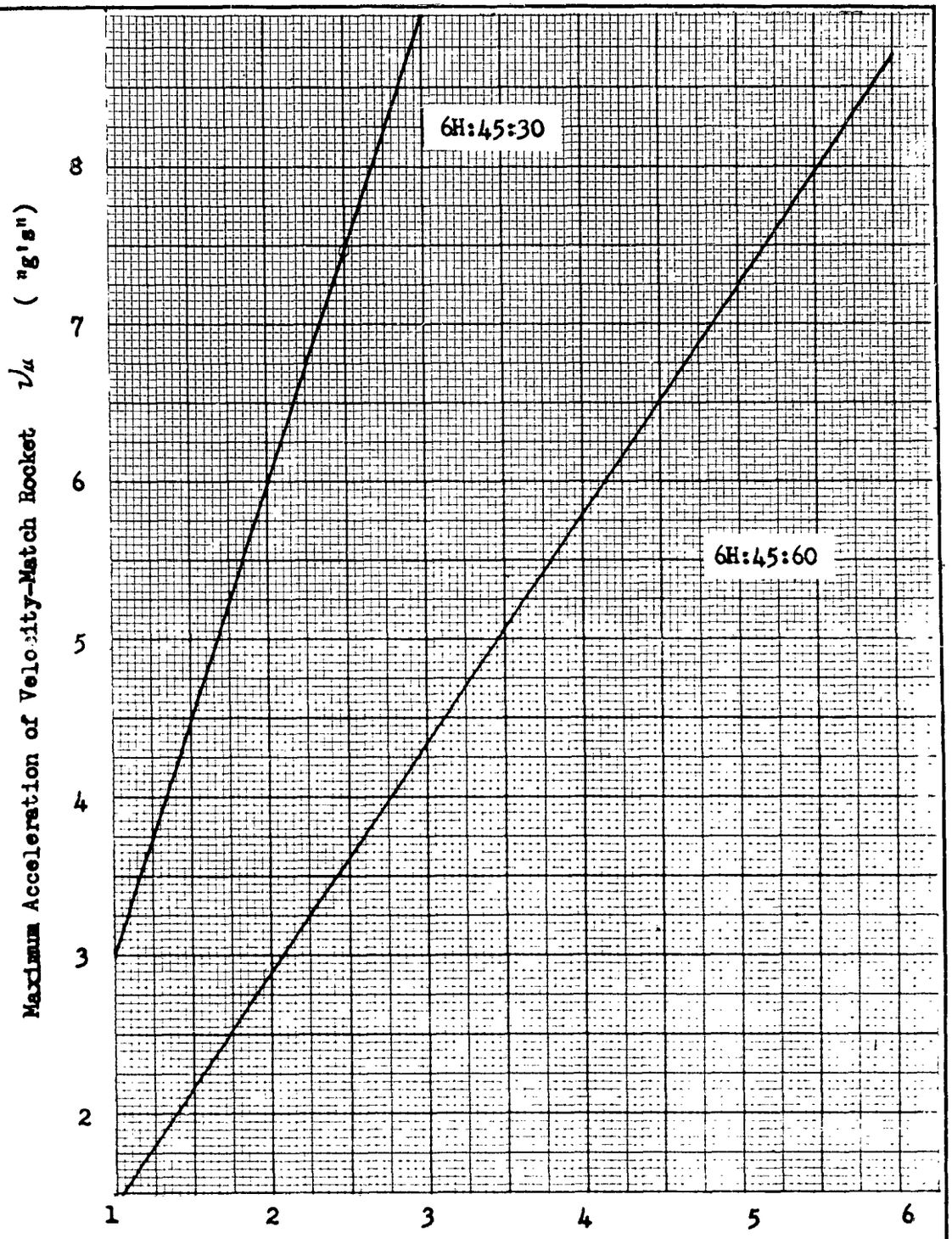

Fig. 6-2

The Effect of β_u on ν_u

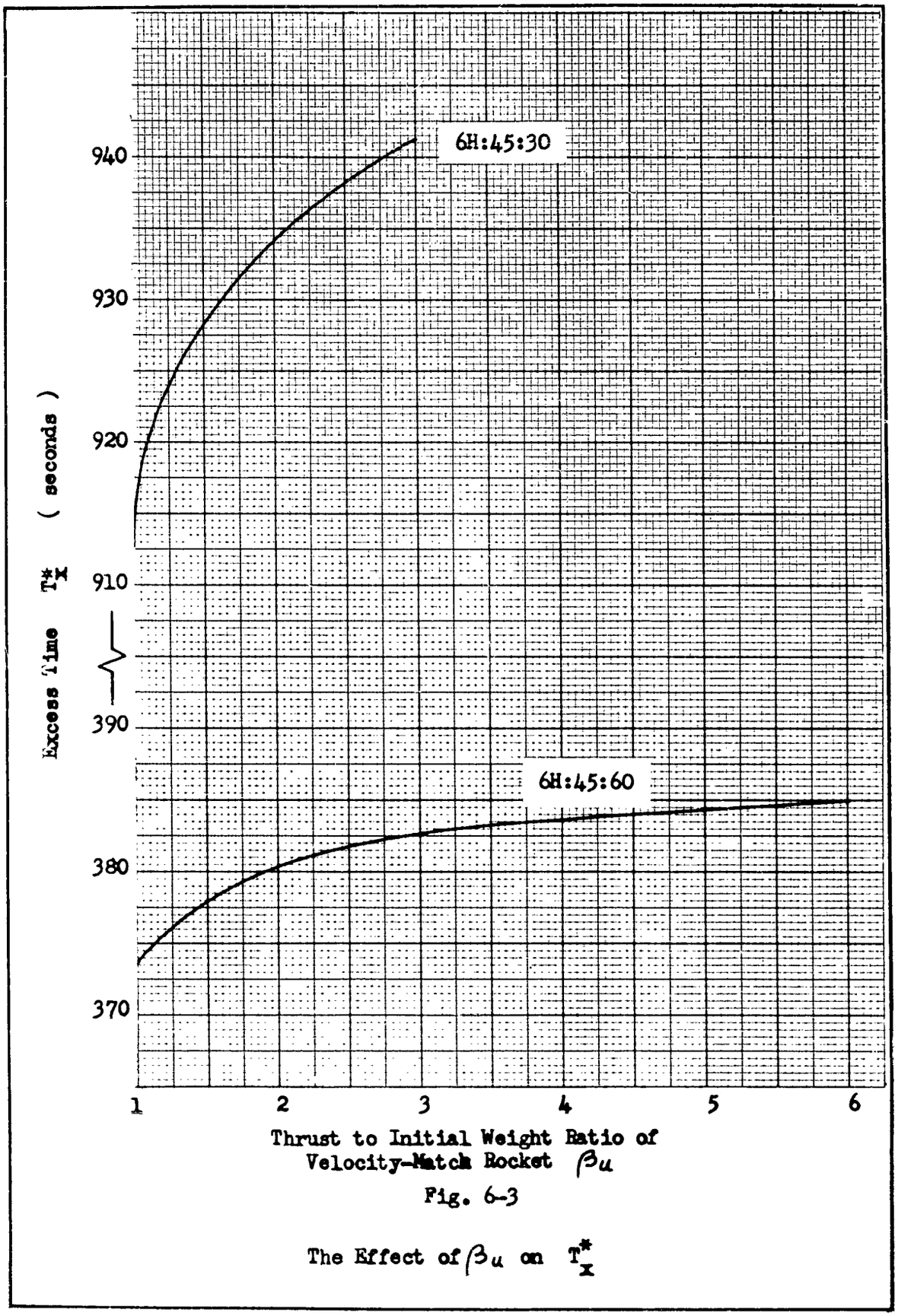

Fig. 6-3

The Effect of β_u on T_x^*

the smaller semi-range angle, and both curves will eventually approach a maximum value of excess time. An increase in β_u from one to three results in an increase in T_x^* of only about 3% and 2.5% for the upper and lower curves respectively. Although this small percent change might be important in some cases, we can safely say that in general β_u is not an important factor as far as time is concerned.

Effect of β on Th_1. Figures 6-4 and 6-5 are plotted from computer data obtained by varying β and holding the other variables fixed as follows:

$$I_s = 250 \text{ seconds}$$
$$n = 10$$
$$\beta_u = 3.0$$
$$k = 3$$

Figure 6-4 shows that for each set of intercept conditions there is an optimum value of β which results in a minimum value of Th_1. These minima are 1.8 and 1.6 for the upper and lower curves respectively. However, since the curves are quite flat in these regions, a value of 1.5 was arbitrarily chosen as a representative value of the optimum β. The existence of these optimum values can be explained by considering Eq (4-44), which shows that the burning times of the boost-phase stages are inversely proportional to β, and the equation

$$Th_1 = \beta \Psi_o \Psi_u \qquad (4\text{-}80)$$

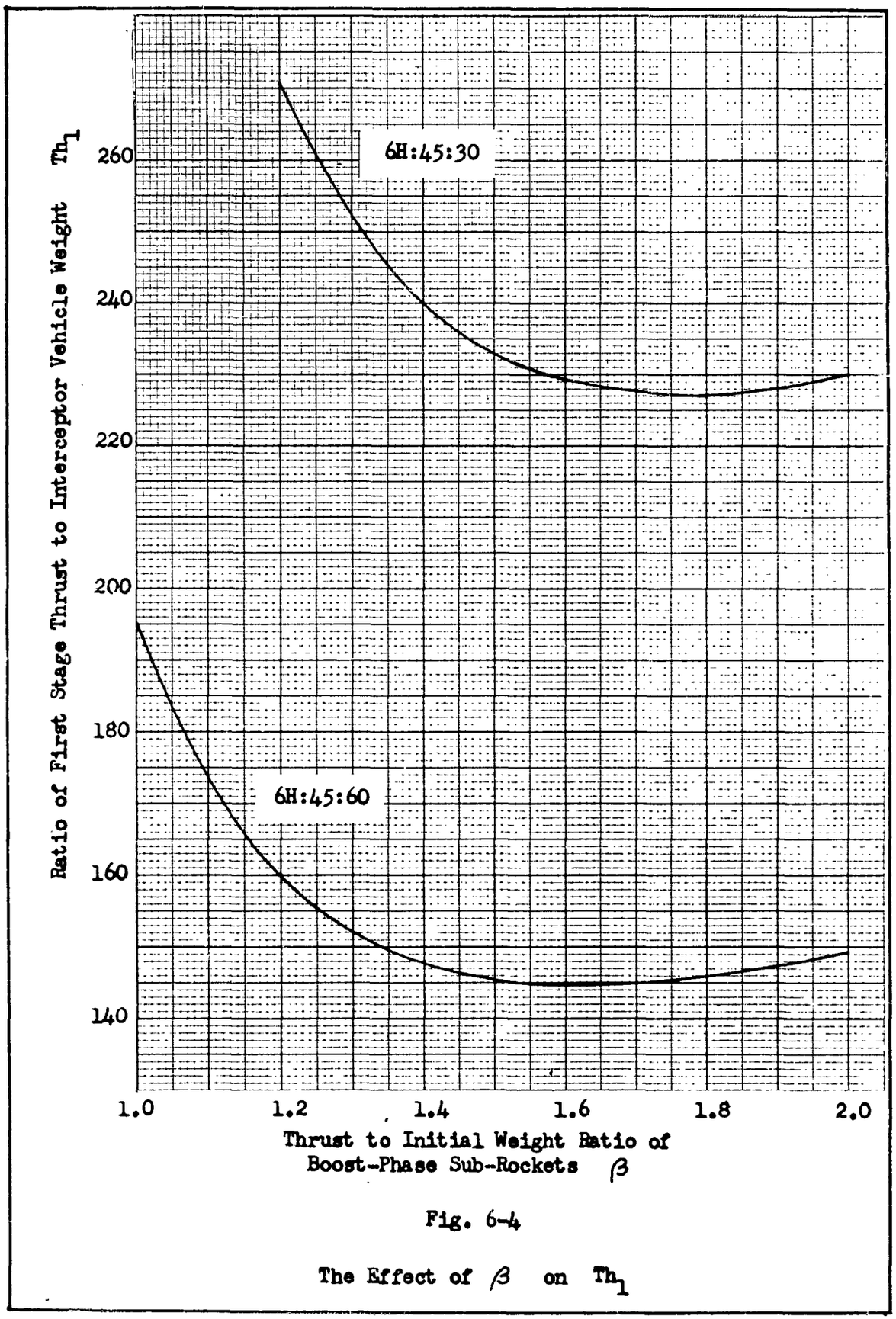

Fig. 6-4

The Effect of β on Th_1

As β is first increased, the burning time shortens, and the velocity loss due to gravity ($\bar{g}t_b$) decreases, thus less fuel is required to reach a given velocity and ψ_o decreases. However, a point is reached where β increases faster than ψ_o decreases. At this point the thrust required, Th_1, is a minimum.

Effect of β on T_x^*. Figures 6-5 shows that an increase in β results in a larger excess time, and that this time approaches some limit asymptotically. The same explanation that was used in discussing the effect of β_u applies here also. We can say that

$$\lim_{\beta \to \infty} (\text{interceptor flight time}) = (\text{free flight trajectory time})$$

which means that for an infinite acceleration we can attain the theoretical launch velocity at the earth's surface and "coast" along the trajectory from the ground up. An increase in β from 1.2 to 1.5 results in increases in T_x^* of approximately 10% and 28% for the upper and lower curves respectively. This means that a considerable advantage is gained by using a high value of β, for the intercept trajectories with larger semi-range angles, ϕ_{mo}, where T_x^* might be critical.

Effect of n on Th_1. The data used to plot the graphs of Th_1 vs n (Fig. 6-6) was obtained by holding the other variables fixed as follows:

$$I_s = 250 \text{ seconds}$$

$$\beta_u = 3.0$$

$$\beta = 1.5$$

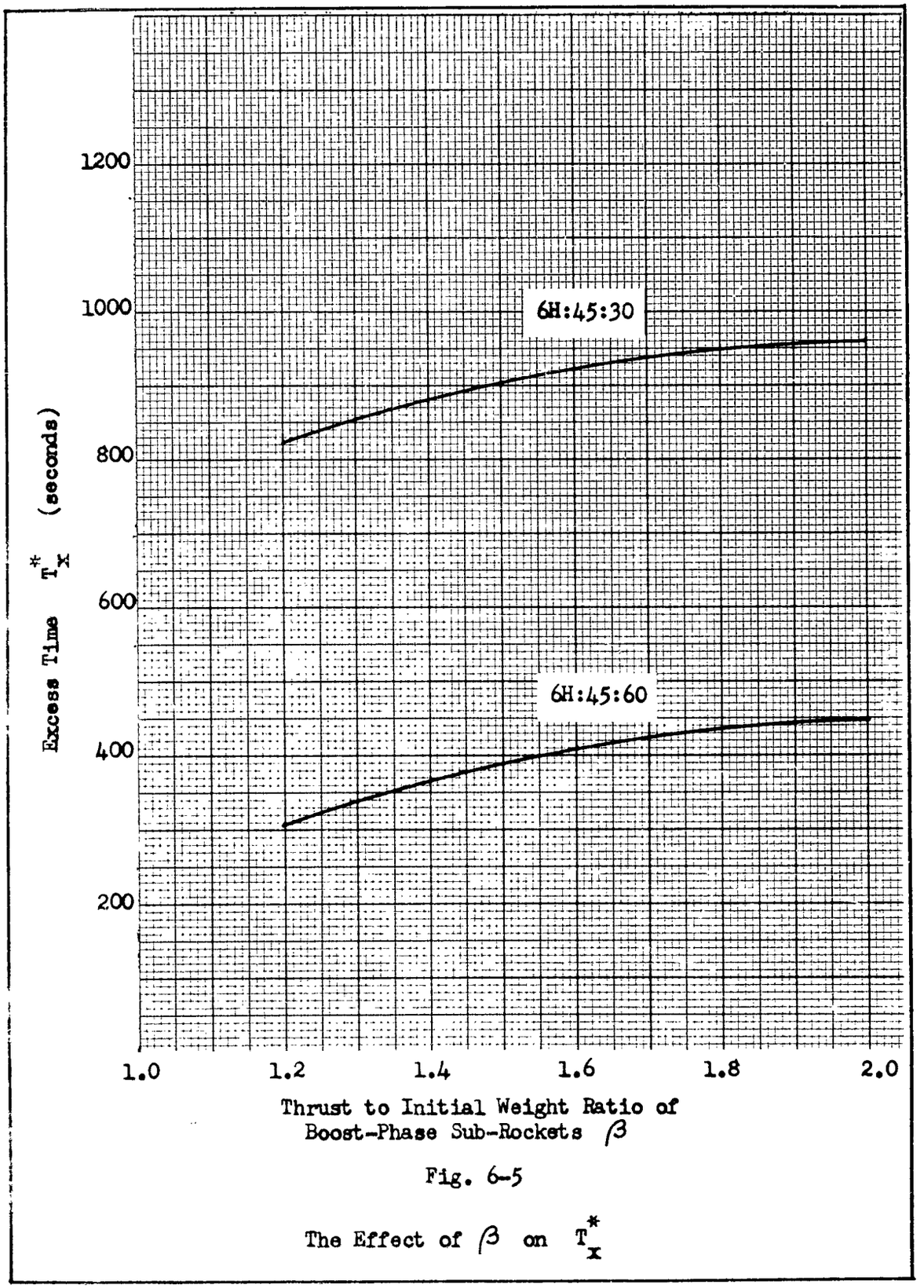

Fig. 6-5

The Effect of β on T_x^*

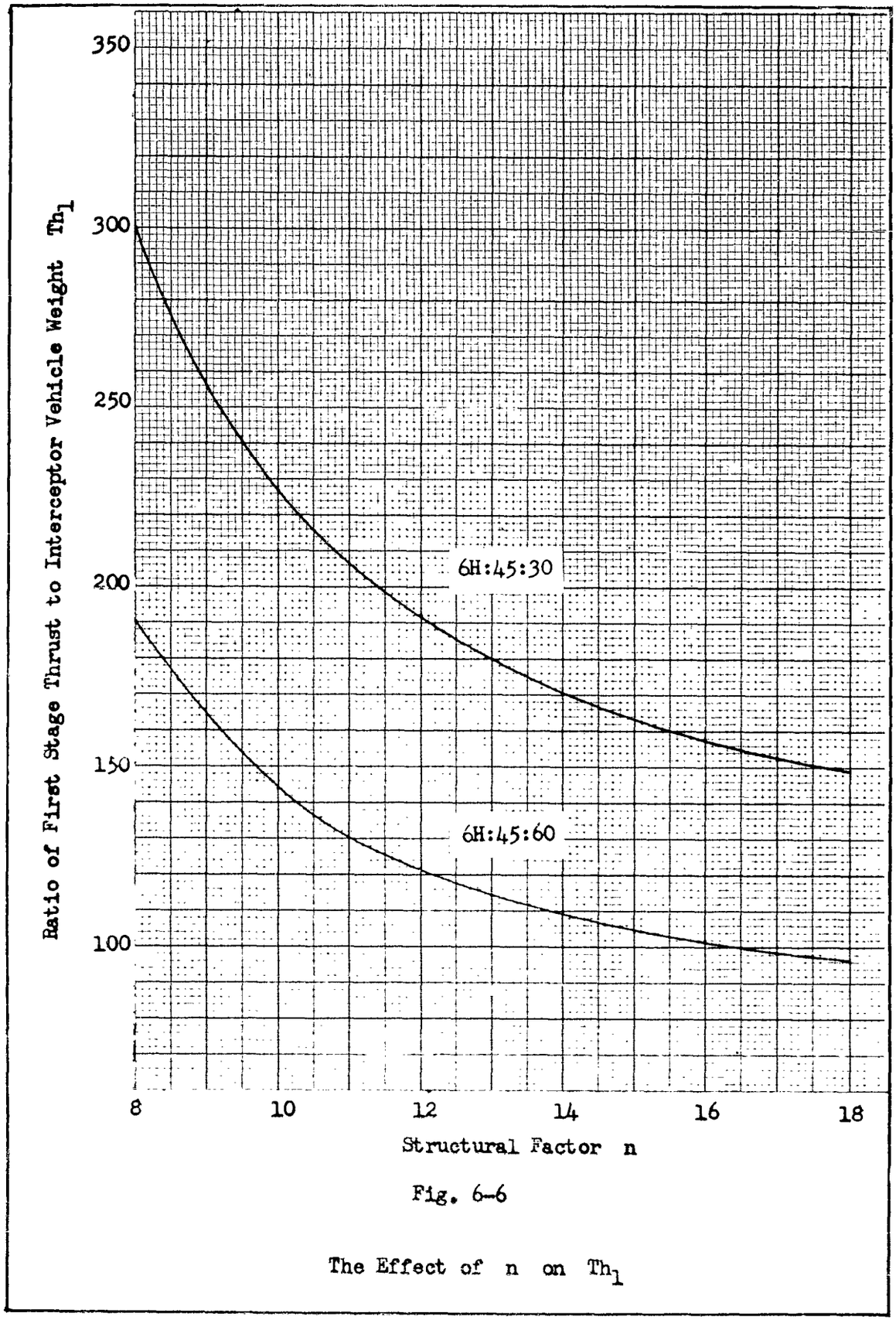

Fig. 6-6

The Effect of n on Th_1

$$k = 3$$

The curves show that advanced structural design techniques (higher n), result in a great reduction in Th_1, but that a point of diminishing returns will be reached, and the curves approach a limiting value. This limiting value is unattainable since as n approaches infinity, the stage weight is equal to the weight of fuel. This assumes that no structure is required to carry this fuel. The structural factor has no effect whatsoever on excess time.

Effect of I_s on Th_1. The curves in Figs. 6-7 and 6-8 were obtained from computer data with the other variables fixed as follows:

$$\beta_u = 3.0$$

$$\beta = 1.5$$

$$n = 10$$

$$K = 3$$

Figure 6-7 clearly shows why great emphasis is placed upon discovering new and exotic rocket fuels. For example, an increase in I_s from 200 to 225 seconds results in decreased thrust requirements of approximately 50%, and an increase in I_s from 225 to 250 seconds results in a further decrease of approximately 40%.

Effect of I_s on T_x^*. Figure 6-8 shows that T_x^* is practically a linear function of I_s. This can also be seen from the equation

$$t_b = \frac{u}{g_c \beta}\left(\frac{D-1}{D}\right) \qquad (4\text{-}44)$$

or

$$t_b = \frac{I_s}{\beta}\left(\frac{D-1}{D}\right)$$

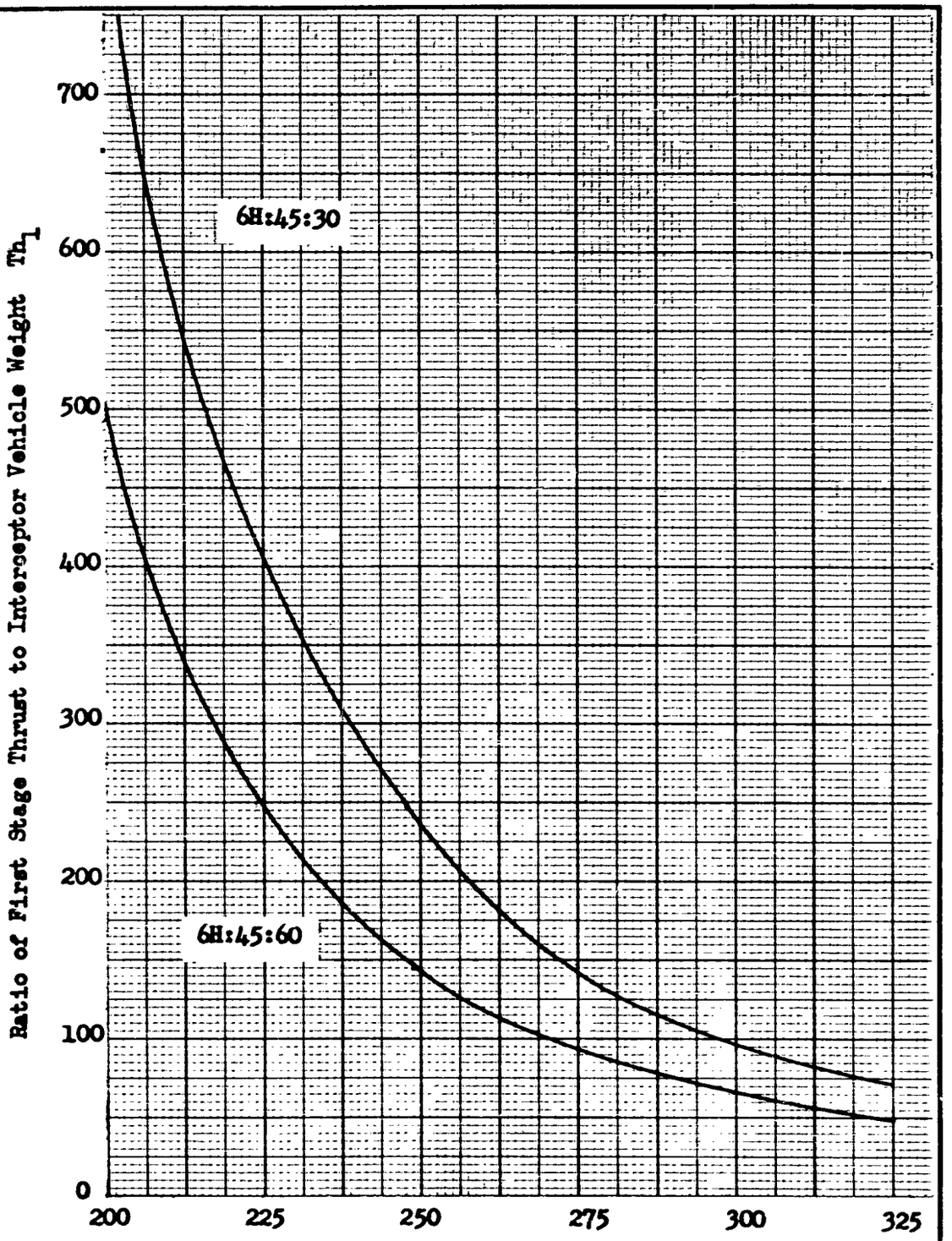

Fig. 6-7

The Effect of I_s on Th_1

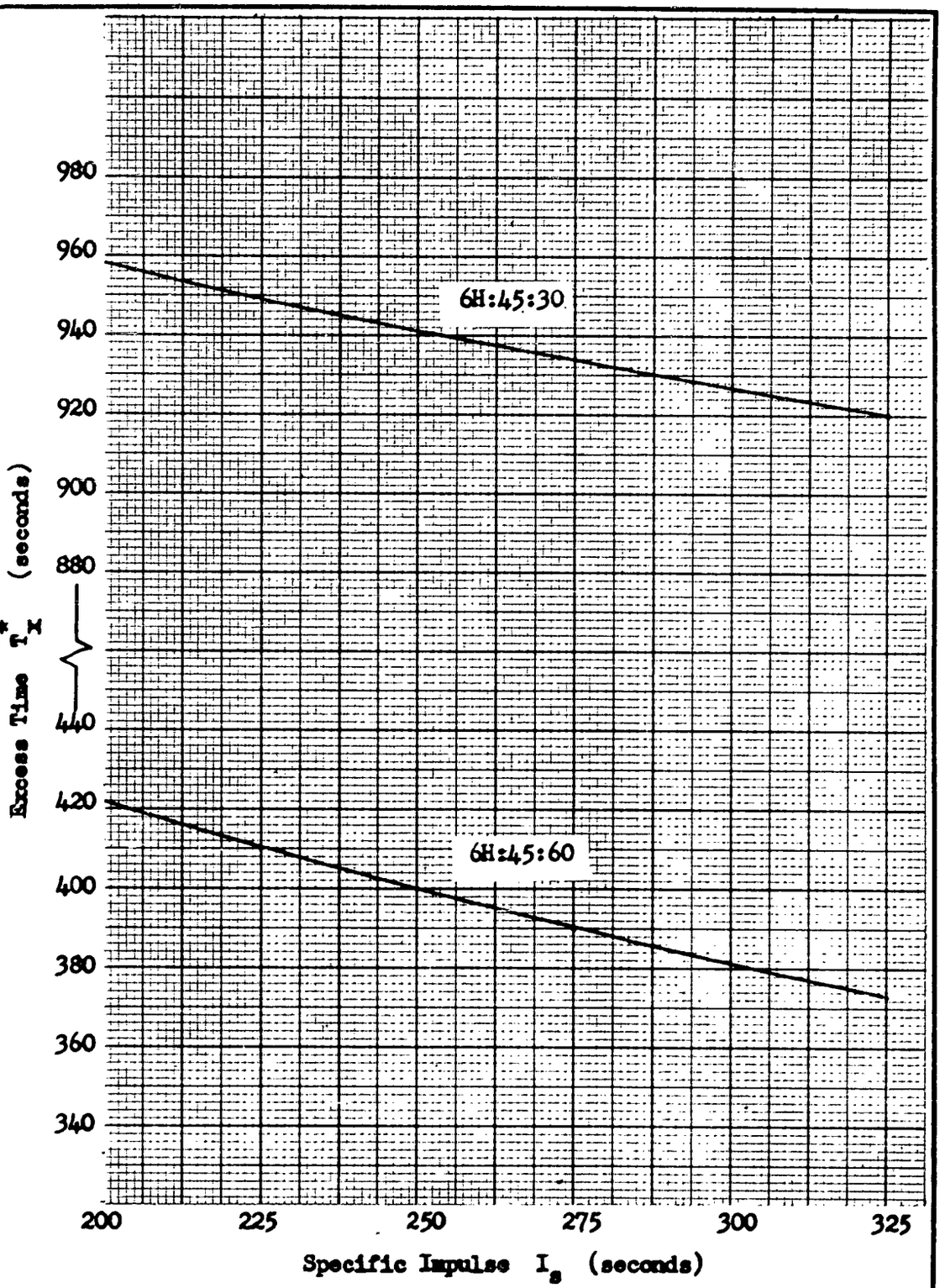

Fig. 6-8

The Effect of I_s on T_x^*

Thus as I_s increases, burning time increases which results in a greater velocity loss due to gravity, and therefore causes a decrease in T_x^*. For the intercept condition 6H:45:60, an increase in I_s from 200 to 225 seconds decreases T_x^* by approximately 2.5%, but this small change is insignificant when compared to the 50% saving in Th_1.

Combined Effect of Changes in I_s and n. For comparison purposes, the effect of combinations of optimistic and pessimistic values of I_s and n upon Th_1 for the 6H:45:60 intercept are determined. These results are shown in Table II.

Table II
Combined Effects of
Specific Impulse and Structural Factor
on Overall Thrust Requirements*

Specific Impulse (sec.)	Structural Factor	Th_1
200	8	796
	20	251
350	8	45
	20	30

* Note: For 6H:45:60 intercept, $\beta = 1.5$, $\beta_u = 3.0$.

Effect of ϕ_{LS_m} and ϕ_{WI} on Th_1 and T_x^*. Figures 6-9, 10, and 11 show the effect of launch site position, ϕ_{LS_m}, on Th_1 for various intercept points on the 6000 nautical mile warhead trajectories. Figures 6-12, 13 and 14 are the curves of T_x^* vs ϕ_{LS_m} which correspond to the Th_1 curves. On the Th_1 graphs, the dotted lines (·····) indicate the approximate position of lines of constant T_x^* (isochrones). The points marked with a star (*) are those points where the maximum acceleration of the velocity-match rocket reached 10 "g's". For all points above the star on each curve, v_u is greater than 10 "g's".

Many of the Th_1 curves appear to approach horizontal and vertical assymptotes. As the launch site is moved up-range from the warhead apogee, ϕ_{moa} approaches ϕ_{wo} and the interceptor and warhead trajectories will eventually coincide and determine the horizontal limit for Th_1. The vertical limit occurs when ϕ_{mo} is equal to zero. However, this is simply a vertical trajectory. The interceptor velocity, v_{mI}, at the intercept point therefore approaches zero as ϕ_{mo} approaches zero, which results in a high Δv, and consequently a much larger velocity-match rocket is required. Thus a much heavier boost-phase rocket with higher thrust is required for these cases.

Illustrations of the Use of the Graphs. To illustrate the use of the curves, let us suppose that we have a 10,000 pound (m_p) manned interceptor vehicle, and desire to intercept a 6000 n.m. minimum-energy warhead trajectory at a point 0.45 radians (ϕ_{WI}) down-range from the apogee. We also select a launch site that is 0.23 radians (ϕ_{LS_m}) up-range. By entering Fig. 6-10 at -0.23 on the

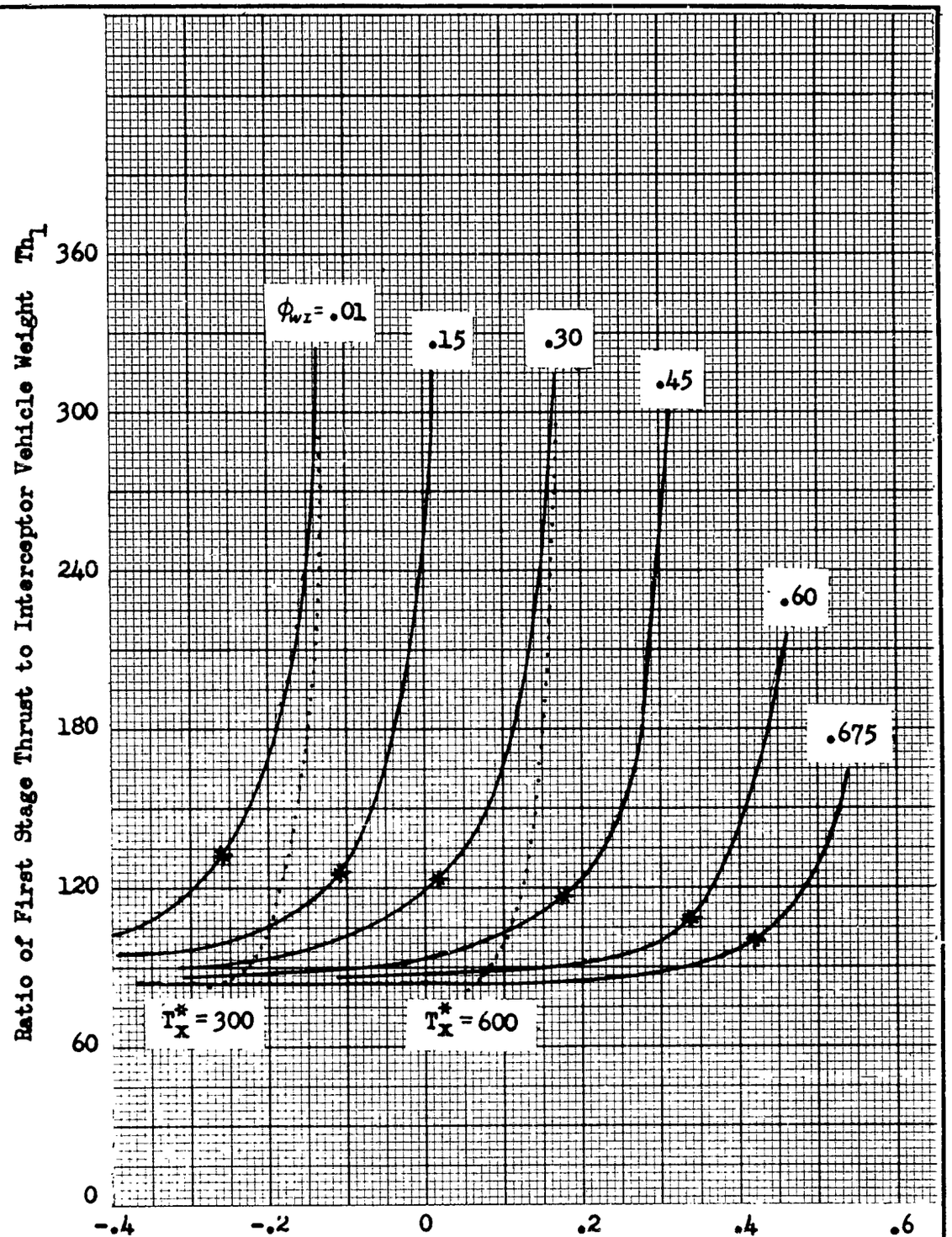

Fig.6-9

The Effect of ϕ_{LS_m} on Th_1 for Various Intercept Points on 6000 n.m. Low Angle Trajectory

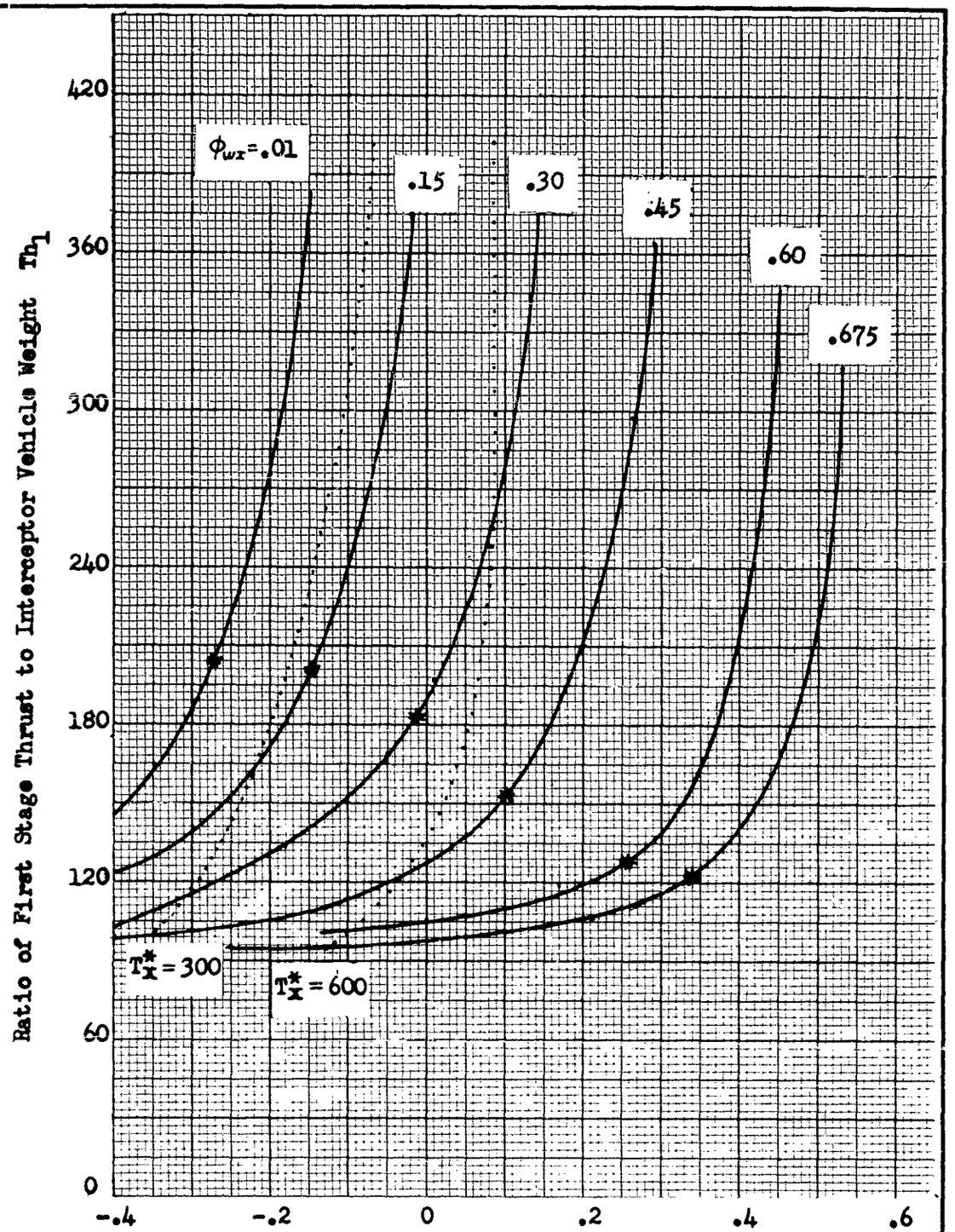

Fig. 6-10

The Effect of ϕ_{LS_m} on Th_1 for Various Intercept Points on 6000 n.m. Minimum Energy Trajectory

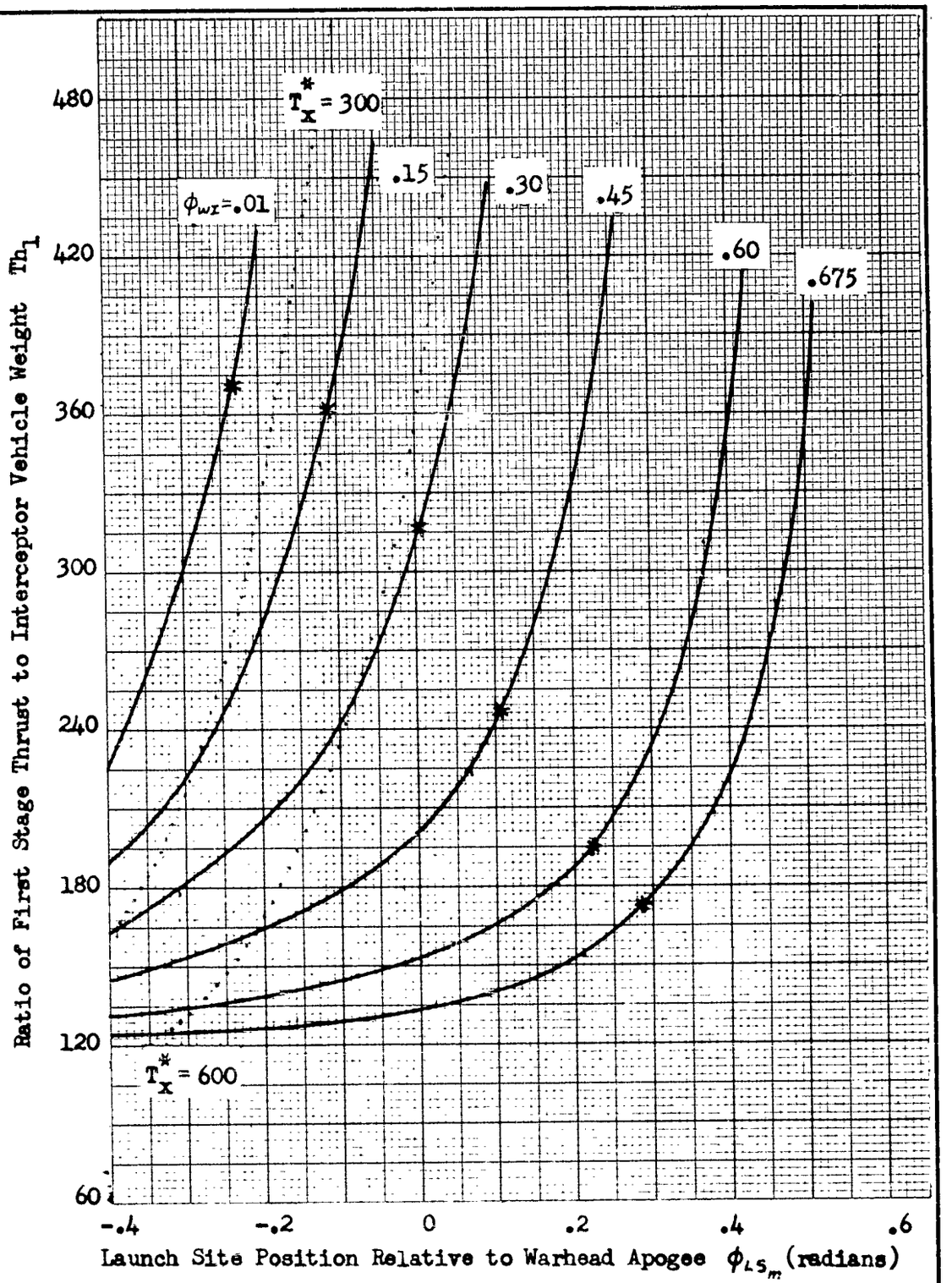

Fig. 6-11

The Effect of ϕ_{LS_m} on Th_1 for Various Intercept Points on 6000 n.m. High Angle Trajectory

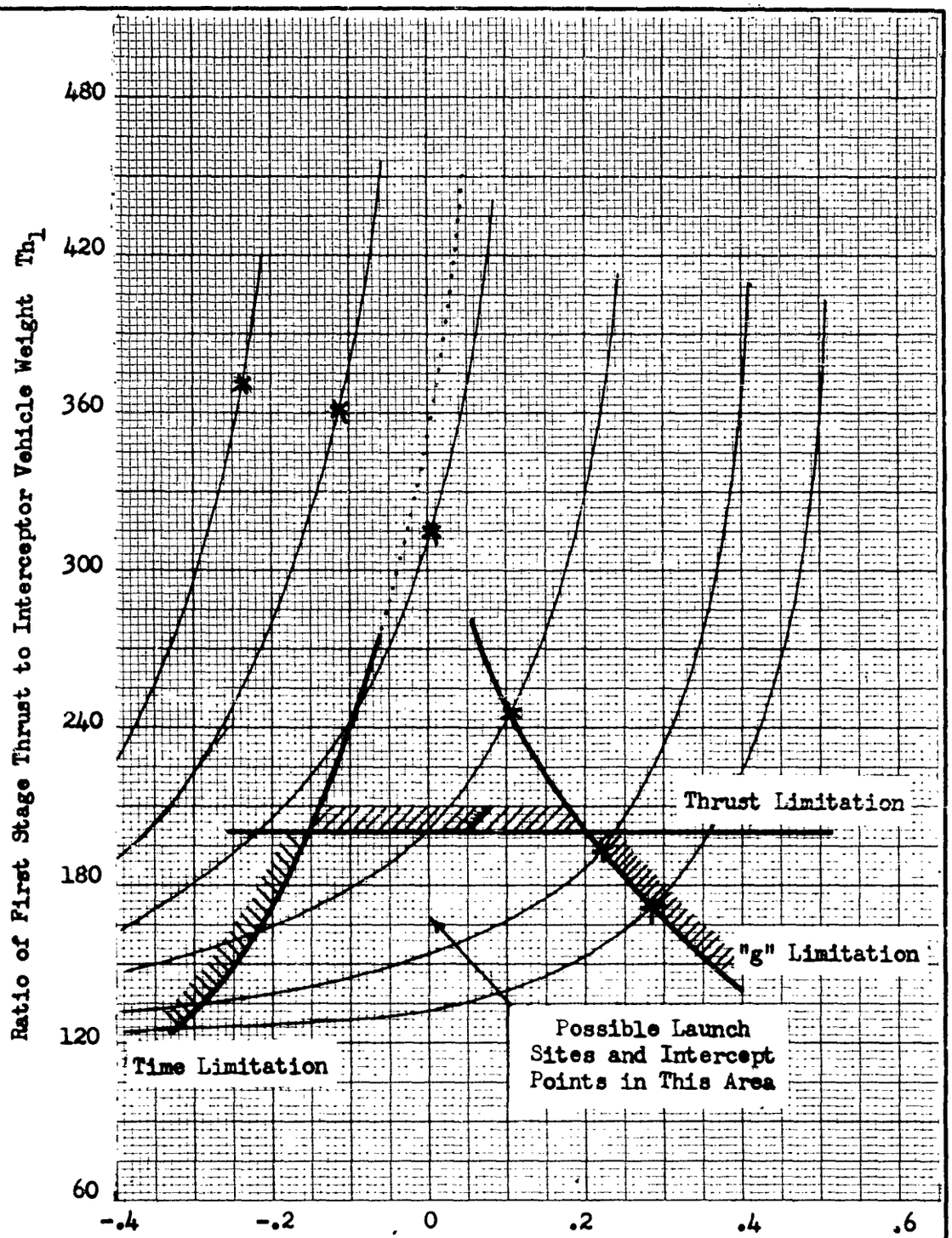

Fig. 6-11a

The Effect of Time, Thrust, and "g" Limitations on Location of Possible Launch Sites and Intercept Points

abscissa, proceeding vertically upward to the curve labeled 0.45, and then horizontally to the ordinate, we find that $Th_1 = 105$. We also see that the maximum acceleration is less than 10 g's and that the excess time is between 300 and 600 seconds. By using the same procedure, and Fig. 6-13, we find that $T_x^* = 410$ seconds. The first stage boost thrust required is

$$T_1 = Th_1 \, m_p = (105)(10{,}000) = 1{,}050{,}000 \text{ lb}$$

The overall weight of the interceptor system is

$$M_o = \frac{T_1}{\beta} = \frac{1{,}050{,}000}{1.5} = 700{,}000 \text{ lb}$$

As a second illustration let us suppose that our restrictions are $T_x^* = 600$ seconds and $\nu = 10$ g's, and we want to intercept a 6000 n.m. high-angle warhead trajectory. Then by referring to Fig. 6-11 we see that we are restricted to operate in the area between the 600 second dotted line and a curve joining the stars. This area defines the possible combinations of intercept point and launch site, and the corresponding values of Th_1 that meet the restrictions. Furthermore, suppose we have a 5000 pound interceptor vehicle, and a first-stage booster rocket with 1,000,000 pounds of thrust, giving us a Th_1 of 200. We are then further restricted to launch sites and intercept points below this horizontal line on Fig. 6-11. Figure 6-11a shows how these restrictions can limit the choice of intercept points and launch sites.

By comparing Figs. 6-9, 10, and 11 it is seen that as we progress from the low angle to the minimum energy to the high angle warhead trajectories, time and g-limitations become less restrictive but higher values of Th_1 are required. The curves of T_x^* (Figs. 6-12, 13, and 14) are also useful for determining the possible launch sites and intercept points for a given time restriction. If, for example, we detected an enemy missile on a 6000 n.m. minimum energy trajectory immediately after it was launched, and we required a minimum of 700 seconds to launch our interceptor system, then we are restricted to use values of ϕ_{WI} and ϕ_{LS_m} on the portions of the curves above a horizontal line at 700 seconds (Fig. 6-13).

Figures 6-15 through 6-20 show basically the same information for the 4000 mile warhead trajectories that was shown in Figs. 6-9 through 6-14 for the 6000 mile trajectories. The dotted-line isochrones are for T_x^* equal to 300 and 450 seconds. The absence of stars on some of the curves indicates that 10 "g's" was never exceeded for these cases. These curves show three important differences for the shorter range warhead trajectory : maximum acceleration is not as restrictive; lower thrusts are required; and time is much more critical. Figures 6-18, 19 and 20 show that for some intercept points near the warhead apogee, T_x^* becomes negative. This means that the interceptor flight time is greater than the warhead flight time, and that the interceptor must be launched <u>before</u> the warhead for these cases. Since this is quite impractical we can say in general that for shorter range enemy missiles, the intercept points must be located further down range, than for longer range trajectories. It is also

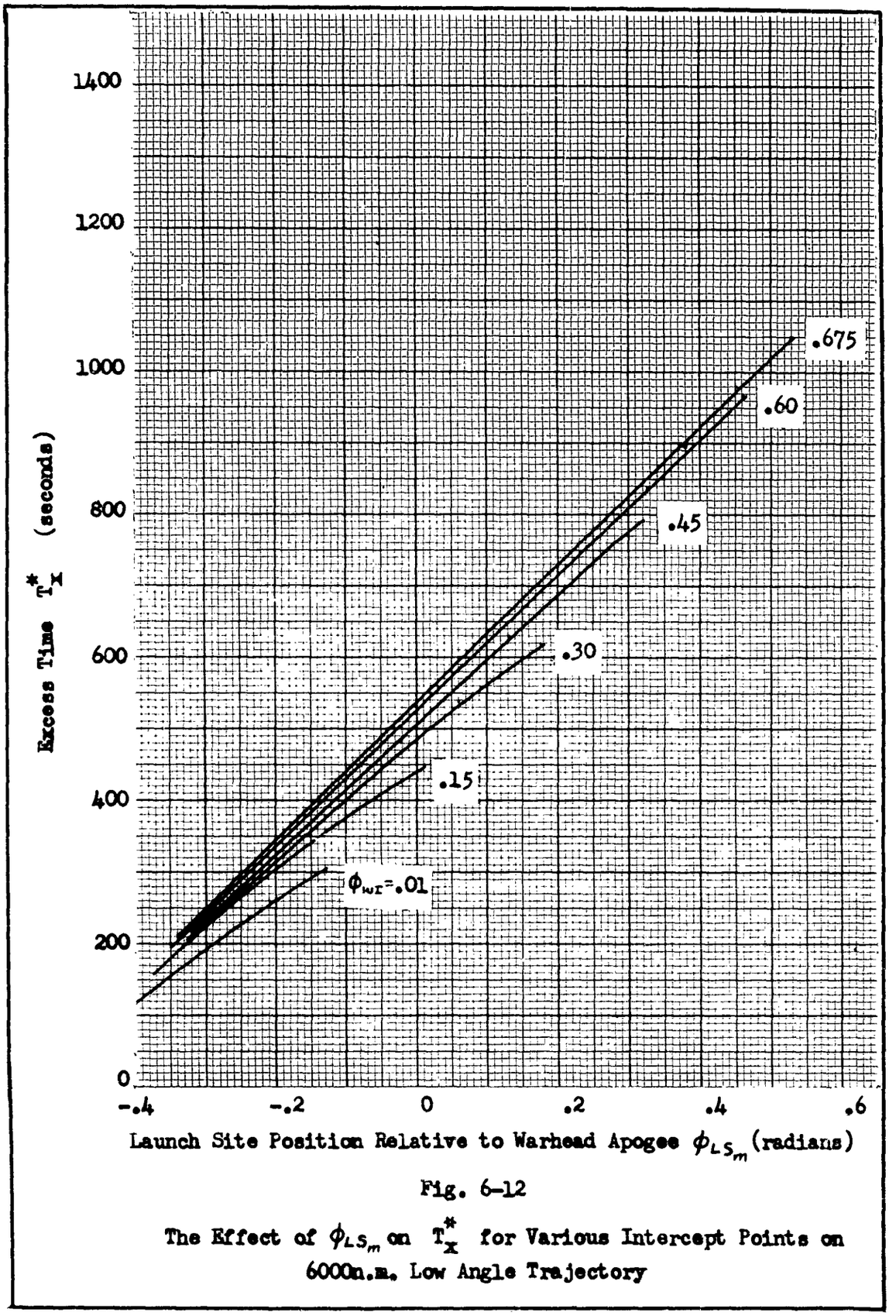

Fig. 6-12

The Effect of ϕ_{LS_m} on T_x^* for Various Intercept Points on 6000n.m. Low Angle Trajectory

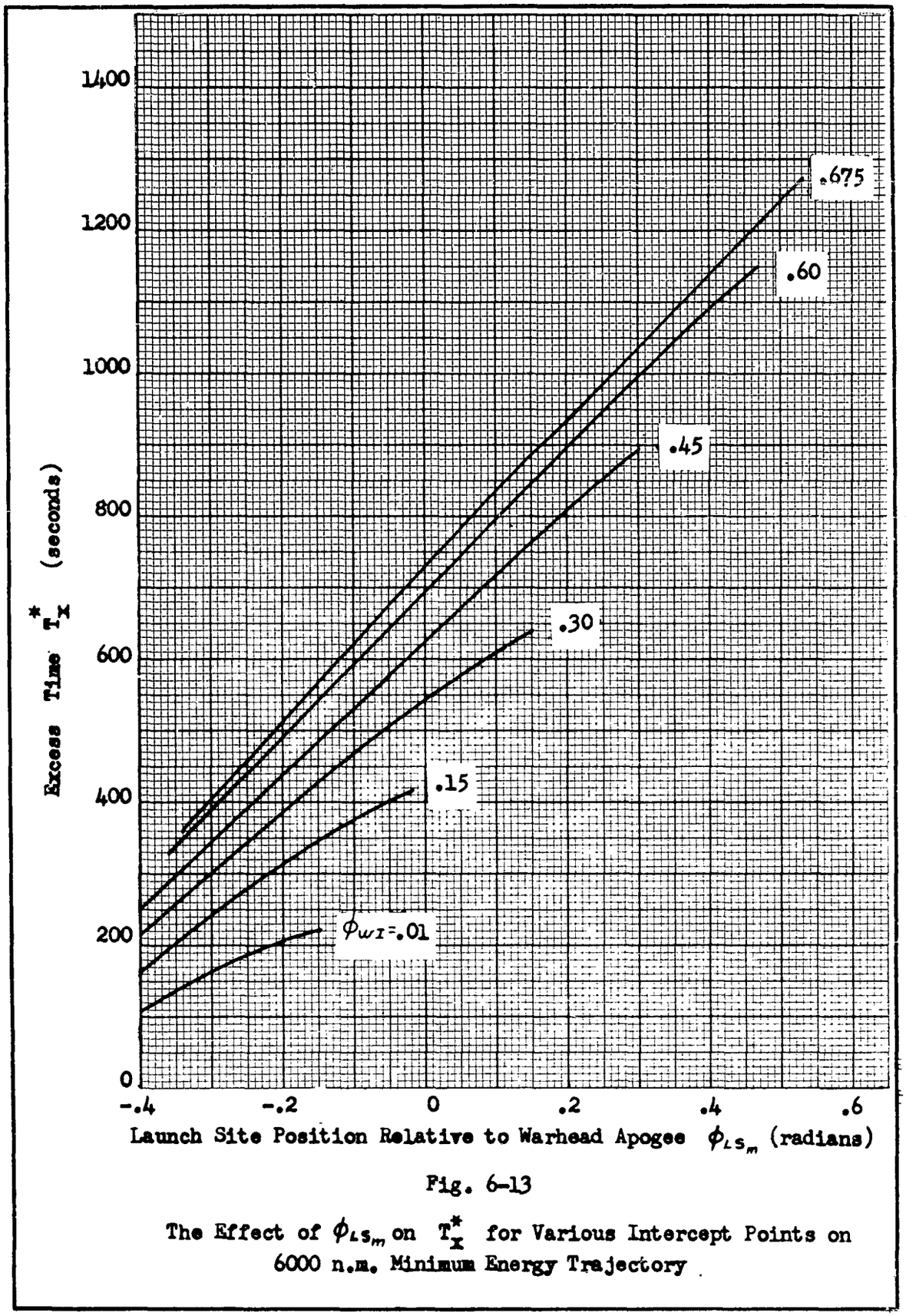

Fig. 6-13

The Effect of ϕ_{Ls_m} on T_x^* for Various Intercept Points on 6000 n.m. Minimum Energy Trajectory

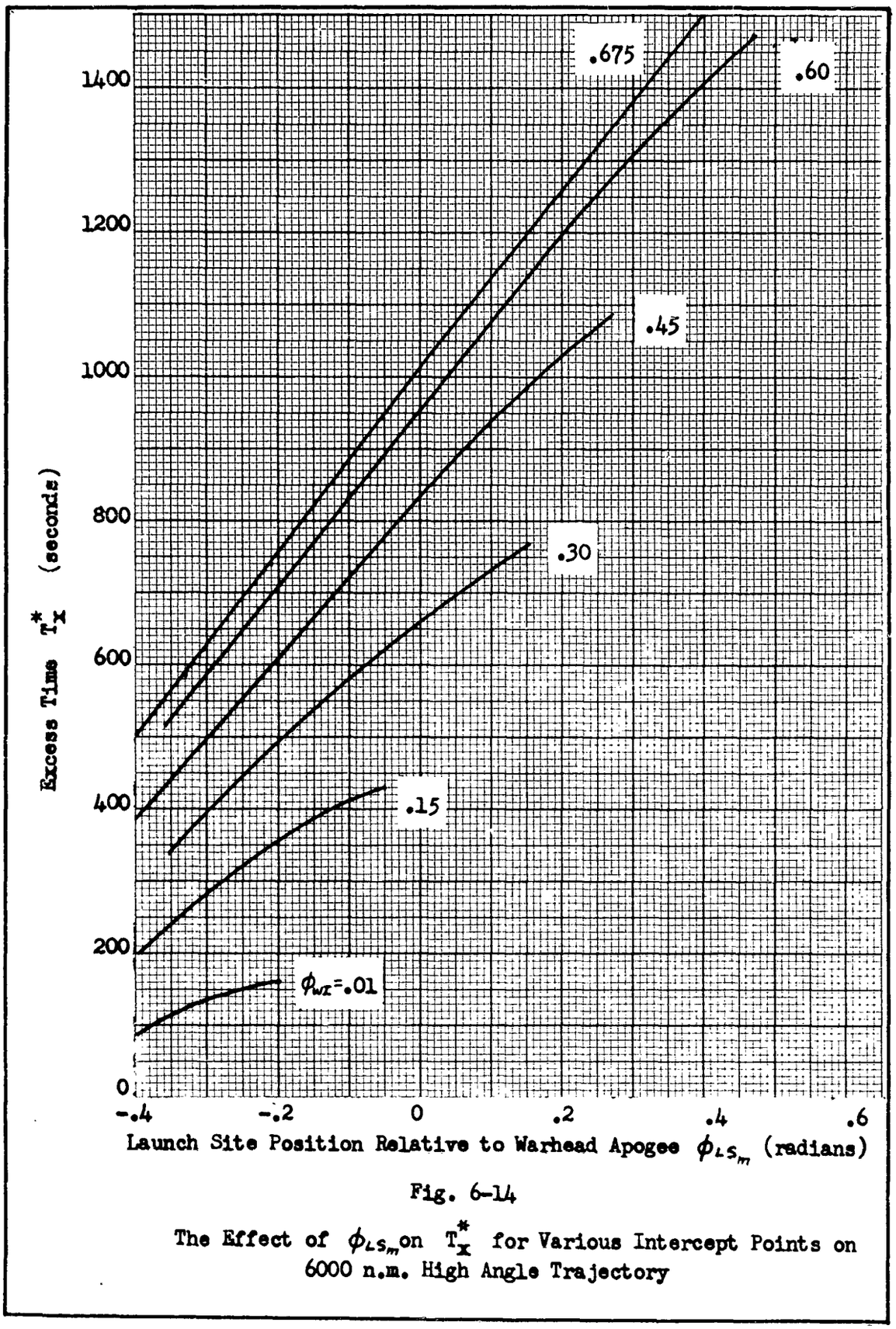

Fig. 6-14

The Effect of ϕ_{LS_m} on T_x^* for Various Intercept Points on 6000 n.m. High Angle Trajectory

reasonable to assume that the interception of an 8000 mile missile would: impose more severe g-limitations; require higher values of first-stage thrust; and increase the excess time.

Summary of Results

1. The thrust to initial weight ratio of the velocity-match rocket, β_u has a negligible effect on overall thrust requirements.
2. β_u has an appreciable effect on maximum accelerations for trajectories with small semi-range angles.
3. β_u has a negligible effect on excess time.
4. There is an optimum value of thrust to initial weight ratio of the boost sub-rockets, β, for each intercept condition which minimizes overall thrust requirements.
5. For values of β close to the optimum value, maximum accelerations are well below human tolerance limits.
6. A small increase in β causes an appreciable increase in excess time, especially for small semi-range angle trajectories.
7. Small increases in both structural factor and specific impulse greatly decrease overall thrust requirements.
8. Specific impulse has a much larger effect on thrust requirements than structural factor does.
9. An increase in specific impulse causes a negligibly small decrease in excess time.
10. Structural factor has no effect on excess time.
11. Excess time decreases as the launch site and intercept point are moved up-range.

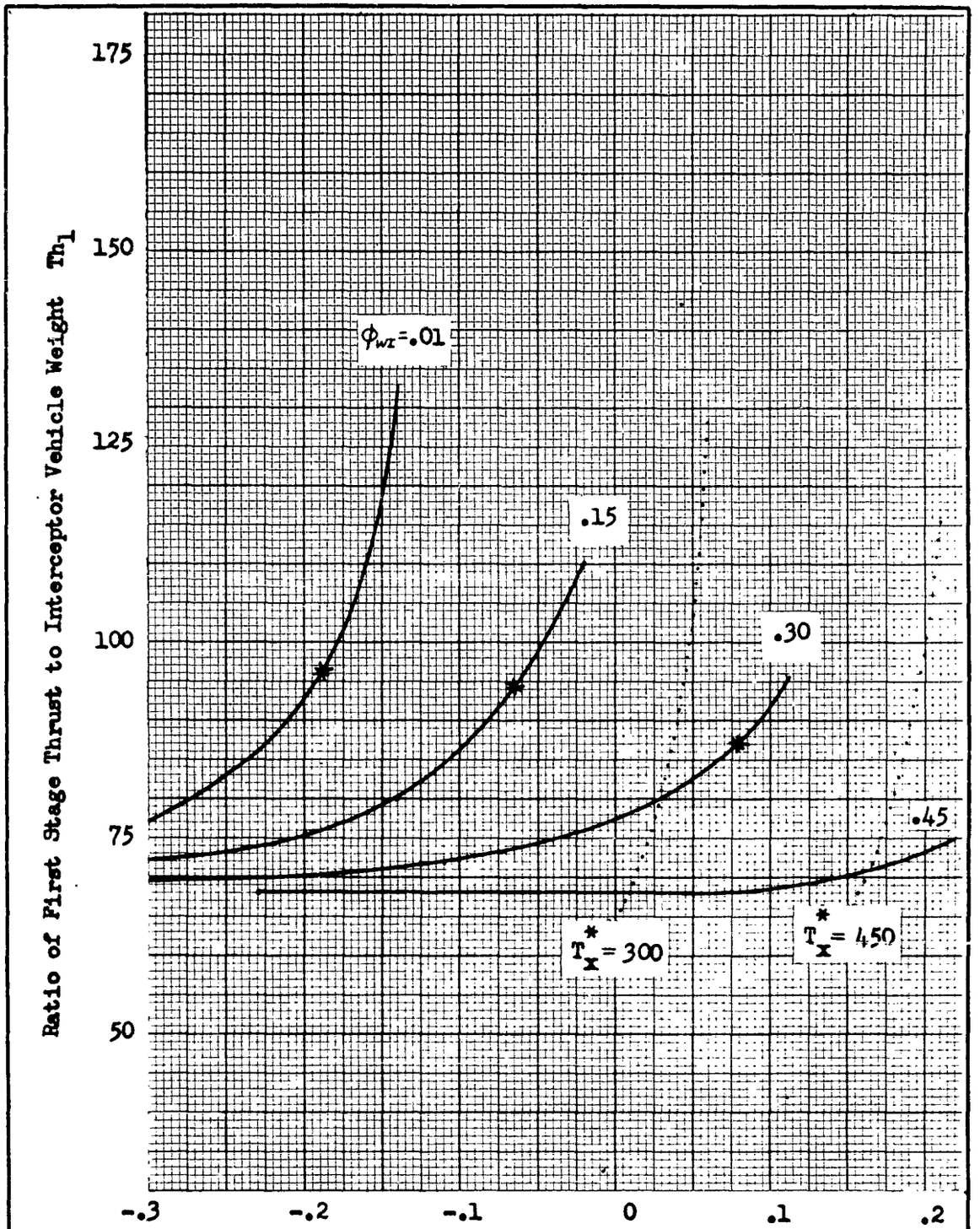

Fig. 6-15

The Effect of ϕ_{LS_m} on Th_1 for Various Intercept Points on 4000 n.m. Low Angle Trajectory

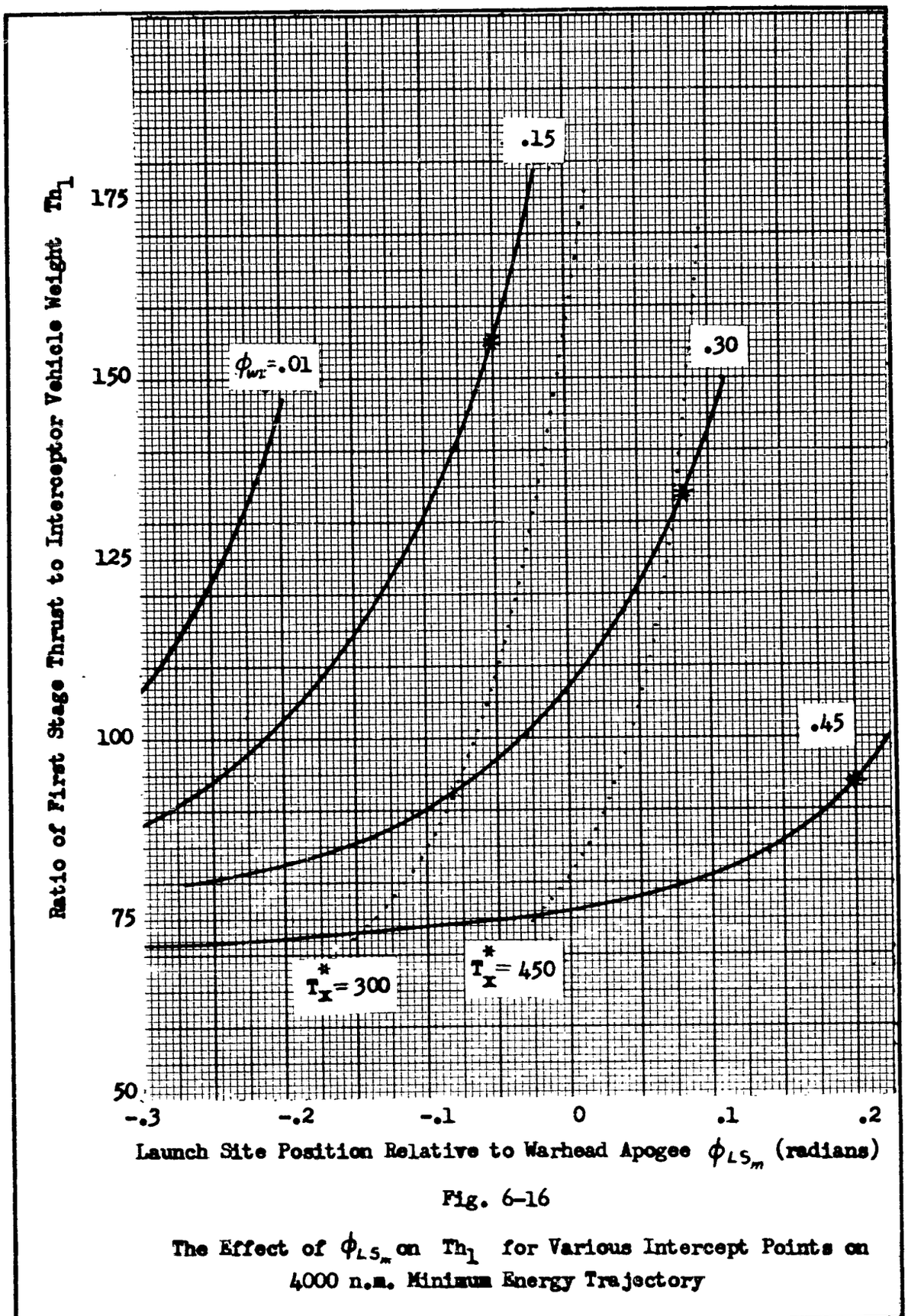

Fig. 6-16

The Effect of ϕ_{LS_m} on Th_1 for Various Intercept Points on 4000 n.m. Minimum Energy Trajectory

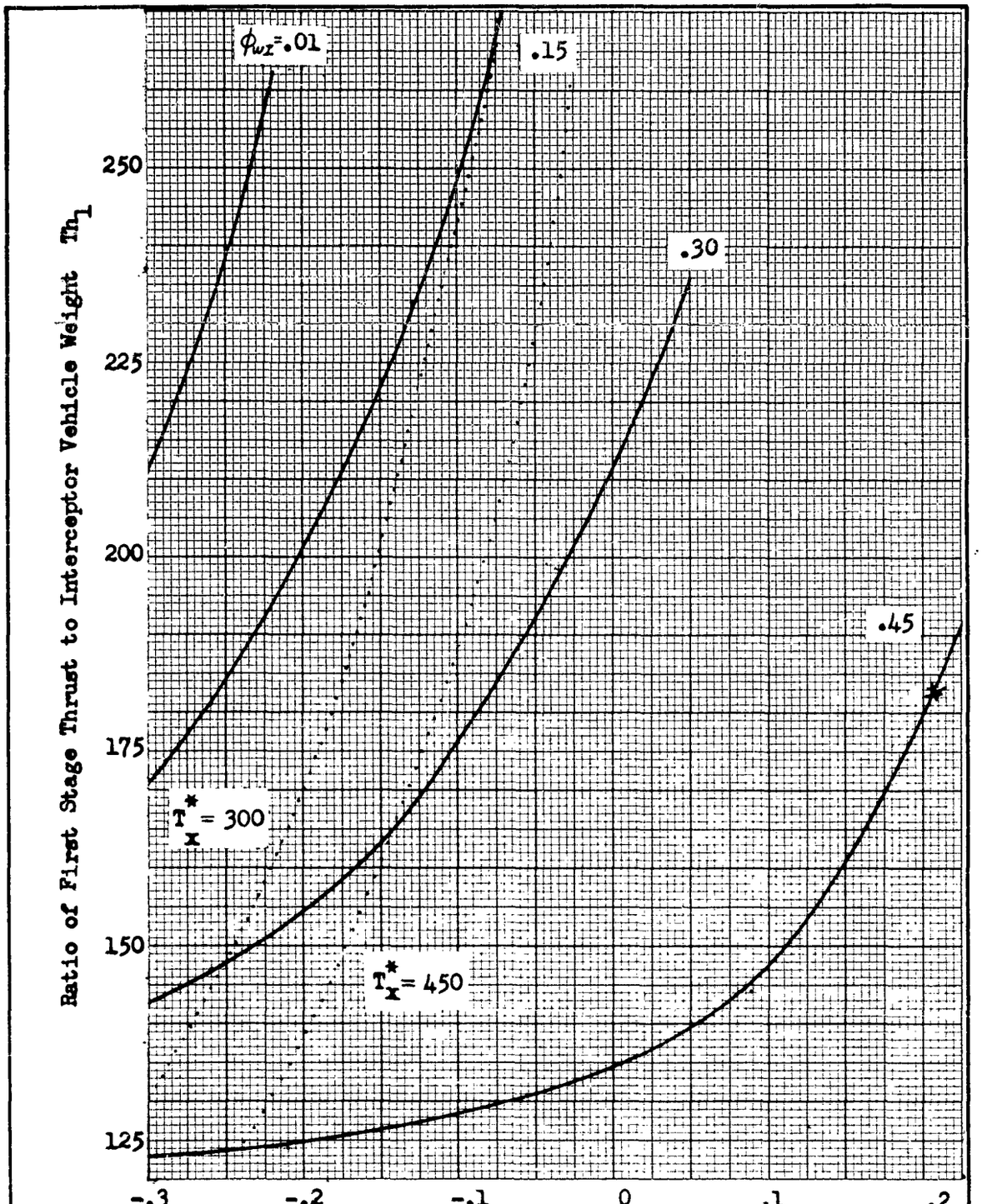

Fig. 6-17

The Effect of ϕ_{LS_m} on Th_1 for Various Intercept Points on 4000 n.m. High Angle Trajectory

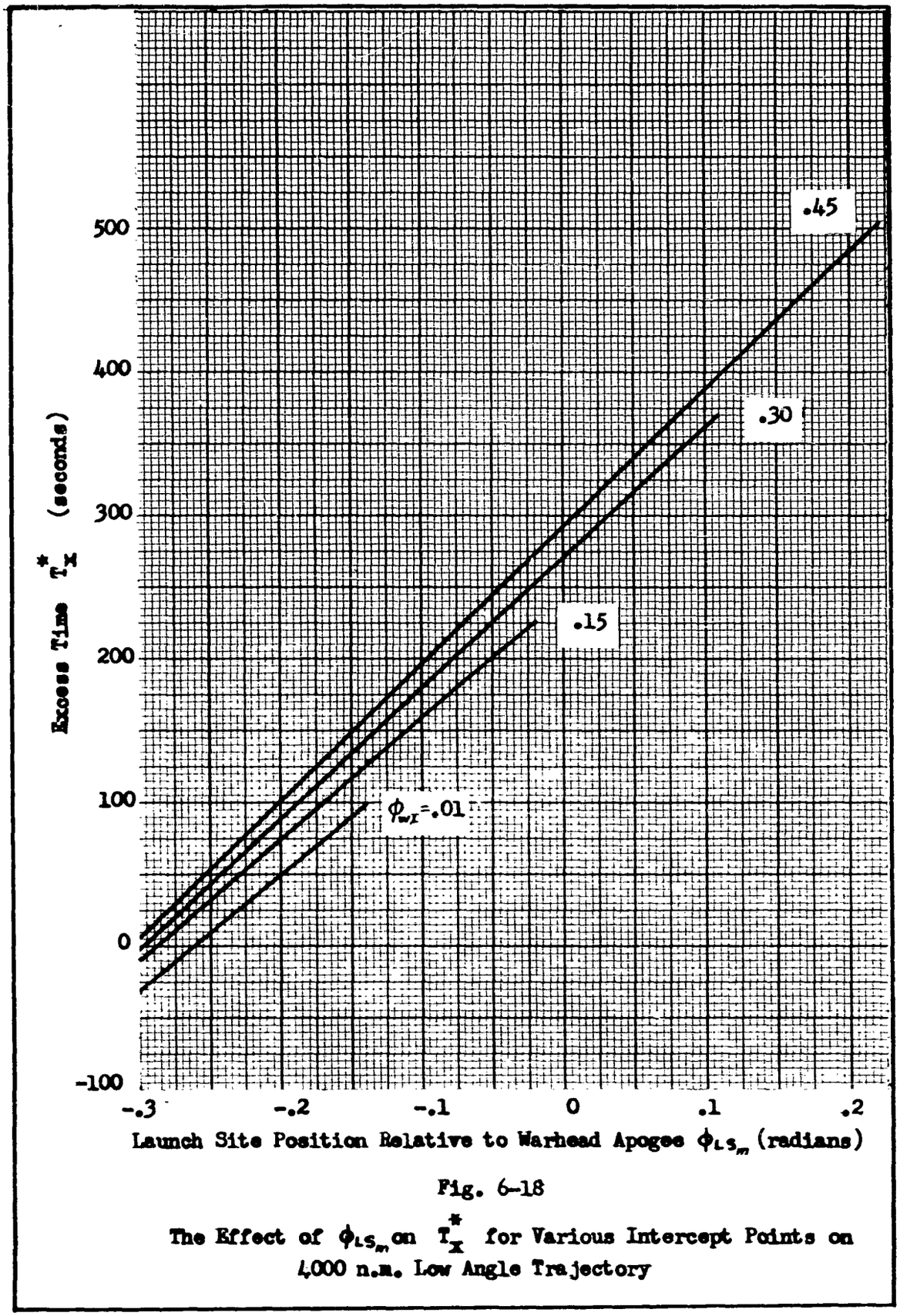

Fig. 6-18

The Effect of ϕ_{LS_m} on T_x^* for Various Intercept Points on 4,000 n.m. Low Angle Trajectory

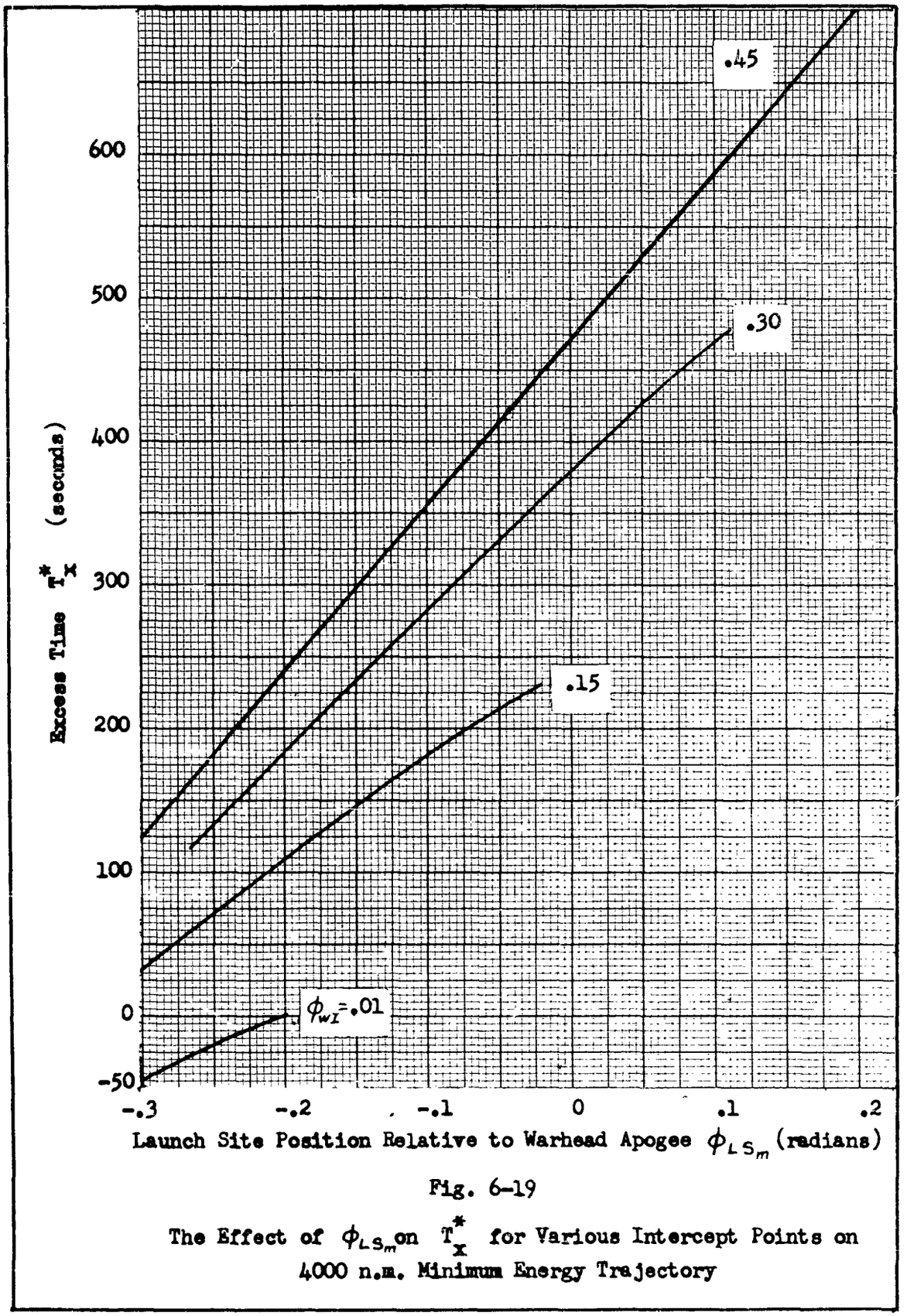

Fig. 6-19

The Effect of ϕ_{LS_m} on T_x^* for Various Intercept Points on 4000 n.m. Minimum Energy Trajectory

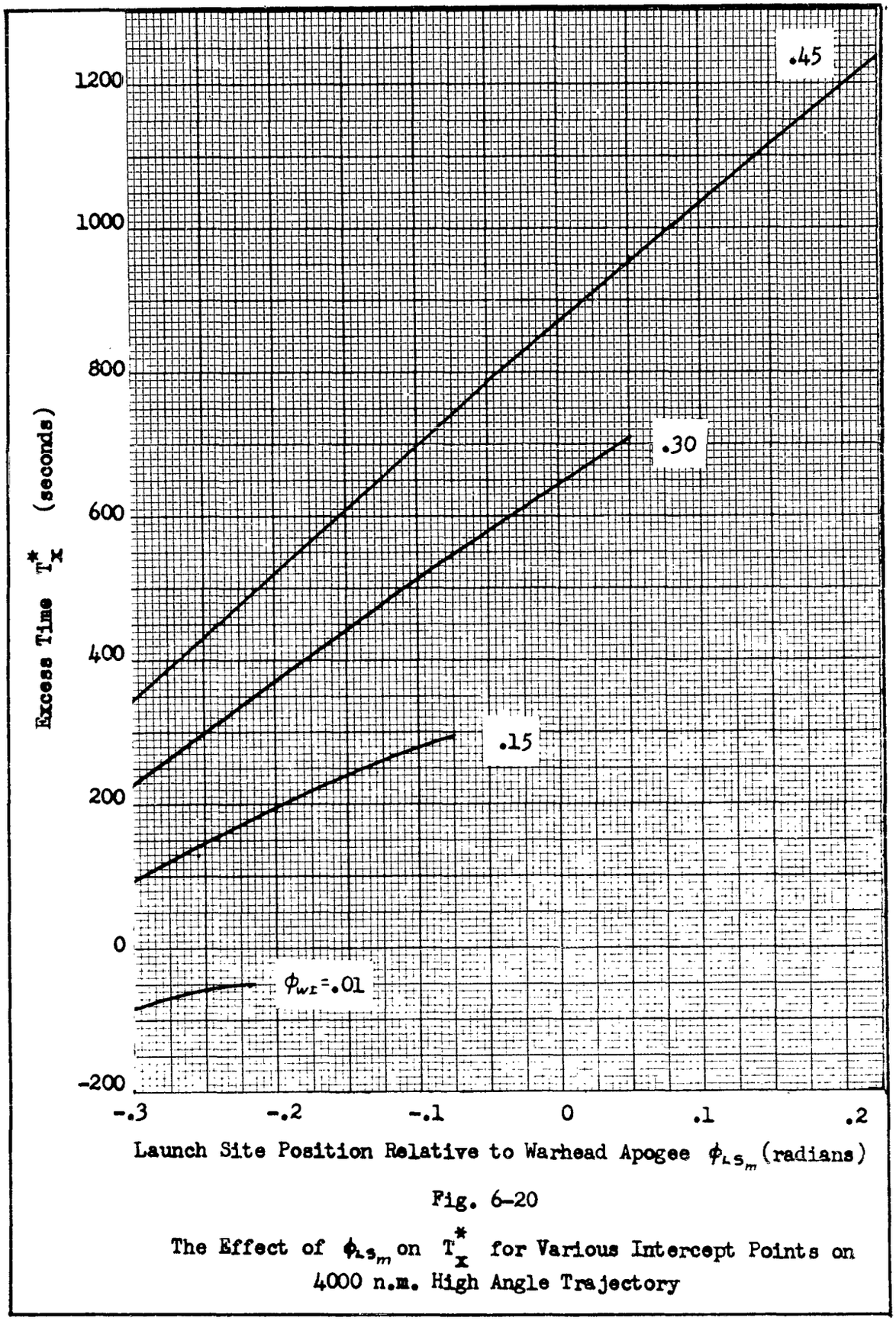

Fig. 6-20

The Effect of ϕ_{LS_m} on T_x^* for Various Intercept Points on 4000 n.m. High Angle Trajectory

12. Thrust and weight requirements increase as the launch site is moved down-range and intercept point is moved up range.
13. Thrust and weight requirements increase as the warhead trajectory altitude increases.
14. Excess time increases as warhead trajectory altitude increases.
15. Higher thrusts and weights are required to intercept longer range trajectories.
16. Excess time decreases as warhead range decreases.
17. Maximum acceleration increases as warhead range increases.
18. Time, thrust, and "g" limitations determine the possible intercept points and launch sites for a given warhead trajectory.
19. The validity of the assumptions made in obtaining the numerical results was verified for a typical intercept trajectory. This makes the graphs a useful tool for obtaining approximate thrust and weight requirements for any size of interceptor vehicle, for the intercept conditions considered.

Conclusions

The trajectory-match intercept technique appears to be theoretically feasible:

1. If first stage rocket engines of sufficient thrust to boost the interceptor vehicle onto the intercept trajectory are made available. Minimizing the weight of the interceptor vehicle is a major factor in satisfying this requirement.
2. If sufficient warning time is available from ballistic missile radar or satellite reconnaissance vehicles.

3. If low reaction times are possible for the interceptor system. One major requirement to meet this restriction is the use of solid or storable-liquid propellants.
4. If guidance systems are developed which can meet the requirements of this intercept technique.

Therefore it is recommended that further study of this technique be made for other warhead trajectories and for different combinations of the boost and velocity-match stages. This study could also be extended to the more realistic situation of a non-planar intercept over a rotating earth.

In addition, if the interceptor is to be manned, a study should be made of the methods which could be used for recovery of the vehicle. Two possibilities are a controlled skip-glide re-entry or a parachute recovery.

Even if all of the above requirements are met for this system, the final decision as to whether or not this intercept technique is the answer to the ICBM defense problem must be based upon an operational analysis, in terms of cost, technical and military manpower requirements, logistics, and many other factors. Thus, the trajectory-match, ICBM intercept technique appears to be theoretically feasible, but a more comprehensive study is necessary to determine if it is militarily practical.

List of References

1. Air Force Cambridge Research Center. Handbook of Geophysics. New York: The Macmillan Co., 1960.

2. Berman, Lawrence J. A Summary of Trajectory Studies for Long Range Ballistic Missiles. WADC TR 57-724. ASTIA Document No. AD 210561. Arlington, Va.: Armed Services Technical Information Agency, December 1958.

3. Bielkowicz, Peter. Notes on Exterior Ballistics, Ch. 15, Multi-Step Rockets. Wright-Patterson AFB, Dayton, Ohio: Aeronautical Engineering Dept., Air Force Institute of Technology, 1956.

4. Bondurant, Stuart, et al. Human Tolerance to Some of the Accelerations Anticipated in Space Flight. WADC TR 58-156. ASTIA Document No. AD 151172. Wright-Patterson AFB, Dayton, Ohio: Aero Medical Laboratory, Wright Air Development Center, April 1958.

5. International Business Machines Corp. IBM 1620 Fortran: Preliminary Specifications. White Plains, N.Y.: April 1960.

6. Lapp, Phillip A. Trajectory Studies. ScD Thesis, Report No. T-63. Cambridge, Massachusetts: Massachusetts Institute of Technology, 1955.

7. Nautical Almanac Office- U.S. Naval Observatory. The American Ephemeris and Nautical Almanac. Washington, D.C.: U.S. Government Printing Office, 1960.

8. Pierce, B.O. A Short Table of Integrals. (3rd Revised Edition). New York: Ginn and Co., 1929.

9. Ralston, Anthony and H.S. Wilf. Mathematical Methods for Digital Computers. New York: John Wilie and Sons Inc., 1960.

10. Sutton, George P. Rocket Propulsion Elements. (Second Edition) New York: John Wiley and Sons, Inc., 1956.

11. Ten Dyke, R.P. Preliminary Design of Rocket Systems. GM-TR-112. Los Angeles, California: Ramo-Wooldridge Corp., 15 July 1957.

12. Traenkle, C.A. Mechanics of the Power and Launching Phase for Missiles and Satellites. WADC TR 58-579. Wright-Patterson AFB, Dayton, Ohio: Aeronautical Research Laboratory, Wright Air Development Center, Sept 1958.

13. Wolover, Lynn E. Ballistic Trajectories Above a Spherical Non-Rotating Earth. WCLJY Internal Memo 57-13. Wright-Patterson Air Force Base, Dayton, Ohio: Aeronautical Research Laboratory, Wright Air Development Center, Sept 1957.

14. Wylie, C.R. Jr. Advanced Engineering Mathematics. New York: McGraw-Hill Book Co. Inc., 1951.

Appendix A

Computer Programs

The computer programs used in this analysis are written in IBM 1620 Fortran Language (Ref 5) for use on the IBM 1620 digital computer. The instructions for the use of these programs are given in this appendix. The actual Fortran Language Program follows each set of instructions. The paper tapes for these computer programs are on file with the Mechanics Department of the Institute of Technology, Wright-Patterson Air Force Base, Ohio.

The values of r_o and μ used in these programs are (Ref 7:430):

$$r_o \text{ (average)} = 3437.747 \text{ nautical miles}$$

$$\mu = 62{,}628. \text{ (nautical miles)}^3/\text{(second)}^2$$

Program: CM-3 General Trajectory Evaluation

This program gives the values for r, v, and γ for any desired position, ϕ, on the ballistic trajectory. It also gives the time of flight between apogee and ϕ.

Operating Instructions.

1. When the computer prints the number (1), the inputs are ϕ_o and γ_o of the trajectory.
2. When the computer prints the number (2), the inputs are the general angle ϕ, which defines the point to be investigated, and $\Delta\phi$, which allows the computer to automatically increase ϕ by $\Delta\phi$ after each computation. This gives the option of determining the values for regular intervals on the trajectory. However, if only one point is desired, make $\Delta\phi$ greater than

ϕ_o, since some value of $\Delta\phi$ must be inserted into the computer memory. When ϕ becomes greater than ϕ_o, the computer sets ϕ equal to ϕ_o, calculates the values, and then returns to the start of the program (ready to accept new values of ϕ_o and γ_o).

3. The results are typed in the following order: ϕ, T^*, r, γ, and v.

4. To change either ϕ or $\Delta\phi$ at any time, turn "Sense Switch 1" on. The computer will then print the number (1), and new values can be inserted in the memory.

Fortran Language Program GM-3

```
U=62628.
RO=3437.747
 5 M=1
PRINT,M
ACCEPT,PO,GA
 IF(PO) 1,2,1
1 E=1.0/(COS(PO)+(SIN(PO))*(COS(GA))/(SIN(GA)))
HS=U*RO*(1.0-E*(COS(PO)))
H=SQR(HS)
W=1.0-(E**2.)
G=(H**3.)/((U**2.)*W)
P=(H**2.)/U
 Z=(SQR(W))/(1.0-E)
Q=2.0/(SQR(W))
6 M=2
PRINT,M
ACCEPT,X,DELTX
8 S=(-E)*(SIN(X))/(1.0-E*(COS(X)))
Y=Z*(SIN(X/2.))/(COS(X/2.))
T=G*(-S+Q*(ATN(Y)))
R=P/(1.0-E*(COS(X)))
A=ATN(S)
V=H/(R*(COS(A)))
PRINT,X,T,R,A,V
IF(SENSE SWITCH 1) 6,7
7 IF(X-PO) 4,5,4
4 X=X+DELTX
IF(X-PO) 8,5,3
3 X=PO
GO TO 8
END
```

Program: CM-11 Combined Boost-Phase and Intercept Analysis

This program contains the intercept and trajectory geometry, rocket equations of motion, and boost-phase approximation equations. These equations are combined as outlined in Chapter IV to give the complete solution to the intercept problem.

Operating Instructions.

1. When the computer prints the number (1), the inputs are n, I_s and β_u.
2. When the computer prints the number (2), the inputs are β and k.
3. When the computer prints the number (3), the inputs are ϕ_{wo} and γ_{wo}.
4. When the computer prints the number (4), the input is ϕ_{wI}.
5. When the computer prints the number (5), the input is ϕ_{mc}.
6. Now the computer solves the problem. The results (for k = 3) will be typed in the order listed below:

ϕ_{moa}	γ_{moa}	ϕ_b	ϕ_{mIa}	ϕ_{LIA}
t_{b_u}	kt_b	ν	ν_u	λ
ψ_u	ψ_o	ψ_1	ψ_2	ψ_3
Th_u	Th_1	Th_2	Th_3	

7. The computer will pause after each line, and the start button must be pushed to continue the computation.
8. When the computation is complete, the operator has several options as to which part of the program the computer will go to for the next set of intercept conditions to be investigated.

These options are controlled by the sense switches as follows:

Change	SW 1	SW 2	SW 3
ϕ_{mo}	Off	--	--
ϕ_{wI}	On	Off	--
β or k	On	On	Off
ϕ_{wo} or γ_{wo}	On	On	On

Program: CM-12 Runge-Kutta Integration

This program is designed to numerically integrate the boost-phase rocket equations of motion for a three stage rocket as a check on the results of the boost-phase approximations.

Operating Instructions.

1. When the computer prints the number (1), the inputs are I_s, β, and t_b.
2. When the computer prints the number (2), the inputs are Th_1, A_1, Th_2, A_2, Th_3, and A_3.
3. When computer prints the number (3), input t_v (duration of vertical flight segment), α (angle between thrust vector and velocity vector during tip-over phase), and Γ (flight path angle where tip-over is complete and α is set equal to zero).
4. When computer prints number (6), input initial conditions for: t (usually zero); $\dot{\phi}$ (usually zero); $\dot{r}$ (usually zero); ϕ_{LS} (usually - ϕ_{moa}); r (usually r_o); and γ_o (usually $\pi/2$).
5. Turn Sense Switch 1 on.
6. When computer prints number (4), input Δt, the incremental time interval of the integration.

7. When computer prints number (5), turn Sense Switch 1 Off. Then input Δt (again), and h, (the factor which determines the print-out interval). The results are printed out for time intervals equal to $h \Delta t$, and are in the following order: t, ϕ , r, γ, and v.

Fortran Language Program CM-11

```
D=3.
TD=1.0E-12
TR=1.0
U=62628.
RE=3437.747
 PIE=3.1415927
M=1
PRINT,M
ACCEPT,F,Z,BU
21 M=2
 PRINT,M
 ACCEPT,B,Q
20 M=3
PRINT,M
ACCEPT,POW,GOW
SPOW=SIN(POW)
CPOW=COS(POW)
SGOW=SIN(GOW)
CGOW=COS(GOW)
AA=SPOW*CGOW/SGOW
EW=1.0/(CPOW+AA)
HWS=U*RE*(1.0-EW*CPOW)
HW=SQR(HWS)
AB=HWS/U
 19 M=4
 PRINT,M
 ACCEPT,PWI
4 SXA=SIN(PWI)
CXA=COS(PWI)
AC=1.0-EW*CXA
AG=EW*SXA/AC
RI=AB/AC
 GI=ATN(AG)
CGI=COS(GI)
VWI=HW/(RI*CGI)
16 M=5
PRINT,M
ACCEPT,PO
ZZ=((RI/RE)-1.0)/AG
CPO=COS(PO)
ZA=SQR(ZZ*ZZ+1.0)
CAZ=CPO/ZA
SAZ=SQR(1.0-CAZ*CAZ)
AZ=-ATN(SAZ/CAZ)
ZB=ATN(ZZ)
 PI=AZ-ZB
SPI=SIN(PI)
CPI=COS(PI)
E=AG/(AG*CPI+SPI)
```

```
HS=U*RE*(1.0-E*CPO)
H=SQR(HS)
VI=H/(RI*CGI)
DVI=VWI-VI
 GC=U/(RE*RE)
EV=Z*GC
DLU=DVI/EV
 DU=EXP(DLU)
WOU=(F-1.)*DU/(F-DU)
WU=WOU-1.
TBU=EV*(DU-1.)/(GC*BU*DU)
QQ=EV*EV*(DU-1.-DLU)/(GC*BU*DU)
AJ=(PIE/2.)-GI
SAJ=SIN(AJ)
CAJ=COS(AJ)
TAK=SAJ/((QQ/RI)-CAJ)
AK=ATN(TAK)
DPI=PIE-AK-AJ
SAK=SIN(AK)
RIA=RI*SAJ/SAK
GIA=AK-(PIE/2.)
CGIA=COS(GIA)
HA=VI*RIA*CGIA
HAS=HA*HA
 REC=HAS/U
ET=(VI*VI/2.)-(U/RIA)
EAS=1.+(2.*ET*REC/U)
EA=SQR(EAS)
AL=U*RE
AM=U*RIA
CPOA=(AL-HAS)/(AL*EA)
CPIA=(AM-HAS)/(AM*EA)
SPOA=SQR(1.-CPOA*CPOA)
SPIA=-SQR(1.-CPIA*CPIA)
POA=ATN(SPOA/CPOA)
PIA=ATN(SPIA/CPIA)
AFL=POA-PIA+DPI
TGO=EA*SPOA/(1.-EA*CPOA)
GO=ATN(TGO)
PB=0.9*POA
DA=0.1*POA
SPB=SIN(PB)
CPB=COS(PB)
12 AN=1.-EA*CPB
TGB=EA*SPB/AN
GB=ATN(TGB)
CGB=COS(GB)
 GBR=GB-DA
SB=SIN(GBR)
CB=COS(GBR)
RB=REC/AN
 VB=HA/(RB*CGB)
VX=VB*CB
 8 DD=D-1.
```

```
DL=LOG(D)
UK=EV*Q
UU=EV*UK
QW=Q-1.
 DB=D*B
YY=DD*CB/(DB*DL)
YZ=SQR(1.-YY*YY)
AP=ATN(YY/YZ)
A=AP+GBR
 SA=SIN(A)
CA=COS(A)
FD=UK*DL*CA-VX
IF(FD*FD-TD) 1,1,2
2 DFA=DD*CA+YY*(DD-DL)*SA/YZ
DFD=UK*DFA/(D*DD)
D=D-(FD/DFD)
GO TO 8
1 AQ=2.*(DD-DL)+QW*DD*DL
AR=UU/(2.*GC*DB)
XC=AR*CA*AQ
YC=AR*SA*AQ-AR*Q*DD*DD/DB
DA=ATN(XC/(YC+RE))
SDA=SIN(DA)
RBA=XC/SDA
IF(RB-RBA) 3,7,9
3 RC=RBA-RB
 GO TO 10
9 RC=RB-RBA
 10 IF(RC-TR) 7,7,11
11 RB=RBA
CPB=(1.-REC/RB)/EA
SPB=SQR(1.-CPB*CPB)
PB=ATN(SB/CPB)
GO TO 12
 7 TB=UK*DD/(GC*DB)
GOO=GO
PBB=PB
 PIAA=PIA
AFLI=AFL
PRINT,POA,GOO,PBB,PIAA,AFLI
PAUSE
DBB=DB
DBU=DU*BU
 ALF=A
PRINT,TBU,TB,DBB,DBU,ALF
PAUSE
AW=(F-1.)*D/(F-D)
WOB=AW*AW
AS=1.-(1./AW)
AU=B/AS
THU=BU*WOU
IF(Q-2.) 13,13,14
13 W1B=WOB*AS
 W2B=(WOB-W1B)*AS
```

```
W0=W0B*W0U
W1=W1B*W0U
W2=W2B*W0U
PRINT,WU,W0,W1,W2
PAUSE
TH1=W0*B
TH2=AU*W2
PRINT,THU,TH1,TH2
GO TO 15
14 W0B=W0B*AW
W1B=W0B*AS
W2B=(W0B-W1B)*AS
W3B=(W0B-W1B-W2B)*AS
W0=W0U*W0B
W1=W0U*W1B
W2=W0U*W2B
 W3=W0U*W3B
PRINT,WU,W0,W1,W2,W3
PAUSE
TH1=W0*B
TH2=AU*W2
TH3=AU*W3
PRINT,THU,TH1,TH2,TH3
15 PAUSE
IF(SENSE SWITCH 1) 17,16
17 IF(SENSE SWITCH 2) 18,19
18 IF(SENSE SWITCH 3) 20,21
END
```

```
PI=3.1415927
EL=LOG(10.)
U=62628.
FM=6080.2011
RE=3437.747
DIMENSION A(4),E(4),C(4),TH(3),Q(5),X(5),Y(5),S(3)
AL=0.
 GC=U/(RE*RE)
M=1
 PRINT,M
ACCEPT,Z,B,TB
EV=Z*GC
 ZB=Z/B
 M=2
PRINT,M
DO 3 K=1,3
 3 ACCEPT,TH(K),S(K)
17 M=3
PRINT,M
ACCEPT,TV,AA,AP
DD=0.
AZ=SQR(0.5)
A(1)=0.5
A(2)=1.-AZ
A(3)=1.+AZ
A(4)=1./6.
 E(1)=2.
E(2)=1.
 E(3)=1.
 E(4)=2.
C(1)=0.5
C(2)=A(2)
C(3)=A(3)
 C(4)=0.5
DO 2 I=1,5
 2 Q(I)=0.
M=6
 PRINT,M
DO 80 I=1,5
80 ACCEPT,Y(I)
ACCEPT,GM
 L=11
K=1
N=1
M=4
PRINT,M
ACCEPT,H
J=1
37 V=SQR(Y(3)*Y(3)+Y(5)*Y(5)*Y(2)*Y(2))
GO TO (52,53,54),N
53 D=0.
 TF=GM-Y(4)
 N=3
```

```
GO TO 4
 54 TA=TF+Y(4)
GO TO 70
52 VV=V*FM
HT=Y(5)-RE
HA=HT-86.67
HB=HT-6.0855
HC=HT-13.487
HD=HT-25.658
HE=HT-28.783
HF=HT-43.586
IF(HA) 18,18,19
18 RH=1./(EXP(EL*(2.624+.10818048*HT)))
GO TO 20
 19 RH=1./(EXP(EL*(12.+.01142854*HA)))
20 IF(HB) 21,22,22
21 AM=.18362-.0040095*HT
GO TO 40
 22 IF(HC) 23,23,24
23 AM=.15922
GO TO 40
 24 IF(HD) 25,26,26
25 AM=.15922+.0018602*HC
GO TO 40
26 IF(HE) 27,27,28
27 AM=.18186
GO TO 40
 28 IF(HF) 29,30,30
29 AM=.18186-.0028798*HE
GO TO 40
30 AM=.13923
40 AN=V/AM
 IF(AN-.6) 31,31,32
31 CD=.25
GO TO 41
32 IF(AN-1.6) 33,34,34
33 CD=AN-.35
GO TO 41
34 IF(AN-2.9) 35,36,36
35 CD=1.73-.3*AN
GO TO 41
36 CD=.86
 41 D=.5*CD*RH*VV*VV*S(K)
4 TA=AL+GM
 70 ST=SIN(TA)
CT=COS(TA)
SG=SIN(GM)
CG=COS(GM)
X(1)=1.
GO TO (73,74,75),K
73 TS=Y(1)
GO TO 76
74 TS=Y(1)-TB
 GO TO 76
```

```
75 TS=Y(1)-2.*TB
76 X(2)=EV*(CT-D*CG/(TH(K)))/(Y(5)*(ZB-TS))-2.*Y(3)*Y(2)/(Y(5))
X(3)=EV*(ST-D*SG/(TH(K)))/(ZB-TS)+Y(5)*Y(2)*Y(2)-U/(Y(5)*Y(5))
X(4)=Y(2)
X(5)=Y(3)
DO 1 I=1,5
WZ=A(J)*(X(I)-E(J)*Q(I))
Y(I)=Y(I)+H*WZ
1 Q(I)=Q(I)+3.*WZ-C(J)*X(I)
IF(Y(2)) 71,72,71
71 TG=Y(3)/(Y(5)*Y(2))
GM=ATN(TG)
 72 J=J+1
 IF(J-4) 37,37,5
5 J=1
IF(Y(1)-TV) 6,7,7
7 IF(GM-AP) 8,8,9
9 AL=AA
GO TO 10
8 AL=0.
10 IF(Y(1)-TB) 6,11,11
11 IF(Y(1)-2.*TB) 97,98,98
97 K=2
 IF(L-22) 95,6,6
95 L=22
GO TO 99
98 IF(Y(1)-3.*TB) 96,93,93
96 K=3
 IF(L-33) 94,6,6
94 L=33
 GO TO 99
93 K=4
L=44
99 PRINT,L
6 IF(SENSE SWITCH 1) 12,13
12 M=5
PRINT,M
ACCEPT,HG,HH
H=HG
 HP=Y(1)+H*(HH-1.)
13 IF(Y(1)-HP) 14,15,15
15 PRINT,Y(1),Y(4),Y(5),GM,V
HP=Y(1)+H*HH
14 IF(K-3) 50,50,16
50 IF(N-1) 49,49,37
49 IF(D-DD) 38,39,39
39 DD=D
GO TO 37
38 IF(D/(TH(K))-.0001) 51,37,37
51 N=2
GO TO 37
16 IF(SENSE SWITCH 3) 3,17
END
```

Appendix B

Check on the Validity of the Boost-Approximations

A numerical integration of the equations of motion of a rocket was performed for one intercept trajectory to determine the validity of the many approximations made in Chapter IV.

The intercept point was chosen to be 0.45 radians down-range from apogee on the 6000 n.m. minimum-energy trajectory. For this point the following information was obtained by using computer program CM-3 (Appendix A):

$$\phi_{wI} = 0.45 \text{ radian}$$

$$r_I = 3917.301 \text{ n.m.}$$

$$\gamma_I = -0.23128 \text{ radian}$$

$$v_{wI} = 3.3681 \text{ n.m. per sec}$$

The design program, CM-11, was used to obtain the following information:

Computer inputs.

$$I_s = 250 \text{ sec}$$

$$n = 10$$

$$\beta_u = 3.0$$

$$\beta = 1.5$$

$$k = 3$$

$$\phi_{mo} = 0.500 \text{ radian}$$

Computer print-outs.

$$\phi_{moa} = 0.50139 \text{ rad}$$

γ_{moa} = 0.50623 rad

ϕ_b = -.41069 rad

ϕ_{mIa} = 0.18201 rad

ϕ_{LIA} = 0.68583 rad

t_{bu} = 32.498 sec

Kt_b = 319.87 sec

ν = 4.1637 "g"

ν_u = 4.9178 "g"

λ = 0.73021 rad

Ψ_u = 0.76462

Ψ_o = 72.974

Ψ_1 = 51.872

Ψ_2 = 15.000

Ψ_3 = 4.3376

Th_u = 5.2939

Th_1 = 109.46

Th_2 = 31.654

Th_3 = 9.1534

By inputting the corrected semi-range angle (ϕ_{moa}) and launch angle (γ_{moa}) for the intercept trajectory, a print out was obtained for points along this trajectory, by using program CM-3.

An interceptor vehicle weight of 10,000 pounds (m_p) was chosen, and by using the above data the boost-stage thrusts, stage weights, and overall system weight were determined to be:

T_1 = 1,094,600. lb

T_2 = 316,540. lb

T_3 = 91,534. lb

M_o = 729,740. lb

m_1 = 518,720. lb

m_2 = 150,000. lb

m_3 = 43,376. lb

The burning times of the three boost stages are equal, and are

$$\frac{k\, t_b}{3} = 106.62 \text{ sec}$$

The total impulse can be calculated by multiplying the thrust of each stage by the burning time of each stage.

Stage 1.	5.84×10^4	ton seconds
Stage 2.	1.68×10^4	ton seconds
Stage 3.	0.49×10^4	ton seconds
Total	8.01×10^4	ton seconds

The equations of motion used are (Ref 2:17)

$$\ddot{r} - r\dot{\phi}^2 = \frac{1}{M}(T\sin\theta + L\cos\gamma - D_r\sin\gamma) - \frac{\mu}{r^2}$$

$$r\ddot{\phi} + 2\dot{r}\dot{\phi} = \frac{1}{M}(T\cos\theta - L\sin\gamma - D_r\cos\gamma)$$

where r = radius from center of earth

ϕ = angle from launch site to radius vector

M = instantaneous mass of interceptor system

T = thrust

L = lift (neglected for this investigation)

D_r = drag

μ = earth's gravitational constant

θ = angle between thrust vector and local horizontal

γ = angle between velocity vector and local horizontal

These equations are broken down into four, first-order, simultaneous differential equations for the computer program (Ref 9: 110-120).

Some estimate of the drag is needed for these equations, since the shape and size of the interceptor system is unknown. A curve of C_d vs M (mach number), (Ref 2:43), for a cylindrical rocket with a 40° apex nose cone, was approximated by straight line segments which resulted in the following estimate for C_d.

$C_d = 0.25 \qquad 0 < M < 0.6$

$C_d = 0.25 + (M - 0.6) \qquad 0.6 < M < 1.6$

$C_d = 1.25 - (M - 1.6) \qquad 1.6 < M < 2.9$

$C_d = 0.86 \qquad 2.9 < M$

The drag is given by the equation

$$D_r = \frac{1}{2} C_d \rho v^2 A$$

where D_r = aerodynamic drag, lb

C_d = coefficient of drag

ρ = atmospheric density, slug per ft^3

v = velocity, ft per sec

A = cross sectional area, ft^2

Now since the coefficient of drag is a function of mach number, and mach number is a function of the speed of sound, we need an estimate for the variation in speed of sound with altitude. This was obtained by fitting straight line segments to a curve of a versus b, where b is the height above the earth (Ref 1:24). By doing this we find that

$$a = 0.18362 - 0.0040095\,b \qquad 0 < b < 6.0855$$

$$a = 0.15922 \qquad 6.0855 < b < 13.487$$

$$a = 0.15922 + 0.0018602\,(b - 13.487) \qquad 13.487 < b < 25.658$$

$$a = 0.18186 \qquad 25.658 < b < 28.783$$

$$a = 0.18186 - 0.0028798\,(b - 28.783) \qquad 28.783 < b < 43.586$$

$$a = 0.13923 \qquad 43.586 < b$$

where a is the speed of sound in nautical miles per second, and b is the height above the earth in nautical miles.

In a similar manner a curve of $\log_{10} \rho$ versus b (Ref 1:21) is approximated by

$$\log_{10} \rho = -(2.624 + 0.1082\,b), \qquad b < 86.67$$

$$\log_{10} \rho = -(12.0 + 0.01143\,b), \qquad b > 86.67$$

The remaining factor in the drag equation is A, the cross sectional area of each stage. We must obtain estimates for all three stages since burned-out stages are jettisoned. To do this, first we assume that the propellant density is 0.06 lb per in^3. This is an average of densities for some commonly used solid propellants (Ref 10: 312, 313). With this density, and the data on stage weights, the approximate volume of each stage is found to be:

Stage 1. . .	5,000.	ft^3
Stage 2. . .	1,445.	ft^3
Stage 3. . .	420.	ft^3

With the volumes known we can now assume some dimensions for the stages and estimate the cross sectional areas. These dimensions are as follows:

	Selected Area-ft^2	Approx. Diam. ft	Approx. Length ft
Stage 1	75	10	67
Stage 2	50	8	29
Stage 3	40	7	11

The velocity-match rocket and interceptor vehicle are, of course, mounted on top of the three boost stages but it is assumed that their cross sectional areas are equal to or less than the third boost-stage area.

The approximate equations for speed of sound, coefficient of drag, and atmospheric density are built into computer program CM-12 (Appendix A), along with the equations of motion. With this program, and the calculated rocket parameters, a trial and error method was used whereby different values of the launch parameters were selected. The values of r_b, v_b, and γ_b, were then compared with points on the desired intercept trajectory printout, to determine new trial input values. After several trials, the following results were obtained:

Launch parameter inputs

t_v = 24 seconds

α = -0.08 radian (4.6°)

Γ = 0.8 radian (45.8°)

where t_v is the duration of the vertical flight segment

α is the angle between the velocity vector and the thrust vector

Γ is the angle where tip-over segment ceases, and the zero-lift (thrust along the velocity vector) segment begins. That is, when γ reaches a value of 0.8 rad, α is set equal to zero.

Computer printouts

	CM-12 (actual)	CM-3 (desired)	Approx. Error
r_b	3637.12 n.m	3639.22 n.m.	0.06%
γ_b	0.44583 rad	0.43464 rad	2.5%
v_b	3.0322 n.m. per sec	3.1342 n.m. per sec	3.3%

The approximate error in overall weight (or thrust) due to the error in required burnout velocity can be found as follows. It can be shown that for a k-stage rocket in field free space,

$$\frac{\psi_{o_1}}{\psi_{o_2}} = \left[\frac{n - D_1 \epsilon^{\frac{v_a - v_1}{ku}}}{(n - D_1)\epsilon^{\frac{v_a - v_1}{ku}}} \right]^k$$

where ψ_{o_1} is the overall mass (or weight) ratio corresponding to D_1,

D_1 is the sub-rocket effective mass ratio required to reach burnout velocity v_1,

ψ_{o_2} and D_2 correspond to burnout velocity v_2.

If we use the preceding computer results, and the above equation, with

$$n = 10$$

$$D_1 = \frac{\nu}{\beta} = \frac{4.1637}{1.5} = 2.7758$$

v_2 = 3.1342 n.m. per second (desired burnout velocity)

v_1 = 3.0322 n.m. per second (actual burnout velocity)

$$u = I_s g = \frac{(250)(32.2)}{6080} = 1.325 \text{ n.m. per second}$$

$$k = 3$$

it is found that

$$\frac{\psi_{o_1}}{\psi_{o_2}} = 0.8987 = \frac{\text{actual weight}}{\text{required weight}}$$

This indicates that there is an approximate error in the overall system weight of 11%. Since the first stage thrust is simply β times the overall weight, this means that 11% more thrust is required to reach the desired burnout velocity, or approximately 1,220,000 lb instead of 1,094,600 lb.

It is felt that after several more trials, a more nearly optimum flight path could be determined, and that the velocity error could be reduced. However, these results indicate that the assumptions used in the mathematical development of Chapter IV do not invalidate the numerical results of Chapter VI. In any case, for heavy interceptor vehicles, where thrust is probably much greater than drag, the graphs in Chapter VI can be used to determine excellent estimates of the thrusts required for different intercept conditions.

Vita

Richard Allen Coffland [redacted] 1950, he entered Iowa State College, and in June 1954 he was graduated with the degree of Bachelor of Science in Chemical Engineering. After receiving his commission as Lieutenant in the USAF Reserve he entered active duty in October 1954. His military assignment prior to his coming to the Institute of Technology was as an Instructor Pilot in the Basic Training Program of Air Training Command.

[redacted]

Charles Allison MacIvor [redacted] he entered Stevens Institute of Technology, Hoboken, New Jersey. He graduated from Stevens in 1953 with the degree of Mechanical Engineer and received a commission as Lieutenant in the USAF Reserve. After being called to active duty in October 1953 he completed pilot training and served as a fighter pilot in Japan. His assignments prior to his coming to the Institute of Technology were as a Ferry Pilot in the Military Air Transport Service, and Flight Service Operations Officer.

[redacted]

This thesis was typed by Joyce M. Kerr.